

A NUMERICAL FORCED CONVECTION HEAT TRANSFER ANALYSIS OF
NANOFLUIDS CONSIDERING PERFORMANCE CRITERIA

A THESIS SUBMITTED TO
THE GRADUATE SCHOOL OF NATURAL AND APPLIED SCIENCES
OF MIDDLE EAST TECHNICAL UNIVERSITY

BY

OĞUZ KİREZ

IN PARTIAL FULFILLMENT OF THE REQUIREMENTS
FOR
THE DEGREE OF MASTER OF SCIENCE
IN
MECHANICAL ENGINEERING

NOVEMBER 2012

Approval of the thesis:

**A NUMERICAL FORCED CONVECTION HEAT TRANSFER ANALYSIS
OF NANOFLUIDS CONSIDERING PERFORMANCE CRITERIA**

Submitted by **OĞUZ KİREZ** in partial fulfillment of the requirements for the degree of Master of Science in **Mechanical Engineering Department, Middle East Technical University** by,

Prof. Dr. Canan Özgen
Dean, Graduate School of **Natural and Applied Sciences**

Prof. Dr. Suha Oral
Head of Department, **Mechanical Engineering**

Assoc. Prof. Dr. Almıla Güvenç Yazıcıoğlu
Supervisor, **Mechanical Engineering Dept. METU**

Prof. Dr. Sadık Kakaç
Co-Supervisor, **Mechanical Engineering Dept. METU**

Examining Committee Members:

Assoc. Prof. Dr. İlker Tarı
Mechanical Engineering Dept., METU

Assoc. Prof. Dr. Almıla Güvenç Yazıcıoğlu
Mechanical Engineering Dept., METU

Dr. Özgür Bayer
Mechanical Engineering Dept., METU

Assist. Prof. Dr. Tuba Okutucu Özyurt
Mechanical Engineering Dept., METU

Assist. Prof. Dr. Nilay Sezer Uzol
Mechanical Engineering Dept., TOBB ETÜ

Date:09/11/2012

I hereby declare that all information in this document has been obtained and presented in accordance with academic rules and ethical conduct. I also declare that, as required by these rules and conduct, I have fully cited and referenced all material and results that are not original to this work.

Name, Last name : Oğuz Kirez

Signature :

ABSTRACT

A NUMERICAL FORCED CONVECTION HEAT TRANSFER ANALYSIS OF NANOFLUIDS CONSIDERING PERFORMANCE CRITERIA

Kirez, Oğuz

M.S., Department of Mechanical Engineering

Supervisor: Assoc. Prof. Dr. Almila Güvenç Yazıcıoğlu

Co-Supervisor: Prof. Dr. Sadık Kakaç

November 2012, 126 pages

A nanofluid is a new heat transfer fluid produced by mixing a base fluid and solid nano sized particles. This fluid has great potential in heat transfer applications, because of its increased thermal conductivity and even increased Nusselt number due to higher thermal conductivity, Brownian motion of nanoparticles, and other various effects on heat transfer phenomenon.

In this work, the first aim is to predict convective heat transfer of nanofluids. A numerical code is created and run to obtain results in a pipe with two different boundary conditions, constant wall temperature and constant wall heat flux. The

results for laminar flow for thermally developing region in a pipe are obtained for Al_2O_3 /water nanofluid with different volumetric fraction and particle sizes with local temperature dependent conductivity approach. Various effects that influence nanofluid heat transfer enhancement are investigated. As a result, a better heat transfer performance is obtained for all cases, compared to pure water. The important parameters that have impact on nanofluid heat transfer are particle diameter of the nanoparticles, nanoparticle volumetric fraction, Peclet number, and viscous dissipation.

Next, a heat transfer performance evaluation methodology is proposed considering increased pumping power of nanofluids. Two different criteria are selected for two boundary conditions at constant pumping power. These are heat transfer rate ratio of the nanofluid and the base fluid for constant wall temperature boundary condition and difference between wall temperature of the pipe at the exit and inlet mean temperature of the fluid ratio for constant wall heat flux case. Three important parameters that influence the heat transfer performance of nanofluids are extracted from a parametric study. Lastly, optimum particle size and volumetric fraction values are obtained depending on Graetz number, Nusselt number, heat transfer fluid temperature, and nanofluid type.

Keywords: nanoparticle, nanofluid, convective heat transfer, numerical simulation, heat transfer performance, constant pumping power

ÖZ

NANOAKIŞKANLARDA ZORLANMIŞ TAŞINIMLA ISI TRANSFERİNİN SAYISAL VE PERFORMANS ÖLÇÜTÜ BAZINDA ANALİZİ

Kirez, Oğuz

Yüksek Lisans, Makina Mühendisliği Bölümü

Tez Yöneticisi: Doç. Dr. Almıla Güvenç Yazıcıoğlu

Ortak Tez Yöneticisi: Prof. Dr. Sadık Kakaç

Kasım 2012, 126 sayfa

Nanoakışkanlar, bir baz akışkan ve nano boyutta parçacıkların karıştırılması ile oluşturulmuş yeni ısı transferi akışkanlarıdır. Nanoakışkanlar, nanoparçacıkların yüksek ısı iletim katsayısı, Brownian hareketi ve başka etkenlerden gelen yüksek ısı transfer katsayısı sayesinde ısı transfer alanında çok yüksek potansiyele sahiplerdir.

Bu çalışmanın amacı, sayısal bir model kullanarak ısı transferi katsayısını doğru bir şekilde hesaplayabilmektir. Tek fazlı akış yöntemi kullanılarak yapılan analizlerde, düz bir boru içerisinde laminer rejimdeki ısı transferi katsayısı, Al_2O_3/su nanoakışkanı için, farklı nanoparçacık boyutu ve hacimsel yüzdeleri için incelenmiş

Analizler sabit duvar sıcaklığı ve sabit duvar ısı akısı sınır koşulları için ayrı olarak yapılmış ve sayısal olarak farklı değerler elde edilmesine rağmen, her iki durum için iyileşme gözlenmiştir. Ayrıca, nanoakışkanlarda ısı transferi etkileyen çeşitli durumların etkisi de kontrollü olarak incelenmiştir. Bu durumlar, Peclet sayısı değişimi, viskoz yitim, nanoparçacık çapı ve nanoparçacık hacimsel yüzdesidir.

Son olarak, sabit pompa gücü durumu düşünülerek, bir ısı transferi performansı yaklaşımı önerilmiştir. Yani, sadece ısı transferi katsayısındaki değişimi gözlemek yerine, artan viskozite ile birlikte artan pompa gücü hesaba katıldığında nanoakışkan kullanmanın faydasının ölçülmesi amaçlanmıştır. İki farklı sınır koşulu için, sabit pompa gücünde iki ayrı performans kıstası belirlenmiştir. Parametrik bir çalışma yapılarak üç önemli etken faktör ortaya çıkarılmış ve başlangıç analizleri yapılmıştır. Nusselt ve Graetz sayılarına, ısı transferi akışkanının sıcaklığına ve nanoakışkan türüne bağlı olarak, her bir durum için bir en iyi nanoparçacık boyutu ve en iyi hacimsel yüzde olduğu sonucuna varılmıştır.

Anahtar Kelimeler: nanoparçacık, nanoakışkan, taşınımli ısı transferi, sayısal benzetim, ısı transferi performansı, sabit pompa gücü

To My Darling

ACKNOWLEDGEMENTS

Firstly, I would like to express my gratefulness to my supervisor Assoc. Prof. Dr. Almıla Güvenç Yazıcıođlu for her advice, support, and encouragement throughout my graduate study.

I would like to thank to Prof. Dr. Sadık Kakaç, Assist. Prof. Dr. Nilay Sezer Uzol and Assist. Prof. Dr. M. Metin Yavuz for their invaluable comments and suggestions on my graduate study.

I would also like to thank to my friends Melih Çelik, M. Emre Esastürk, Süleyman Polat, Abdullah Yelmer, Büryan Apaçođlu, E. Begüm Elçiođlu, İ. Ozan Sert, Göker Türkakar, and Mustafa Uslu for their friendship and contributions to my thesis.

My efforts would not be meaningful without the support of my wife Büşra, and my family.

Lastly, I would like to thank to TÜBİTAK for its financial support during my academic study.

TABLE OF CONTENTS

ABSTRACT	iv
ÖZ.....	vi
ACKNOWLEDGEMENTS	ix
TABLE OF CONTENTS	x
LIST OF TABLES	xiii
LIST OF FIGURES.....	xiv
LIST OF SYMBOLS.....	xviii
CHAPTERS	
INTRODUCTION.....	1
1.1. Heat Transfer Enhancement with Nanofluids	1
1.2. Nanofluid Composition	3
1.3. Nanofluid Preparation	3
1.4. Motivation and Organization of the Thesis.....	4
THERMOPHYSICAL PROPERTIES OF NANOFUIDS	6
2.1. Introduction	6
2.2. Literature Survey of Thermophysical Properties	7
2.2.1. Density.....	7
2.2.2. Specific Heat	8
2.2.3. Thermal Conductivity.....	9
2.2.4. Viscosity.....	15
2.3. Impact of Nanoparticles	20
2.4. Impact of Base Fluid	24

CONVECTIVE HEAT TRANSFER OF NANOFLUIDS.....	31
3.1. Introduction	31
3.2. Survey of Experimental, Theoretical and Numerical Studies in Literature ...	32
3.2.1. Experimental Studies.....	32
3.2.2. Theoretical Studies and Empirical Correlations.....	37
3.2.3. Numerical Studies	41
3.3. Modeling of the Nanofluid Convective Heat Transfer in a Pipe.....	42
3.3.1. Governing Equations of the Problem	44
3.3.2. Boundary Conditions.....	48
3.3.2.1. Constant Wall Temperature.....	48
3.3.2.2. Constant Wall Heat Flux	49
3.3.3. Numerical Method to Solve the Energy Equation.....	49
3.3.3.1. Finite Difference Method	50
3.3.3.2. Discretization of Interior Nodes	51
3.3.3.3. Discretization of Boundary Nodes	53
3.3.4. Verification of the Numerical Study	53
3.3.4.1. Mesh Dependency Analysis	54
3.3.4.2. Validation of the Code with Pure Water	55
3.3.5. Demonstrative Parameters.....	56
RESULTS OF THE NUMERICAL STUDY AND DISCUSSION	58
4.1. Introduction	58
4.2. Comparison with Experimental Results	58
4.3. Comparison of Five Different Thermal Conductivity Models for the Two Boundary Conditions.....	61
4.3.1. Constant Wall Temperature.....	61
4.3.2. Constant Wall Heat Flux	65
4.4. Nusselt Number of the Two Boundary Conditions	68
4.5. Other Affecting Parameters.....	69
4.5.1. Temperature Dependent Variable Thermal Conductivity	69

4.5.2. Peclet Number	72
4.5.3. Particle Size	73
4.5.4. Axial Conduction	75
4.5.5. Viscous Dissipation	76
4.6. Conclusion.....	79
HEAT TRANSFER PERFORMANCE EVALUATION OF NANOFLUIDS WITH PUMPING POWER CONSIDERATION.....	80
5.1. Introduction	80
5.2. Survey of the Performance of Nanofluids in Literature	81
5.3. Evaluation Criterion and Problem Geometry	86
5.4. Pressure Drop and Pumping Power of Nanofluids.....	87
5.5. Performance Ratio for the Two Boundary Conditions.....	89
5.5.1. Constant Wall Temperature.....	89
5.5.2. Constant Wall Heat Flux	92
5.6. Investigation of Affecting Parameters in Fully Developed Region	94
5.6.1. The Parameter Nu_f/Gz_f	94
5.6.2. The Parameter β	96
5.6.3. The Parameter h_r	98
5.7. Maximum Heat Transfer Performance and Optimum Nanofluid Type	100
SUMMARY AND CONCLUSION.....	105
6.1. Summary	105
6.2. Conclusion.....	107
6.3. Future Work	111
REFERENCES	113
APPENDICES	
A. NUMERICAL STUDY CODE ALGORITHM	123
B. CONVECTIVE HEAT TRANSFER ANALYSIS DIMENSIONAL VALUES AND RESULTS	124
C. PARAMETRIC STUDY OF CHAPTER 5	126

LIST OF TABLES

Table 1	Empirical c_4 Values for Different Materials Used in Eq. (11) [25]	11
Table 2	Thermophysical Properties of Materials [64] Generally Used in Nanofluid Preparation	21
Table 3	Selected Base Fluid Properties Affecting Nanofluid Heat Transfer at 20°C [64] with Desired Tendency for Better Enhancement.....	26
Table 4	Dimensional Geometrical and Boundary Condition Values for the Figures (18-30).....	124
Table 5	Constant and Variable Property Results of Al_2O_3 (50nm) /water Nanofluid in the Fully Developed Region for Different Peclet Numbers.....	124
Table 6	Effect of Axial Conduction for Al_2O_3 (50nm) /water Nanofluid in the Fully Developed Region.....	125
Table 7	Effect of Viscous Dissipation for Al_2O_3 (50nm) /water Nanofluid in the Fully Developed Region.....	125

LIST OF FIGURES

Figure 1 Relative thermal conductivities of Al ₂ O ₃ /water nanofluids at different particle diameters using the three models [6, 23, 28] at temperature 20 °C as a function of nanoparticle volumetric fraction (Eq. 9, 12, 19).....	15
Figure 2 Relative thermal conductivity of Al ₂ O ₃ /water nanofluids using the three models [6, 23, 28] for different particle diameters at volumetric fraction 5% ($\phi=0.05$) as a function of temperature (Eq. 9, 12, 19).....	16
Figure 3 Relative viscosity of water based nanofluids for three different particle diameters using the three models [28, 46, 47] at 20°C as a function of nanoparticle volumetric fraction (Eq. 21, 22, 24).	19
Figure 4 Relative thermal conductivity of water based nanofluids with different nanoparticle types using the two models [23, 28] with particle diameter 10 nm at 20°C as a function of nanoparticle volumetric fraction (Eq. 9, 19).	22
Figure 5 Relative volumetric heat capacity of water based nanofluids with different types of nanoparticles at 20°C as a function of nanoparticle volumetric fraction (Eq. 3, 4, 5, 7)	23
Figure 6 Relative density of water based nanofluids with different types of nanoparticles at 20°C as a function of nanoparticle volumetric fraction (Eq. 3, 5). .	23
Figure 7 Relative thermal conductivities of Cu (10 nm) nanofluids with different base fluids at 20°C, with the two models [23, 28] as a function of nanoparticle volumetric fraction (Eq. 9, 19).	27
Figure 8 Relative viscosity of Cu (10 nm) nanoparticle nanofluids with different base fluids at 20°C as a function of nanoparticle volumetric fraction (Eq. 24)	28

Figure 9	Relative density of Cu (10 nm) nanoparticle nanofluids with different base fluids at 20°C as a function of nanoparticle volumetric fraction (Eq. 3, 5).	28
Figure 10	Relative volumetric heat capacity of Cu (10nm) nanofluids with different base fluids at 20°C as a function of nanopart. vol. frac. (Eq. 3, 4, 5, 7).....	29
Figure 11	Prandtl numbers of the selected base fluids as a func. of temp.....	30
Figure 12	Geometry of the convective heat transfer problem	44
Figure 13	The problem geometry and nodes used in numerical solution, number of nodes is shown arbitrarily.	51
Figure 14	Mesh sensitivity analysis of the numerical study at Peclet number 2000 with pure water as a function of 2nd dimensionless axial length (Nux is Nusselt number and $x+= x/(D \cdot Re \cdot Pr)$ the reverse of Graetz number.).....	54
Figure 15	Validation of the code with Equation (72) [90] for pure water solution at Peclet number 1000	56
Figure 16	Comparison of the local heat transfer coefficient from the current study with experimental data from Kim et al. [74] for pure water and Al ₂ O ₃ /water nanofluid using Corcione's thermal conductivity model	59
Figure 17	Comparison of the local heat transfer coefficient from the current study with experimental data from Rea et al. [71] for pure water and Al ₂ O ₃ /water nanofluid using Corcione's thermal conductivity model	60
Figure 18	Local heat transfer coefficient of Al ₂ O ₃ (20 nm) /water nanofluid at Peclet number 2000 by using the five conductivity models ($\phi=1\%$) for CWT	63
Figure 19	Local heat transfer coefficient of Al ₂ O ₃ (20 nm) /water nanofluid at Peclet number 2000 by using the five conductivity models ($\phi=4\%$) for CWT	63
Figure 20	Local heat transfer enh. of Al ₂ O ₃ (20 nm) /water nanofluid at Peclet number 2000 by using the five conductivity models ($\phi=1\%$) for CWT condition ...	64
Figure 21	Local heat transfer enh. of Al ₂ O ₃ (20 nm) /water nanofluid at Peclet number 2000 by using the five conductivity models ($\phi=4\%$) for CWT condition ...	64

Figure 22	Local heat transfer coefficient of Al ₂ O ₃ (20 nm) /water nanofluid at Peclet number 2000 by using the five conductivity models ($\phi=1\%$) for CHF	66
Figure 23	Local heat transfer coefficient of Al ₂ O ₃ (20 nm) /water nanofluid at Peclet number 2000 by using the five conductivity models ($\phi=4\%$) for CHF	66
Figure 24	Local heat transfer enh. of Al ₂ O ₃ (20 nm) /water nanofluid at Peclet number 2000 by using the five cond. models ($\phi=1\%$) for CHF condition	67
Figure 25	Local heat transfer enh. of Al ₂ O ₃ (20 nm) /water nanofluid at Peclet number 2000 by using the five conductivity models ($\phi=4\%$) for CHF condition	67
Figure 26	Local Nusselt number along the channel for the Al ₂ O ₃ (20 nm) /water nanofluid at $\phi=4\%$ and the pure water using Corcione model with CWT and CHF boundary conditions at Peclet number 2000	69
Figure 27	Local Nusselt number with variable and constant thermal conductivity assumptions for Al ₂ O ₃ (20 nm) /water nanofluid at $\phi=4\%$ and pure water at Peclet number 2000 using Corcione model (CHF condition is applied)	71
Figure 28	Local heat transfer enh. along the channel for Al ₂ O ₃ (20 nm) /water nanofluid at $\phi=4\%$ with variable cond. and constant cond. assumptions at Peclet number 2000 using Corcione model (CHF condition is applied)	72
Figure 29	Local heat transfer enhancement along the channel for different Peclet numbers for Al ₂ O ₃ (20 nm) /water nanofluid at $\phi=4\%$ using Corcione model (CHF condition is applied)	73
Figure 30	Local heat transfer enhancement along the channel for Al ₂ O ₃ /water with different nanoparticle diameters nanofluid at $\phi=4\%$ using Corcione model (CHF condition is applied)	74
Figure 31	Local Nusselt number along the channel with and without the axial conduction term in Eq. 60 assumptions for pure water and Al ₂ O ₃ (20 nm) /water nanofluid at $\phi=5\%$ using Corcione model ,(CHF condition is applied), (ON:axial conduction considered, OFF:axial conduction neglected)	76
Figure 32	Local Nusselt number along the channel with and without negligible viscous dissipation assumptions for pure water and Al ₂ O ₃ (20 nm) /water nanofluid,	

(CHF condition is applied), ($\phi=5\%$, ON: viscous dissipation conduction considered, OFF: not considered).....	78
Figure 33 Fully developed Nusselt number with varying channel diameter with and without negligible viscous dissipation assumptions for pure water and Al_2O_3 (20 nm) /water nanofluid, (CHF condition is applied), ($\phi=4\%$, ON: viscous dissipation conduction considered, OFF: not considered).....	78
Figure 34 Variation of heat transfer performance ratio with in fully developed region as a function of Nuf/Gzf (Eq. 100 or 109)	95
Figure 35 Variation of β parameter with changing volumetric fraction at different particle sizes for Cu/water nanofluid at 20°C (Eq. 5, 7, 24, 102).....	97
Figure 36 Variation of β parameter with changing volumetric fraction at different particle sizes for Cu/EG nanofluid at 20°C (Eq. 5, 7, 24, 102).....	97
Figure 37 Variation of the parameter h_r with changing volumetric fraction at different particle sizes for Cu/water nanofluid at 20°C (Eq. 19, 103).....	99
Figure 38 Variation of the parameter h_r with changing volumetric fraction at different particle sizes for Cu/EG nanofluid at 20°C (Eq. 19, 103).....	99
Figure 39 Heat transfer performance ratio for Cu/water nanofluids at different particle diameters for CHF case with fully developed region at Graetz number 20 as a function of volumetric fraction.....	102
Figure 40 Heat transfer performance ratio for Cu/water nanofluids at different particle diameters for CHF case with fully developed region at Graetz number 20 as a function of volumetric fraction.....	102
Figure 41 Heat transfer performance ratio for Cu/EG nanofluids at different particle diameters with for CHF case with fully developed region at Graetz number 20 as a function of volumetric fraction	103
Figure 42 Heat transfer performance ratio for Cu/EG nanofluids at different particle diameters with for CHF case with fully developed region at Graetz number 20 as a function of volumetric fraction	103

LIST OF SYMBOLS

- B : Boltzman constant, 1.381×10^{-23} , J/K
- C : specific heat, $J/kg \cdot K$
- c_{1-19} : empirical or theoretical constant in related equations
- CHF : constant wall heat flux boundary condition
- CWT: constant wall temperature boundary condition
- D : pipe diameter, m
- d_f : base fluid molecular diameter, nm
- d_p : nanoparticle diameter, nm
- \mathbf{F} : body force vector, N
- f : friction factor in straight pipes
- Gz : Graetz number
- h : heat transfer coefficient, $W/m^2 \cdot K$
- i : node number in axial direction
- j : node number in radial direction
- k : thermal conductivity, $W/m \cdot K$
- k_d : thermal dispersion coefficient, $W/m \cdot K$
- L : pipe length, m
- l : nanolayer thickness, nm
- M : molecular mass, kg/mol
- m : mass flow rate, kg/s
- n : shape factor (Eq. 9)
- NTU : number of transfer units in heat exchanger

Nu	: Nusselt number
OFF	: related term neglected
ON	: related term added
P	: pressure, Pa
P	: pumping power to circulate flow, W
Pe_d	: nanoparticle Peclet number
Pe	: channel flow Peclet number
Pr	: Prandtl number
Q	: total heat transfer rate, W
q''	: wall heat flux, W/m^2
q'''	: volumetric heat generation, W/m^3
r	: radial direction
r_0	: radius of the pipe
Re	: channel flow Reynolds number
Re_B	: Brownian velocity based Reynolds number (Eq. 13)
$Re_{B,2}$: Brownian velocity based Reynolds number 2 (Eq. 20)
T	: temperature, $^{\circ}C$
t	: time, s
UA	: overall heat transfer coefficient \times area, W/K
\mathbf{V}	: velocity vector, m/s
v	: flow velocity, m/s
x	: axial direction

Greek letters

δ_v^+	: laminar sublayer thickness in turbulent flow
λ_f	: mean free path of base fluid, nm
ϵ	: heat transfer efficacy (Eq. 82)
Φ	: viscous dissipation, W/m^3

$\beta = \rho_r C_r / \mu_r^{1/2}$: property related heat transfer performance parameter
$\gamma = Nu_r k_r$: property related heat transfer performance parameter
η	: performance comparison criterion (Eq. 81)
θ	: dimensionless temperature
μ	: viscosity, N·s/m ²
ρ	: density, kg/m ³
φ	: angular direction
ϕ	: nanoparticle volumetric fraction in nanofluid

Subscripts

b	: bulk value over the channel
f	: base fluid
fr	: freezing point
i	: inlet condition
l	: liquid layering
m	: average of inlet and exit
nf	: nanofluid
o	: exit condition
p	: nanoparticle
r	: ratio of nanofluid to base fluid related parameter
w	: wall condition
x	: local value
v	: property in laminar sublayer in turbulent flow

Superscripts

*	: dimensionless value (Eq. 59)
+	: dimensionless value (Eq. 72)

CHAPTER 1

INTRODUCTION

1.1. Heat Transfer Enhancement with Nanofluids

Throughout history, people worked on the subject of heat transfer phenomenon for a better heat transfer performance, which directly affects the standard of their life. With the development of heat engines, heat pumps and similar devices, the requirement for a better heat transfer became more important. Heat exchanger devices, heat transfer fluids or other components related with heat transfer were invented and improved with thriving technology. Usage of more compact, larger heat transfer area heat transfer devices are common in today's industry. However, heat transfer requirements of these devices are becoming larger while their sizes are becoming smaller. At this point, increasing the heat transfer area of a device may no longer be a solution because the practical limitations of manufacturing smaller channels or components can be a problem with usage of conventional methods.

Researchers targeted two different ways to overcome these problems in the heat transfer research world, which are improving micro or nano sized channels and different types of heat transfer fluids. The second alternative includes nanofluid improvement and usage in heat transfer applications such as heat exchangers and heat sinks.

Certainly, thermal conductivities (k) of the heat transfer fluids like water, ethylene glycol or engine oil are relatively low, thus; a heat transfer fluid which should be used in a convective heat transfer system possesses a higher heat transfer resistance compared to metallic components of a device. Therefore, a direct intervention to the heat transfer fluids to improve the performance of the systems is an attractive idea. Thermal conductivity plays a crucial role in the heat transfer coefficient of the system so that high performance cooling can be obtained by increasing the thermal conductivity of fluids.

Addition of small particles, which have high thermal conductivity into a base fluid, comes from this notion and it was firstly proposed by Ahuja [1, 2] to acquire a heat transfer enhancement. Although Ahuja was able to achieve a heat transfer enhancement with mini sized Polystyrene particles in his system, clogging of the channels became a serious problem because of deposition of the particles. The research required smaller (nano) sized particles called nanoparticles. They were dispersed in a base fluid, mixed and homogenized with special techniques. The pioneer scientist who used it in a heat transfer system was Choi [3].

The heat transfer enhancement using nanofluids is important because of the reasons mentioned above. The heat transfer enhancement was defined as ratio between heat transfer coefficient of nanofluid and heat transfer coefficient of base fluid (described in the next section) at a constant parameter. The constant parameter may be different in various studies. Typically, it is selected as velocity, Reynolds number or Peclet number. Researchers thought that the enhancement was directly related to Nusselt number ($Nu = h \cdot D/k$) and thermal conductivity enhancement of a fluid in a system according to notion of comparison of heat transfer coefficients in a system. Thermal conductivity enhancement was defined as ratio between nanofluid thermal conductivity and base fluid thermal conductivity. A comparison can be made between the base fluid and the nanofluid, thus; it can be observed that how much heat transfer coefficient enhancement is achieved. The challenging topic on this issue is accurate prediction of heat transfer enhancement.

1.2. Nanofluid Composition

Nanofluids are made from generally one type of base fluid and one type of nanoparticles. As it is mentioned above, the aim is to increase the thermal conductivity of the fluid matrix which is going to be used in a heat transfer application. For this reason, the nanoparticles are generally selected as metallic or metal oxide materials which have higher thermal conductivity [4-8]. Common metallic and metallic oxide nanoparticles used in this area are Alumina (Al_2O_3), Copper Oxide (CuO), Copper (Cu), Titanium di Oxide (TiO_2). Other types of materials such as graphite, carbon and diamond are also used in research [9-14]. In addition to enhancement in thermal conductivity, an enhanced Nusselt number is also observed in the experiments.

Common heat transfer fluids can also be used as the base fluid of the nanofluid. The important point of the selection of the base fluid is still dependent on suitability for a specific heat transfer application. All heat transfer base fluids can be used for nanofluid production as long as they are suitable for production techniques. However, it is important to note that the addition of nanoparticles in a fluid provides more enhancement if the fluid has poor heat transfer capabilities. In other words, it is much more beneficial to use the nanoparticle addition technology when the working base fluid of a system has low thermal conductivity.

1.3. Nanofluid Preparation

The technology for nanofluid preparation gives two way of production of nanofluids using a base fluid and nanoparticles. These are single step and two step methods that have been used by different researchers. A detailed survey about preparation of nanofluids is made by Li et al. [15].

Single step was used by many researchers with different type of nanofluids. This step gives chance to mix the fluid and the particles in one step, as said. A solid particle source is heated up and vaporized particles are directly contacted to the fluid, thus; directly solidified as nano sized particles. Although it has advantages, e.g. stability of nanofluids, this method is a quite newly found way and requires investigation.

Two step method involves the following steps. First, production of nanoparticles is achieved using suitable methods such as “dry powder by inert gas condensation, chemical vapor deposition, and mechanical alloying” [15]. Second, previously prepared nanoparticles are dispersed into the base fluid. This method provides an easier solution for production of nanofluids because literature has knowledge about such nanoparticle production techniques. However, there exists a stability problem with this method and other additional techniques (e.g. ultrasonic vibration) for homogenous mixing of the particles in the fluid must be implemented.

1.4. Motivation and Organization of the Thesis

Most researchers have accepted that usage of a nanofluid instead of a base fluid helps to increase heat transfer coefficient. Although a common point of view about nanofluids is obtained, there is a significant discrepancy in results of nanofluid researches because amount of heat transfer enhancement could not be predicted well. In fact, the motivation behind this thesis study is several gaps in the literature which are described as follows.

First, usage of thermal conductivity and viscosity models in various experimental and numerical studies is arbitrarily and traditional models are widely used. On the other hand, it is vital to select suitable models which correctly describe the real situation for specific cases. In this study, some of models which represent individual or similar ideas are tested and compared. Therefore, a comparison is made, then; the most suitable models are chosen for generalized nanofluid heat transfer cases. In addition, there is a lack of information of the nanoparticle and the base fluid impact on nanofluids. Different types of nanoparticles and base fluids are compared as a primitive study.

Second, it was stated that traditional heat transfer correlations and analytical solutions are not capable of accurate estimation of heat transfer coefficient of nanofluids. This may be caused by thermal conductivity variation in nanofluid flow and any other mechanisms which are not considered in traditional models. As an original work, a numerical study is composed and performed on nanofluid convective heat transfer

behavior. It is aimed to acquire reasonable results and observe heat transfer enhancement for nanofluids by considering variable thermal conductivity (including Brownian motion effect which will be discussed later) and single phase approach.

Third, evaluation of heat transfer performance of nanofluids in terms of heat transfer and flow is not an extensively debated issue in the literature. The heat transfer enhancement definition cannot be sufficient to explain heat transfer performance because it says nothing about increased pumping power of flow by replacing the base fluid with the nanofluid. Thus, a study about this topic is to be very helpful for understanding the absolute benefit of the nanofluid heat transfer. An innovative study about this issue is developed, suggested, and related analyses are performed in Chapter 5.

In conclusion, the thesis aims to serve as a guide on thermophysical property model usage for nanofluids, estimation of heat transfer coefficient and enhancement, and heat transfer performance of nanofluids.

CHAPTER 2

THERMOPHYSICAL PROPERTIES OF NANOFLUIDS

2.1. Introduction

Nanofluid heat transfer enhancement idea comes from their higher thermal conductivity, hence; thermophysical properties and especially the thermal conductivity is a vital issue in nanofluid heat transfer phenomena. On the other hand, prediction of conductivity has been a serious challenge until now because there are many parameters that affect the thermal conductivity values. Temperature, type of the fluid, nanoparticle type, size, shape, and volumetric fraction, and production and mixing methods may greatly change the thermal conductivity values. Actually, the key issue in nanofluid heat transfer research is accurate prediction of nanofluid thermal conductivity. The literature research on thermal conductivity of nanofluids is a guide to understand how different parameters affect the values and what kind of thermal conductivity model should be selected for the current study.

Secondly, viscosity is also very important in nanofluid heat transfer performance, because it also increases with nanofluid usage compared to base fluid. Hence, there is an increase in the pumping power required for the circulation fluid. Prediction of viscosity of nanofluids is also a challenging topic and this is widely researched. The similar parameters that affect thermal conductivity affect viscosity values. Besides, viscosity estimation is also important in heat transfer coefficient estimation especially for turbulent flow because it exists in Reynolds number.

Lastly, the density and the specific heat affect the heat transfer performance of nanofluids. Fortunately, prediction of these thermophysical properties is simpler than that of other properties.

Thermophysical properties of nanofluids are often compared with base fluid properties in nanofluid heat transfer research in order to reach a conclusion. For better understanding of descriptions and conclusions, relative thermal conductivity, relative viscosity, relative density, and relative specific heat are presented in following equations, respectively.

$$k_r = \frac{k_{nf}}{k_f} \quad (1)$$

$$\mu_r = \frac{\mu_{nf}}{\mu_f} \quad (2)$$

$$\rho_r = \frac{\rho_{nf}}{\rho_f} \quad (3)$$

$$C_r = \frac{C_{nf}}{C_f} \quad (4)$$

In Equations (1-4), μ is viscosity, ρ is density, C is specific heat, and subscripts refer to nanofluid and base fluid, respectively. These definitions are used often in all chapters of the current study.

2.2. Literature Survey of Thermophysical Properties

2.2.1. Density

Density prediction does not require complicated correlations or models. It can be estimated with mixing theory [16] as following equation:

$$\rho_{nf} = \phi \rho_p + (1 - \phi) \rho_f \quad (5)$$

Here, ϕ represents the volumetric fraction of the nanoparticles in nanofluid. The subscript refers to nanoparticle. Pak and Cho [16] showed that the model matches with experimental data.

In addition, an experimental study on the density of nanofluids was also investigated by Sommer and Yerkes [17]. Their results were 5% higher than the mixing theory estimations, at maximum.

As a summary, there is lack of experimental data for density of nanofluids but it is also reasonable to assume that it agrees with mixing theory. Equation (5) is used in the current study when the density estimation is required in Chapters 4 and 5.

2.2.2. Specific Heat

Specific heat is a distinctive marker for heat transfer applications because heat carrying capacity should be high for an effective heat transfer. The same weighted fraction method is widely used in calculation of specific heat of nanofluids [16], as with density, but there is a debate regarding this method.

$$C_{nf} = \phi C_p + 1 - \phi C_f \quad (6)$$

However, it can be understood that Equation (6) is not suitable when the unit of the specific heat is considered (e.g. J/kg·K). This property is on per unit mass and must be calculated according to this consideration. A mass based weighted fraction method (thermal equilibrium model) gives Equation (7) as it is stated in [18] and it is more consistent with experimental results [19].

$$C_{nf} = \frac{\phi \rho C_p + 1 - \phi \rho C_f}{\rho_{nf}} \quad (7)$$

The nanofluid specific heat estimation is made from the Equation (7) in Chapters 4 and 5 in the current study.

2.2.3. Thermal Conductivity

As discussed at the beginning of the chapter, the conductivity is the most important thermophysical property that affects nanofluid heat transfer. The aim is to keep it as high as possible while maintaining a practical, long term heat transfer capability. On the other hand, there are several difficulties such as particle agglomeration, and sedimentation [20]. In fact, the first issue is to obtain a robust heat transfer fluid which has a high thermal conductivity. The second consideration is to predict the conductivity accurately.

Nanofluid thermal conductivity is a hot research area, and theoretical and experimental investigations have been made for several years. Generally, researches focused on determining the affecting parameters first and obtaining a theoretical or an empirical model for nanofluid heat transfer.

Maxwell [21] introduced a thermal conductivity model for conventional suspensions with spherical non-nano sized particles. The interaction between the particles is neglected; hence, the importance of the shape of the particles is not taken into account. The model is described below.

$$k_r = \frac{k_{nf}}{k_f} = \frac{k_p + 2k_f + 2 \frac{k_p - k_f}{k_p + k_f} \phi}{k_p + 2k_f - \frac{k_p - k_f}{k_p + k_f} \phi} \quad (8)$$

The pioneers of the nanofluid research, Choi and Eastman [22] proposed to use Hamilton & Crosser model [23] that was proposed for suspensions with particles larger than nanoparticles. This model was prepared considering Effective Medium Theory and is similar to Maxwell's model. However, as a first approximation, it can be used to observe how nanoparticle type, shape, and volume fraction alter the thermal conductivity of nanofluids. It is shown as follows:

$$k_r = \frac{k_p + n - 1 \frac{k_p - k_f}{k_p + k_f} \phi}{k_p + n - 1 \frac{k_p - k_f}{k_p + k_f} \phi} \quad (9)$$

Here, n is the shape factor. It is equal to 3 for spherical particles and the equation reduces to Maxwell model.

Das et al. [4] investigated Al₂O₃ (38 nm)/water and CuO (29 nm)/water nanofluids with volumetric fractions from 1 to 4%. The results show that CuO/water nanofluids have higher thermal conductivity than Al₂O₃/water nanofluids at different volumetric fractions. In addition, thermal conductivity of nanofluids increases with volumetric fraction and temperature. The temperature effect is important because thermal conductivity ratio of nanofluid to base fluid increases with increasing temperature. The findings are consistent with Lee et al.'s results [24], who have studied the thermal conductivity of nanofluids which were prepared using Al₂O₃ and CuO nanoparticles, and water and ethylene glycol base fluids. However, Hamilton Crosser model (Eq. 9) under predicts the values at higher temperatures than room temperature.

Chandrasekar et al. [5] investigated thermal conductivity of Al₂O₃ (43 nm)/water nanofluid with volumetric nanoparticle concentrations between 0.3-3% at room temperature. They observed an increasing trend in the conductivity values with increasing volumetric fraction. The results were compared with Das et al.'s [4] results and a similar behavior was observed. In addition, a model proposed by Chandrasekar et al. [5] closely predicts the experimental results. This model is shown below.

$$k_r = \frac{C_{nf}}{k_f}^{c_1} \frac{\rho_{nf}}{\rho_f}^{c_2} \frac{M_f}{M_{nf}}^{c_3} \quad (10)$$

Here, M is the average molecular mass of nanofluid and base fluid according to subscript and c_1 , c_2 , and c_3 are empirical constants.

Koo and Kleinstreuer [25] developed a thermal conductivity model for nanofluids, theoretically. They considered that the conductivity of nanofluids can be explained by two parts called as "static" and "Brownian". In other words, the thermal conductivity of nanofluids is separated into two parts. It was stated that the first part represents the thermal conductivity enhancement for dilute suspensions, hence; it can be selected as Hamilton Crosser model in Equation (9), and the second part is related with Brownian

motion. They created an explanation for the dynamic Brownian part theoretically considering particle size, temperature and particle volume fraction. It was mentioned that Brownian motion part of the model is especially important for ethylene glycol fluid. The model is as follows:

$$k_r = \frac{k_p + n - 1}{k_f + n - 1} \frac{k_f + n - 1}{k_p - k_f} \frac{k_p - k_f}{\phi} + 5 \times 10^4 c_4 \phi \rho_f C_f \sqrt{\frac{B \cdot T}{\rho_p d_p}} c_5 \quad (11)$$

where c_4 and c_5 are experimentally determined coefficients that contribute the effects of interaction between particles and temperature, respectively. c_5 is taken as 1 because of lack of experimental data and c_4 is given in Table 1 for different materials. Besides, d_p is particle diameter, B is the Boltzman constant, and T is temperature of the fluid.

Chon et al. [6] measured thermal conductivity of Al₂O₃ (11, 47, 150 nm)/water nanofluid with volumetric fractions 1 and 4%. They created a Brownian motion based empirical correlation for the conductivity. The results state that the conductivity increases with increasing volumetric fraction and decreasing particle size. Besides, the temperature range for the measurements is 21-71°C, which can be thought as a wide range for heat transfer applications. The model is stated as follows:

$$k_r = 1 + 64.7 \cdot \phi^{0.746} \frac{d_f}{d_p}^{0.369} \frac{k_p}{k_f}^{0.7476} Pr_f^{0.9955} Re_B^{1.2321} \quad (12)$$

$$Re_B = \frac{\rho_f B \cdot T}{3\pi\mu_f^2\lambda_f} \quad (13)$$

Table 1 Empirical c_4 Values for Different Materials Used in Eq. (11) [25]

Material type	c_4	Fraction
CuO	$0.0011 \cdot 100\phi^{-0.7272}$	$\phi > 1\%$
Al ₂ O ₃	$0.0017 \cdot 100\phi^{-0.0841}$	$\phi > 1\%$

Here, Re_B is Brownian velocity based Reynolds number which is shown in Equation (13). The symbol λ_f represents mean free path of the base fluid.

Duangthongsuk and Wongwises [7] conducted experiments on TiO₂ (21 nm & 40 nm)/water nanofluids with nanoparticle volumetric fractions 0.2%, 0.6%, 1.0%, 1.5% and 2.0%. Relative thermal conductivity of nanofluids was found as temperature dependent and slightly decreasing with temperature. The volumetric fraction also positively affects thermal conductivity. The nanoparticle size decrement increases conductivity.

Sitprasert et al. [26] studied on interfacial layer between base fluid and nanoparticle. According to Leong et al. [27], it has a very dominant effect of thermal conductivity of nanofluids and they developed a nanolayer dependent thermal conductivity. Sitprasert et al. extended this study and made the theoretical model sensitive to temperature change. The equation which shows the Sitprasert model is as in the following equation:

$$k_r = \frac{k_p - k_l \phi k_l 2c_7^3 - c_6^3 + 1 + k_p + 2k_l \beta_2^3 \phi c_6^3 k_l - k_f + k_f}{c_7^3 k_p + 2k_l - k_p - k_l \phi c_7^3 - c_6^3 + 1} \quad (14)$$

Here, k_l , the thermal conductivity of nanolayer, and c_6 and c_7 are defined as:

$$c_6 = 1 + \frac{l}{d_p/2} \quad (15)$$

$$c_7 = 1 + \frac{l}{d_p} \quad (16)$$

$$l = 0.01 T - 273 d_p/2^{0.35} \quad (17)$$

$$k_l = c_8 \frac{l}{d_p/2} k_f \quad (18)$$

Here, l is the thickness of the nanolayer and c_8 is an experimental constant.

Corcione [28] developed an empirical thermal conductivity correlation using the data available in the literature [4, 24, 25, 26, 29-34]. In this study, four types of nanoparticles, TiO₂, Al₂O₃, CuO, Cu and two types of base fluid, water and ethylene glycol were used. The nanoparticle size, thermal conductivity, volumetric fraction and the base fluid freezing temperature are the key parameters affecting thermal conductivity of the nanofluid. In addition, it is emphasized that the temperature of the nanofluid is important because relative thermal conductivity of nanofluids increases with temperature. Increment of particle diameter negatively and increment of volumetric fraction positively affect thermal conductivity values as stated in the literature generally. The background of the model is Brownian based enhanced thermal conductivity of nanofluids. Thermal conductivity values higher than Hamilton Crosser model is attributed to Brownian motion of nanoparticles. This model is shown as in the following equation:

$$k_r = 1 + 4.4Re_{B,2}^{0.4}Pr_f^{0.66} \frac{T}{T_{fr}}^{10} \frac{k_p}{k_f}^{0.03} \phi^{0.66} \quad (19)$$

$$Re_{B,2} = \frac{2\rho_f B \cdot T}{\pi\mu_f^2 d_p} \quad (20)$$

Here, T_{fr} is the freezing temperature of the base fluid and $Re_{B,2}$ is an another definition for the Brownian velocity based Reynolds number.

This model is a practical one and accuracy of it is good enough for generalized problems. The usage of two base fluids while creating the correlation is also an advantage for engineering problems.

There are numerous thermal conductivity models and conducted experiments in the literature, which can be used for analyses. Review articles that describe mechanisms behind enhanced thermal conductivity of nanofluids, describing theoretical and empirical models, and comparing experimental and theoretical studies for consistency are available in the literature.

Özerinç et al. [35] composed a review article that explains theoretical and empirical models for thermal conductivity of nanofluids. The detailed information about enhancement mechanisms can also be obtained from this study.

Chandrasekar et al. [36] surveyed experimental studies of thermal conductivity and prepared a review article. They reviewed 25 different experimental studies and stated their findings in terms of maximum enhancement, volumetric fraction, particle size and nanofluid type. The enhancement mechanisms are listed in this study as: “(i) Brownian motion of nanoparticles [24,37-40], (ii) nanolayering of the liquid at the liquid/particle interface [ref-ref], (iii) the nature of heat transport in the nanoparticles [41-43], (iv) clustering of particles [20,44,45]”.

The thermal conductivity estimations of nanofluids including different nanosized particles are observed in two Figures. Figure (1) shows relative thermal conductivity of Al_2O_3 (10, 40, 70 nm)/water nanofluids with the different models. As seen, nanoparticle volumetric fraction increases the conductivity but slopes are different for the three models. Actually, Corcione and Chon models give higher values and are close to each other. In addition, 10 nm particle sized nanofluid conductivity is significantly higher than others while Hamilton Crosser model cannot predict this difference.

Figure (2) predicts relative thermal conductivities again but this time the variable is the temperature of the nanofluids. Hamilton Crosser model provides a constant behavior with changing temperature while the other two models predict increasing relative thermal conductivity with temperature. This is caused by the Brownian effect on nanoparticles.

Finally, the five models selected from the literature are Hamilton Crosser, Koo Kleinstreuer, Chon, Sitprasert, and Corcione thermal conductivity models. These are used in the current study in the forced convective heat transfer analyses separately. The comparison among the heat transfer results are presented in Section 3 of Chapter 4. Because the analyses with Corcione model are the most reliable ones, this model is used in the rest of the Chapter 4, and in Chapter 5.

2.2.4. Viscosity

Most flow applications require low viscosity fluids because low viscosity means low pumping power to transport the fluid. In heat transfer applications, transportation of fluid also needs an extra pumping power for active systems. During nanofluid heat transfer in convective systems, viscosity of nanofluids may increase required pumping power of the system while increasing heat transfer. This is the drawback of nanofluids and should be critically analyzed because increment in viscosity of fluids may diminish the advantage of increment in thermal conductivity.

In nanofluid flow, viscosity depends on several factors such as nanoparticle concentration, type, size and shape, base fluid type, and ph value of the nanofluid. Similar to thermal conductivity enhancement, viscosity increases with increasing particle loading and smaller size of the particle. On the other hand, increment in the temperature slightly decreases relative viscosity of nanofluid.

Maiga [47] correlated three different sets of experimental data and obtained the viscosity model described in Equation (22). This model is limited to certain types of nanofluids, therefore; the only criterion for viscosity is particle volumetric fraction.

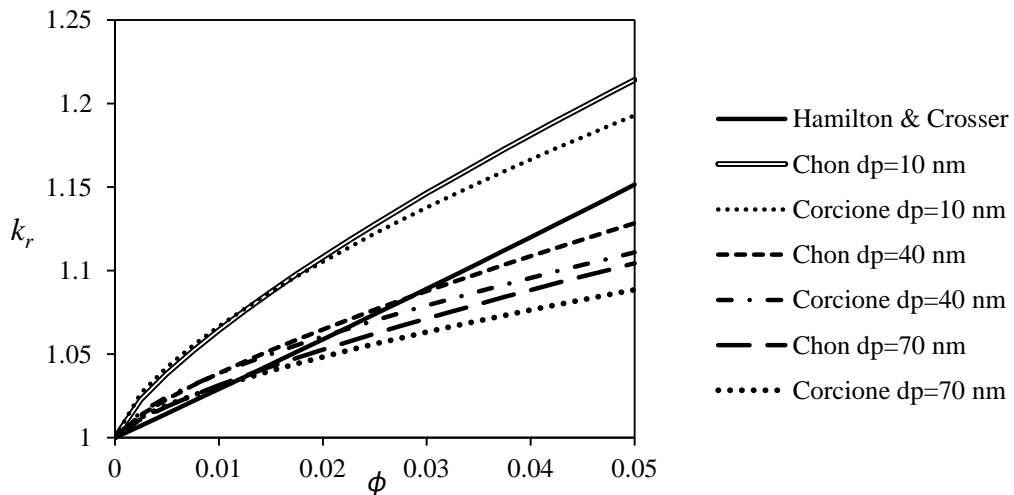


Figure 1 Relative thermal cond. of $\text{Al}_2\text{O}_3/\text{water}$ nanofluids at different particle diameters using the three models [6, 23, 28] at temp. 20 °C as a function of nanopart. vol. frac.

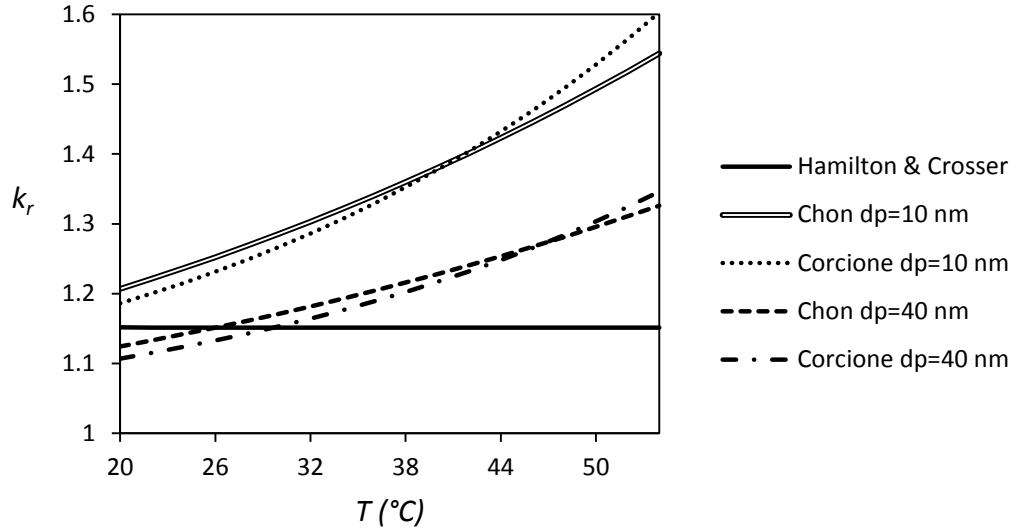


Figure 2 Relative thermal conductivity of Al_2O_3 /water nanofluids using the three models [6, 23, 28] for different particle diameters at volumetric fraction 5% ($\phi=0.05$) as a function of temperature (Eq. 9, 12, 19)

$$\mu_r = \frac{\mu_{nf}}{\mu_f} = 1 + 2.5\phi \quad (21)$$

$$\mu_r = 1 + 7.3\phi + 123\phi^2 \quad (22)$$

Duangthongsuk and Wongwises [7] performed viscosity measurements of TiO_2 (21 nm & 40 nm)/water nanofluids with nanoparticle volumetric fractions 0.2%, 0.6%, 1.0%, 1.5%, and 2.0%. The viscosity increases with decreasing temperature and increasing volumetric fraction. They concluded that Einstein's viscosity model [46] for conventional suspensions severely under predicts the experimental data.

Nguyen et al. [48] made experiments with nanofluids Al_2O_3 (36 and 47 nm)/water in the particle range 1%-9.4% and not surprisingly obtained increasing nanofluid viscosity with increasing nanoparticle concentration. However, contrary to common view, they obtained higher viscosity for 47 nm nanoparticle sized nanofluid at the

same particle volume fraction. More importantly, a hysteresis phenomenon on viscosity occurred for high nanoparticle fraction nanofluids; nanofluid viscosity decreased with increasing temperature up to a critical point but suddenly and sharply increased after the critical point. This situation was observed in the 22-75°C temperature range and the critical point depends on the particle volumetric fraction. This result caused doubts about heat transfer performance of nanofluids because the viscosity increment is not the desired case. Moreover, reliability of the nanofluid may be greatly weakened by this phenomenon since it is very case dependent.

Chandrasekar et al. [5] investigated both thermal conductivity and viscosity of nanofluids as stated above. The nanofluid type is Al₂O₃ (43 nm)/water with nanoparticle volumetric fraction 0.3-5%. The experiments were conducted at room temperature. The viscosity measurement showed that the volumetric fraction increment exponentially increases the viscosity of the nanofluid. The results are consistent with Nguyen et al.'s [48] experimental study. However, Einstein model predicts dramatically lower viscosity values than the results in the experiments. Besides, a newly suggested viscosity model by the researchers that is described in Equation (23) coincides with the experimental results.

$$\mu_r = 1 + c_9 \frac{\phi}{1 - \phi}^{c_{10}} \quad (23)$$

Here, c_9 and c_{10} are empirical constants.

Prasher et al. [49] studied Al₂O₃/PG (propylene glycol) nanofluid with volumetric fractions 0.5% to 3% using variable particle diameters (27, 40, 50 nm). The particle loading increases viscosity of the nanofluid and the results show that increment of diameter of nanoparticles slightly decreases nanofluid viscosity. On the other hand, unlike thermal conductivity, relative viscosity of nanofluid does not change with temperature variation.

Murshed et al. [32] performed experiments on TiO₂ (15 nm)/water and Al₂O₃ (80 nm)/water nanofluid and found higher viscosity values than pure water and increasing

values with volumetric fractions from 1% to 5%. They compared their results with the literature and concluded that the differences among studies are caused by different production techniques of nanofluids and particle clusters.

Vasheghani et al. [50] measured the viscosity of Al₂O₃ (20 nm)/engine oil nanofluid. Experimental setup was a rotational viscometer and they conducted the experiment with only 3% weighted fraction of nanofluids ($\phi = 0.7\%$). Viscosity of the nanofluid is available for the temperature range of 25-75°C and decrease with increasing temperature. Actually, there is a considerable difference between the base fluid and nanofluid viscosity at room temperature. However, the difference disappears with increasing temperature. In addition, they investigated shear stress – shear rate relationship and observed a Newtonian fluid behavior.

In general, each experimental study creates its own empirical correlation or theoretical studies are fitted to experimental results. On the other hand, it is imperative to compose a widely applicable viscosity model because the nanofluid applications may consist infinitely large number of nanofluid types. Corcione [28] made an empirical study using data available in the literature [16, 29, 48, 51-59] for water, ethylene glycol, ethanol and propylene glycol based nanofluids. Because it has a wide application range, particle diameter, particle volumetric concentration, and molecular diameter of base fluid are the affecting parameters. The nanoparticle material effect is neglected. The following Equation shows the viscosity model:

$$\mu_r = 1 - 34.87 \frac{d_f^{0.3}}{d_p} \phi^{1.03} \quad (24)$$

Here, d_f is the molecular diameter of base fluid.

Kumar et al. [60] reviewed theoretical viscosity models based on various knowledge of nanoparticle research. The liquid layering, particle size, particle shape, particle interaction, and dispersion techniques are the key parameters that affect the nanofluid viscosity. Therefore, the composed theoretical studies are based on them.

The estimations of three different models with different nanoparticle sizes and volumetric fractions are investigated.

Figure (3) shows relative viscosity of water based nanofluids with three models, Einstein [46], Maiga [47], and Corcione [28]. Einstein and Maiga are based on only nanoparticle volumetric fraction, hence; particle diameter is not important for them. As seen, there is a significant difference among different sized nanoparticle based nanofluids when they are predicted by Corcione model. Particle diameter greatly alters the relative viscosity.

Einstein [46], K-D [61], Niesen [62] and Bachelor [63] models are classical models and other models were derived by using them.

On the other hand, temperature and nanoparticle material (e.g. Al_2O_3 , CuO) has no effect on viscosity according to the three models, thus; these are all applicable for the common nanoparticle types used in research.

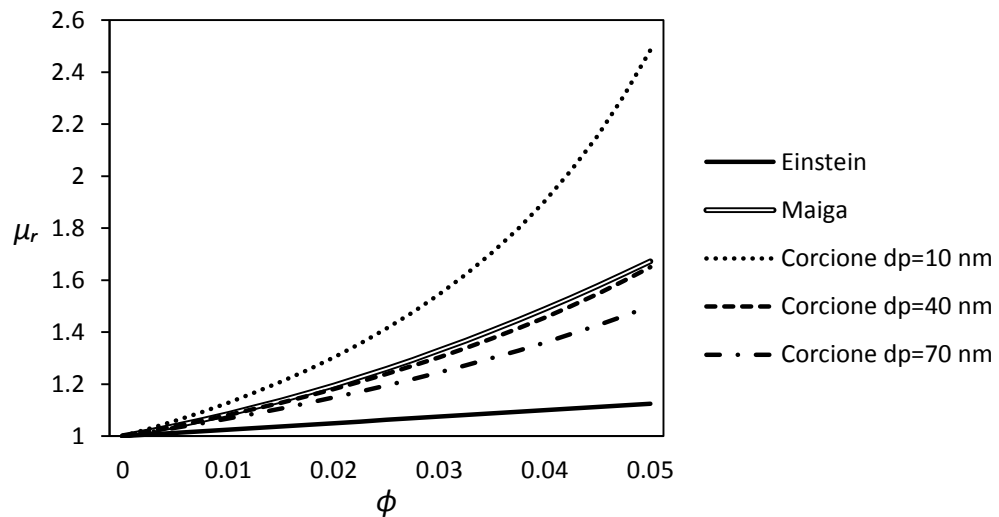


Figure 3 Relative viscosity of water based nanofluids for three different particle diameters using the three models [28, 46, 47] at 20°C as a function of nanoparticle volumetric fraction (Eq. 21, 22, 24).

Finally, it is decided to use Corcione viscosity model when viscosity estimation is required in the current study because of its wide range applicability. Convective heat transfer analyses in the Chapter 4 are not affected by viscosity value, except viscous dissipation investigation (see Section 4.5.5). On the other hand, viscosity estimation is directly related with pumping power required to maintain the nanofluid flow. Therefore, the usage of the suitable model is extremely important when heat transfer and pumping power performance is considered simultaneously as it is done in Chapter 5. In fact, the accurate viscosity prediction is as important as accurate conductivity estimation because the pumping power performance is also as important as heat transfer performance.

2.3. Impact of Nanoparticles

Nanofluid suspensions are generally made from metallic or metal oxide nanoparticles because of their high thermal conductivities. Although the preparation of the nanofluids require great knowledge and effort, this section aims to simply determine the most effective nanoparticles to be used with a base fluid by looking at only thermophysical properties. This section provides as a guide to the types of materials to be used in nanofluid research. Actually, there is no available data in the literature about selection of nanoparticles except practical considerations. However, the theoretical approach is also important because it gives an idea which materials may be beneficial.

Table (2) shows thermophysical properties of common materials, adopted from Incropera's heat transfer textbook [64], used in nanofluid preparation and research. Most researchers focused on thermal conductivity of nanoparticles and nanofluids but density and specific heat have also vital importance in the heat transfer performance of nanofluids as will be explained in Chapter 5. As a first approximation, density, volumetric heat capacity (the product of density and specific heat), and thermal conductivity of the materials are compared by looking over the Table (2). It is concluded that Al_2O_3 , CuO and Cu are the most proper candidates to use in nanofluid heat transfer applications. A more detailed analysis is performed on them by

comparing relative density, relative multiply of density and specific heat, and relative thermal conductivity as follows.

The first issue is the origin point of the nanofluid, thermal conductivity of nanoparticles. It is clearly an advantage to have a high thermal conductivity particle in nanofluid production because it is going to increase heat transfer coefficient of convective heat transfer in nanofluid flow without causing any disorder. Figure (4) demonstrates the difference among water based nanofluids made from different nanoparticles. In the Figure, the relative thermal conductivity is shown, calculated through two models, Hamilton Crosser, a classical model and Corcione, an empirical model based on extensive data. As it is seen, Corcione model with Cu/water nanofluid gives the best result because the relative thermal conductivity of Cu is the highest. Predictions by Hamilton Crosser model give nearly the same values for different nanoparticle types while Corcione predictions give relatively different results. Hamilton Crosser predictions for Al₂O₃ and CuO nanoparticle type nanofluids are given in the same line because the difference cannot be observed in the Figure.

Table 2 Thermophysical Properties of Materials [64] Generally Used in Nanofluid Preparation

Nanopart. Material	ρ_p (kg/m ³)	C_p (J/kg·K)	$(\rho C)_p$ (J/m ³ ·K·10 ⁵)	k_p (W/m·K)
Al	2702	903	24.4	237
Al ₂ O ₃ , sapphire	3970	765	30.4	46
Cu	8933	385	34.4	401
CuO	6500	560	36.4	20
Ag	10500	325	24.7	429
SiC	3160	675	21.3	490
SiO ₂	2400	691	16.6	16
TiO ₂	9110	235	21.4	13
TiO ₂ , polycrystalline	4157	710	29.5	8.4

The second issue is volumetric heat capacity (ρC_p). The higher the volumetric heat capacity, the better the heat transfer performance. This situation may seem ambiguous but explained in Chapter 5, which investigates evaluation of heat transfer performance of nanofluids. In fact, volumetric heat capacity is as important as thermal conductivity of particles. Figure (5) shows relative volumetric heat capacity, which is defined in Equation (25), for three different nanoparticles. CuO/water nanofluid gives the highest value (0.994 for $\phi = 0.05$) but the difference are very small compared to change in other properties. Unfortunately, the relative volumetric heat capacity is always slightly smaller than 1 for water based nanofluids.

$$\rho C_r = \frac{\rho C_{nf}}{\rho C_f} \quad (25)$$

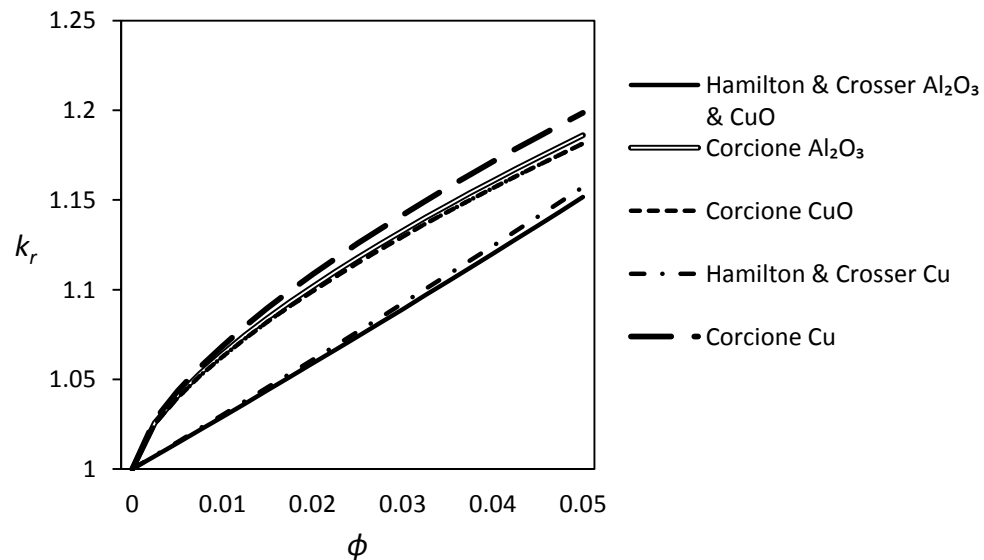


Figure 4 Relative thermal conductivity of water based nanofluids with different nanoparticle types using the two models [23, 28] with particle diameter 10 nm at 20°C as a function of nanoparticle volumetric fraction (Eq. 9, 19).

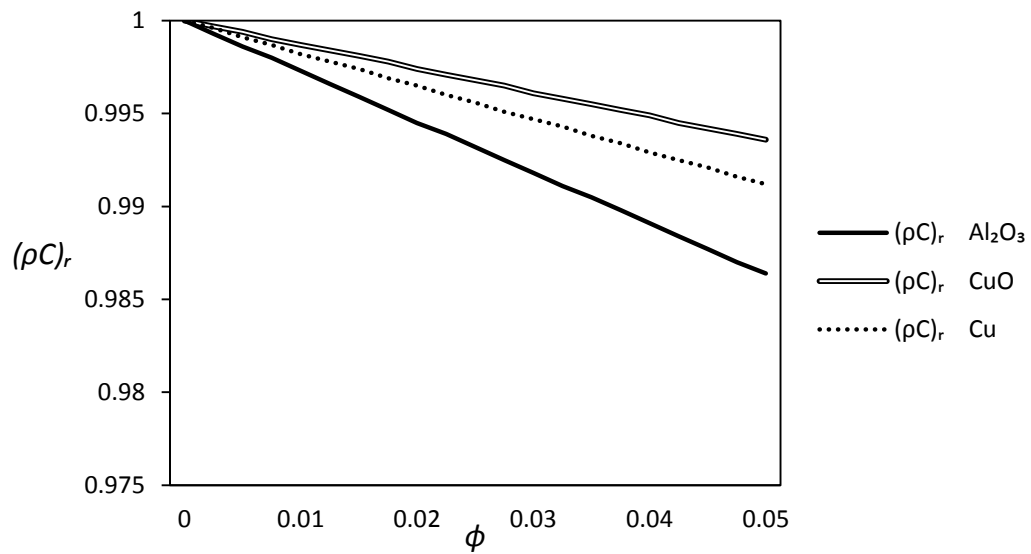


Figure 5 Relative volumetric heat capacity of water based nanofluids with different types of nanoparticles at 20°C as a function of nanoparticle volumetric fraction (Eq. 3, 4, 5, 7)

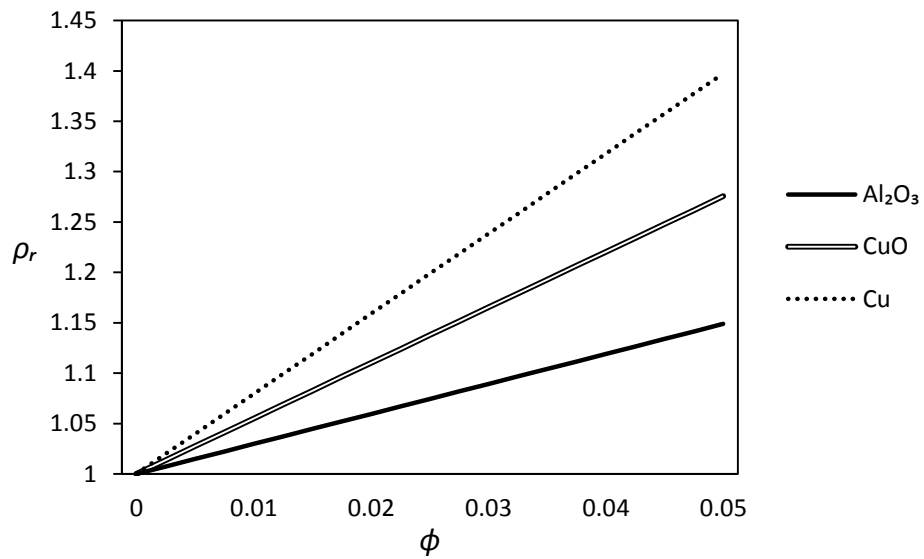


Figure 6 Relative density of water based nanofluids with different types of nanoparticles at 20°C as a function of nanoparticle volumetric fraction (Eq. 3, 5).

The density of the nanoparticle is an important parameter independently because Reynolds number ratio, extracted from the pumping power consideration, which will be described in Chapter 5, depends directly on the relative density. Relative density, presented in Figure (6), is especially important for turbulent flow but it is also important for laminar flow in developing region of convective heat transfer. In the Figure, the variation of relative density for nanofluids prepared with three different nanoparticles with particle volumetric fraction between 0-5% is shown. Cu/water nanofluid gives significantly high values with increasing nanoparticle volumetric fraction.

The Corcione viscosity model, the most reliable one, states that the viscosity of nanofluids is not affected by the nanoparticle material, hence; the viscosity is not discussed in this section.

Once the nanoparticle material is selected, volumetric fraction and size of particles should be considered. There are many parameters that affect heat transfer performance; such as thermophysical properties and non-conventional convective heat transfer behavior of nanofluids, thus; it is not easy to reach a solid conclusion only looking at thermophysical properties even if they are predicted accurately. Instead, optimum values should be determined first theoretically, then; they should be checked by experiments as will be discussed in following chapters. Actually, the optimum values for Cu/water and Cu/Ethylene Glycol nanofluids are obtained in Chapter 5. On the other, there is no significant difference between different types of nanoparticle material selections according to Chapter 5.

2.4. Impact of Base Fluid

In this section, relative enhancements on thermophysical properties of heat transfer base fluids by adding nanoparticles to them are compared. For example, relative densities of water based and ethylene glycol based nanofluids are compared by using Cu as the nanoparticle material. Absolute thermophysical properties or heat transfer performances of different nanofluids are not considered to obtain an objective result.

As an exception, Prandtl number of the base fluid plays a crucial role in nanofluid heat transfer performance as it will be described in Chapter 5.

A heat transfer application system requires one type of fluid because of several reasons; such as high thermal performance, non-corrosiveness, low freezing or boiling point. Therefore, it may not be suitable to replace the base fluid with another one. However, once one type of fluid is selected; its performance can be increased by adding nanoparticles in it.

A first approximation can be made by looking at only thermophysical properties of base fluids and nanofluids. Hence, a decision can be made on which system is more suitable for the usage of nanofluids with its own base fluid.

Table (3) denotes thermophysical properties, molecular diameter and freezing point temperature of common heat transfer base fluids, which are important in nanofluid heat transfer phenomena. Unlike in the case of material selection, it is not straight forward which property should be kept lower or higher. Therefore, this is demonstrated in the Table pointing up or down for better heat transfer enhancement. While deciding the direction of the arrows, relative increment or decrement on nanofluid properties is observed. For example, it is investigated the effect of addition of nanoparticle to water on the properties. Then, the enhancement results can be compared with ethylene glycol's (EG) results. It is more advantageous to use the nanoparticles in base fluids which provides higher relative enhancement. In other words, a base fluid that agrees with given tendencies gives higher enhancement by adding nanoparticles than other fluids. For instance, engine oil (EO) properties have lower capability than water properties in terms of heat transfer but enhancement with nanoparticles in EO gives higher enhancement than water based nanofluids. On the other hand, it is not stated that this newly found fluid is the best heat transfer fluid.

Desired tendency of Prandtl number is increment. This means a heat transfer fluid, which has a higher Prandtl number takes advantage of nanofluid usage in its system more significantly than fluids with lower Prandtl number. Namely, if a fluid has a

Table 3 Selected Base Fluid Properties Affecting Nanofluid Heat Transfer at 20°C [64] with Desired Tendency for Better Enhancement

Fluid Type	Pr	C (J/kg·K)	ρ (kg/m ³)	k (W/m·K)	μ (N·s/m ²)	$\sim d_f$ (nm)	T _{fr} (K)
Desired Tendency	↑	↓	↓	↓	↓	↓	↓
Water	7.00	4184	998	0.599	0.10·10 ⁻³	0.38	273
EG(ethylene glycol)	209	2383	1117	0.250	0.22·10 ⁻¹	0.56	261
r-134a	3.51	1405	1225	0.083	0.21·10 ⁻³	0.64	247
EO (engine oil)	10863	1881	888	0.145	0.84	1.17	-

Prandtl number higher than any other fluid, it has more potential about nanofluid heat transfer enhancement.

The same analogy is valid for other parameters in the Table (3) with reverse tendency. It means a lower specific heat, density, thermal conductivity, viscosity, molecular diameter, and freezing temperature fluid experiences a better heat transfer enhancement by adding nanoparticles in it. The desired tendency conclusion for conductivity, viscosity, molecular diameter and freezing temperature is made by considering Corcione models on thermal conductivity and viscosity in Equations (19) and (24).

According to Corcione model in Equation (19), relative thermal conductivity of the nanofluid increases with increment in density of base fluid because of dependence of Brownian Reynolds number, $Re_{B,2}$, on density but it is neglected because it is smaller compared to relative density increment with decreasing base fluid density. Relative thermal conductivity also increases with decreasing base fluid conductivity, freezing temperature, and viscosity because of “ $k_p/k_f^{0.03}$ ”, “ T/T_{fr}^{10} ”, and “ $Re_{B,2}$ ” terms, in Equation (19) respectively. Figure (7) shows nanofluids with different base fluids with addition of Cu particles. Two thermal conductivity models, Hamilton-Crosser and Corcione, are presented and it is seen that H-C model does not give different results for each nanofluid while Corcione model does. Ethylene glycol (EG) has the

highest relative conductivity. In the Figure, the solid line corresponds to Hamilton Crosser model for all fluids in shown in Table 3.

Viscosity model shown in Equation (24) states that base fluid average molecular diameter should be smaller for lower relative viscosity. However, it is important to note that these models were fitted to water and ethylene glycol based nanofluids. Their validity is not known for other types of base fluids and it is not possible to check this because of lack of experimental data on this issue in the literature. Fig. (8) presents the results for relative viscosity of water and EG obtained through the Corcione model (Eq. 24).

Relative density of nanofluids prepared with different base fluids is demonstrated in Figure (9). It can be observed that there is quite significant difference among nanofluids as in material selection case.

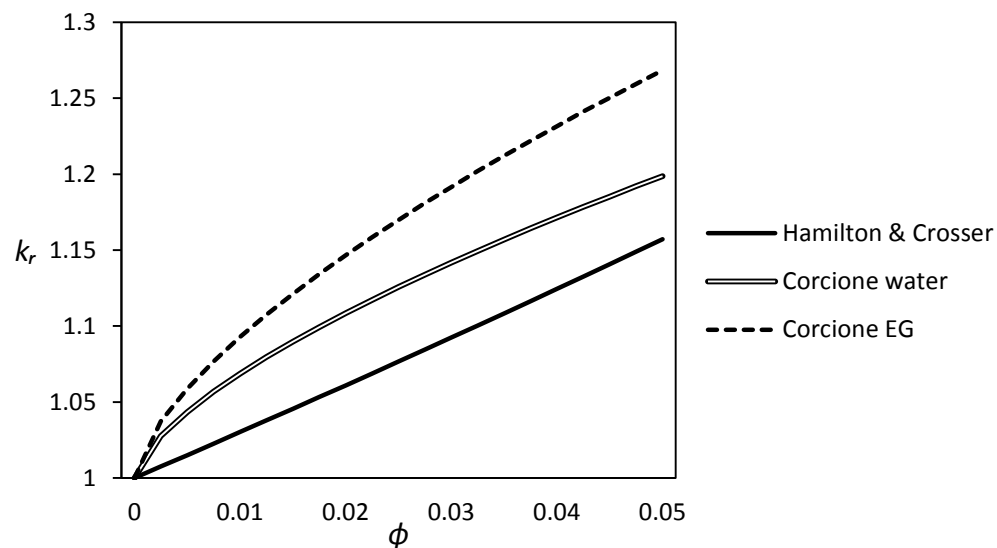


Figure 7 Relative thermal conductivities of Cu (10 nm) nanofluids with different base fluids at 20°C, with the two models [23, 28] as a function of nanoparticle volumetric fraction (Eq. 9, 19).

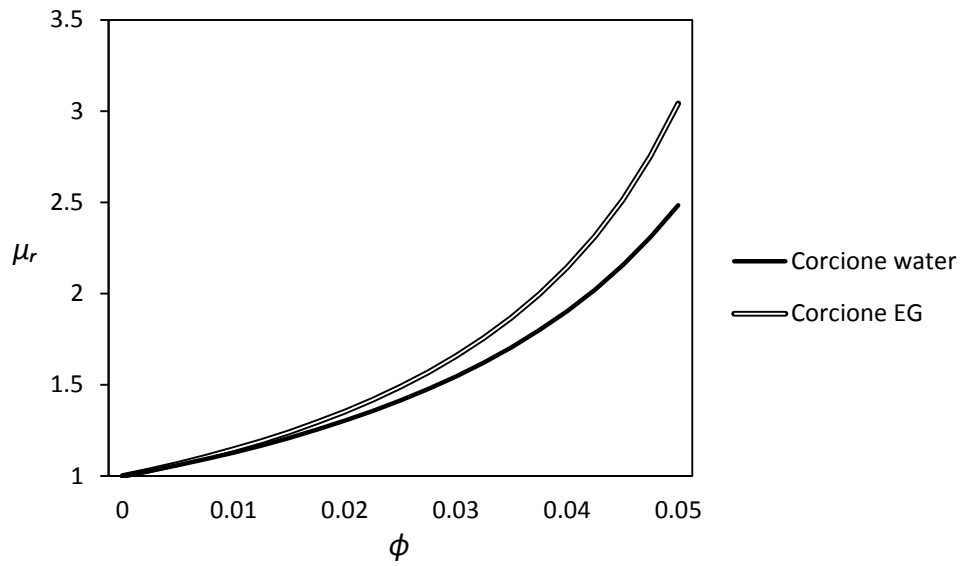


Figure 8 Relative viscosity of Cu (10 nm) nanoparticle nanofluids with different base fluids at 20°C as a function of nanoparticle volumetric fraction (Eq. 24)

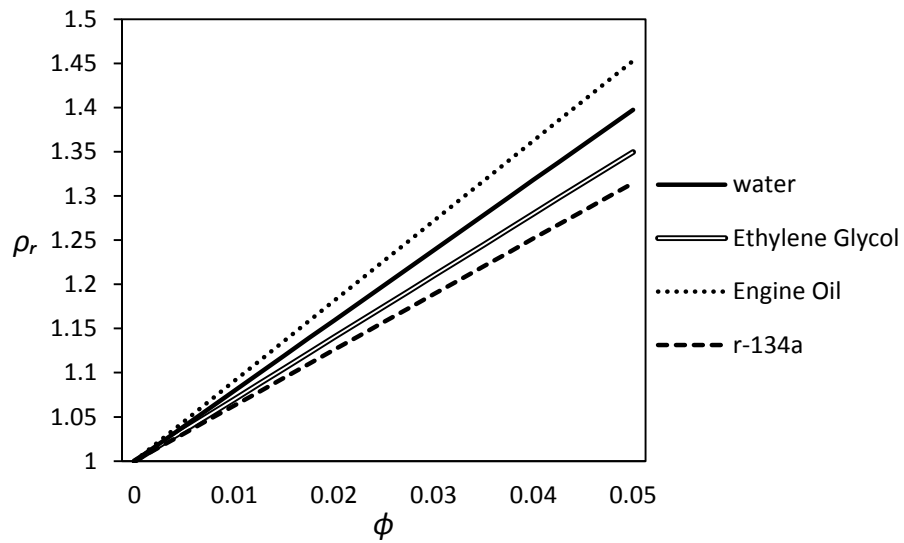


Figure 9 Relative density of Cu (10 nm) nanoparticle nanofluids with different base fluids at 20°C as a function of nanoparticle volumetric fraction (Eq. 3, 5).

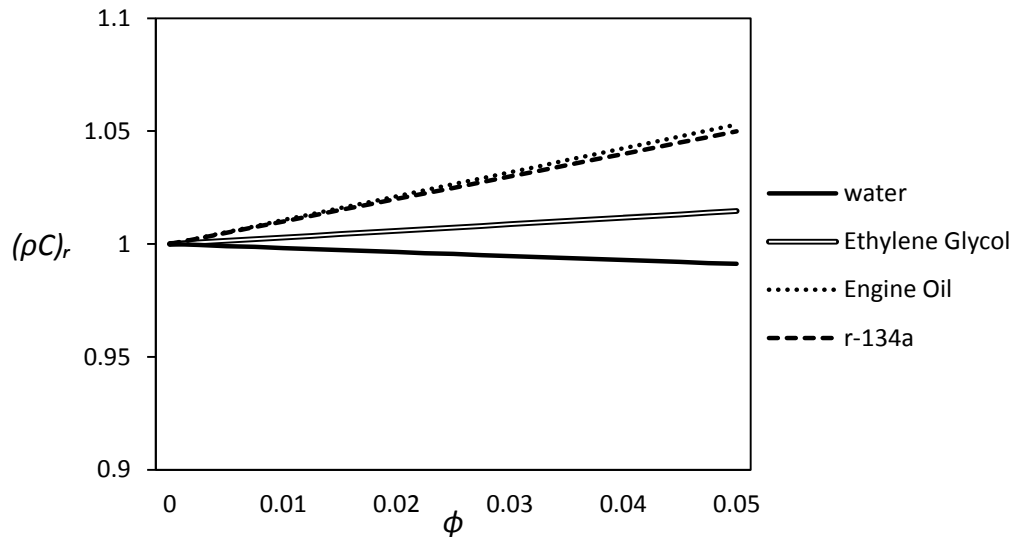


Figure 10 Relative volumetric heat capacity of Cu (10nm) nanofluids with different base fluids at 20°C as a function of nanopart. vol. frac. (Eq. 3, 4, 5, 7).

Relative volumetric heat capacity of nanofluids is shown in Figure (10) for four different base fluids. It can be seen that water is the worst in this case. Other fluid values have increasing relative volumetric heat capacity with the addition of nanoparticles, while water values decrease but there is a small decrement in water's case. However, EO and r-134a values increase up to 5%.

As it will be described in Chapter 5, base fluid Prandtl number is also a very important parameter for heat transfer enhancement in nanofluids. Here, Prandtl number is the base fluid Prandtl number (not relative Prandtl number) and it affects directly the nanofluid heat transfer performance. Higher Prandtl number means higher heat transfer performance while taking other parameters as constant. Figure (11) shows temperature dependent Prandtl numbers of base fluids. In the Figure, it is shown that Prandtl number of EO is significantly larger than other base fluids and its temperature dependency is also stronger. EG has a moderate trend compared to other fluids while water and r-134a have lower Prandtl numbers and temperature dependency. Chapter 5 presents the related descriptions on the affecting parameters and explains why high

Prandtl number fluids have more potential on performance enhancement with nanofluids.

In conclusion, it can be said that base fluid parameters may significantly alter heat transfer performance of nanofluids. However, it is not easy to determine which property is the most important one. In order to make a better decision, a detailed analysis should be performed as it will be done in Chapters 4 and 5.

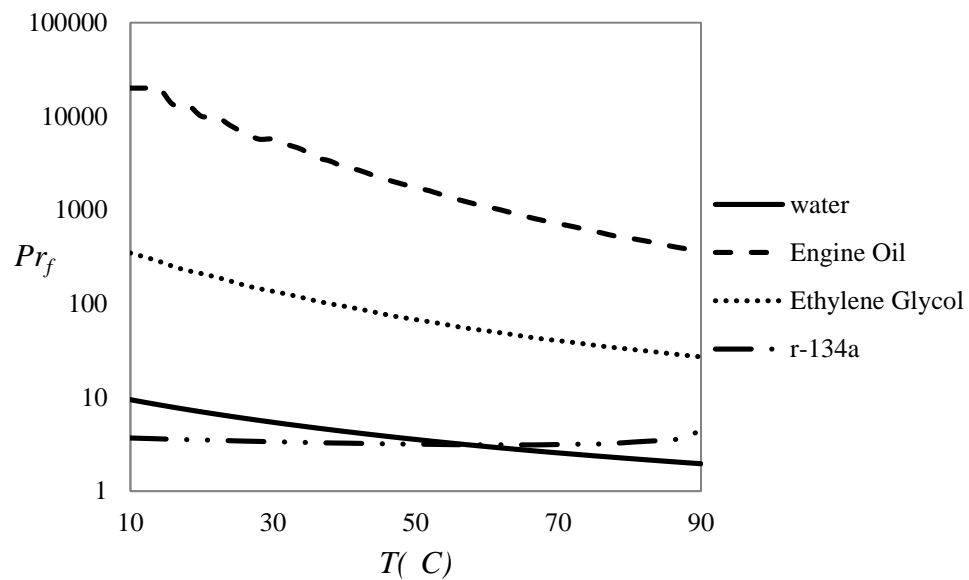


Figure 11 Prandtl numbers of the selected base fluids as a func. of temp.

CHAPTER 3

CONVECTIVE HEAT TRANSFER OF NANOFLUIDS

3.1. Introduction

Forced convective heat transfer is preferred and used in heat transfer applications because of its controllability and applicability. Since it has been widely used in order to obtain desired heat transfer, investigations on prediction of it has also been studied extensively. There are many theoretical and empirical approaches which cover laminar and turbulent flow and heat transfer phenomena.

Empirical studies usually result in individual correlations, which predict different types of flows on different geometries or other boundary conditions. Theoretical studies also predict heat transfer of different cases by improving or expanding a theoretical idea. Governing differential equations were extracted by researches and their solutions are achieved by analytical or numerical methods.

The prediction of convective heat transfer has a vital importance because it directly affects design and operational conditions. It means that the better the prediction, the higher the heat transfer performance. Although conventional heat transfer applications are accurately predicted by heat transfer correlations or solutions to differential equations, there are still debates on estimation of relatively new subjects such as convective heat transfer of nanofluids.

The literature states generally higher heat transfer coefficient and Nusselt number for convective nanofluid heat transfer than predicted by conventional theories but there are also contradictions in experimental results of nanofluids, unfortunately.

The original study about estimation of the nanofluid convective heat transfer is presented in this Chapter after the literature survey. The theory behind the nanofluid convective heat transfer is investigated and a model using numerical methods is suggested which will be used in Chapter 4.

3.2. Survey of Experimental, Theoretical and Numerical Studies in Literature

3.2.1. Experimental Studies

Forced convection analysis of nanofluids in a circular pipe has been widely investigated by researches.

Pak and Cho [16] studied nanofluid flow and heat transfer with constant heat flux boundary condition using Al_2O_3 (13nm)/water and TiO_2 (27nm)/water nanofluids in a range of nanoparticle concentration 1%-10%. The flow was in the turbulent flow regime with Reynolds number 10^4 - 10^5 . In addition to heat transfer and pressure drop experiments, viscosities of these fluids were measured and it was found that the viscosity of 10% volumetric fraction of Al_2O_3 /water nanofluid is 200 times larger than the viscosity of pure water. Pressure drop measurements in the flow showed that the nanofluid flow is similar to single phase fluid flow because it provides the same friction factor with Blasius correlation for friction factor [65], thus; the pumping power increment is caused by only viscosity increment. Heat transfer coefficient and Nusselt number was higher than pure water in the constant Reynolds number case and the maximum heat transfer coefficient enhancement was 75% with 1.34% volumetric fraction of Al_2O_3 /water nanofluid. On the other hand, a heat transfer coefficient and Nusselt number decrement was observed at constant velocity case because increment in the viscosity decreased the Reynolds number. The authors used larger sized nanoparticles to overcome the viscosity increment appearing with the usage of very small nanoparticles.

Li and Xuan [66] measured the forced convective heat transfer coefficient of CuO (d_p = nanoparticle diameter < 100nm) /water nanofluids under laminar and turbulent flow regime with volumetric fractions from 0.3% to 2%. The Reynolds number range for the experiments was 800-25000 and the boundary condition was constant wall heat flux. The results were presented in the constant Reynolds number case and constant mean velocity case and heat transfer enhancement was observed for both cases. The maximum enhancement was 60% for 2% volumetric fraction of nanofluid and it was said that an abnormal heat transfer enhancement took place. This means that there are other mechanisms than thermal conductivity enhancement that affects heat transfer coefficient positively.

Xuan and Li [67] made experiments in turbulent flow with CuO/water nanofluids with nanoparticle concentration range 0.3%-3%. Average velocity of the fluid was taken as constant and analyses were made between Reynolds number 10000 and 25000. Nusselt number and heat transfer increment was observed for both constant velocity and constant Reynolds number cases. It was noted that increasing the nanoparticle concentration increases the heat transfer enhancement and the maximum case (3% volumetric fraction) gives 60% enhancement. The important point was that the enhancement with nanofluids cannot be predicted by conventional turbulent flow heat transfer correlations such as Dittus-Boelter [68]. It was stated that the abnormal heat transfer is caused by thermal dispersion. In addition, pressure drop of nanofluid flow was measured and it was concluded that there is no additional pressure drop for constant Reynolds number.

Wen and Ding [69] investigated laminar flow heat transfer and they also found that nanoparticle concentration increment increases the heat transfer enhancement at constant Reynolds number. They obtained a maximum of 47% heat transfer coefficient enhancement with 1.6% nanoparticle concentration. They have concluded that the extension of thermal development of the flow and particle migration due to force on the particles provide an abnormal heat transfer enhancement that cannot be explained with Graetz solution [86] for laminar flow.

Heris et al. [70] studied heat transfer enhancement in laminar flow experimentally with constant wall temperature boundary condition unlike the previous researchers. $\text{Al}_2\text{O}_3/\text{water}$ (20nm) type nanofluid was the fluid at nanoparticle concentrations from 0.2% to 2.5% and results were presented at constant Peclet numbers. Maximum enhancement, 41%, at 2.5% nanoparticle concentration was observed and extra enhancement in addition to conductivity was committed to thermal dispersion, similar to Xuan and Li [67].

Rea et al. [71] studied Alumina/water (50nm) and Zirconia/water (50nm) nanofluids in the entrance and fully developed region of laminar flow. The nanoparticle concentrations of Alumina and Zirconia nanofluids were 0.6% to 6% and 0.32% to 1.32%, respectively. The experimental data were obtained in constant velocity case and Nusselt number and heat transfer enhancement figures were provided. It was noted that there is no abnormal heat transfer enhancement for both entrance and fully developed regions, that is, the traditional correlations and analytical solutions for pure fluids can be implemented to predict heat transfer phenomena of these nanofluids. The enhancement resulted from the thermophysical property changes and it depends on the density, specific heat and conductivity for the entrance region and conductivity for the fully developed region. The maximum enhancement was found as 27% for Alumina and the Zirconia/water nanofluid enhancement was only 3%. In addition, it was emphasized that pressure drop is proportional with the viscosity and it is 7.2 times higher than that of water for the maximum enhancement case. It is important to note that the working temperature range for this study was maximum 15°C and this may cause to see no abnormal heat transfer enhancement. The Nusselt number results of this study are compared with the current study in Chapter 4.

Anoop et al. [72] made an experimental study on Alumina/water nanofluid in the entrance and fully developed region of laminar flow. They investigated the heat transfer enhancement at constant Reynolds number and the effect of the size of nanoparticles which compose the nanofluids. They used 45 nm and 150 nm spherical particles, and they prepared mixtures with weighted fractions from 1 wt% to 6 wt%. In contrast to other researchers who reported nanofluid concentrations in terms of

volumetric fraction, Anoop et al. reported weighted fractions. The maximum heat transfer coefficient enhancement, 31%, was at a concentration of 4 wt% and with 50 nm nanoparticles in the entrance region. Finally, they proposed a correlation that depends on the particle size and volumetric concentration, for the entrance and fully developed region of laminar flow. However, it is a very case dependent correlation because only 6 different types of nanofluid were used to propose it.

Dunangthongsuk and Wongwises [73] studied TiO₂/water (21nm) nanofluids in the turbulent flow regime with volumetric fractions from 0.2% to 2%. Before conducting the convective heat transfer experiment, they measured the thermal conductivity and the viscosity of the nanofluids and found similar results with Yu and Choi model [44] for conductivity and Wang et al. model [52] for viscosity. An approximate constant wall heat flux boundary condition was applied with a double pipe heat exchanger for heat transfer experiments. They found maximum 32% enhancement with 1% concentration in the 3000-18000 Reynolds number interval with constant Reynolds number comparison. Thus, unlike the other experiments, there was no systematic increase with increasing concentration. Conversely, there was a heat transfer decrement for 2% nanoparticle concentration. It was stated that this may have been caused by the increment in the viscosity and particle agglomeration at high nanoparticle concentration. Furthermore, the traditional friction factor correlations were reasonable for pressure drop calculation of nanofluids but they suggested a more accurate correlation for nanofluids as a function of Reynolds number and nanoparticle concentration.

Kim et al. [74] experimentally investigated Al₂O₃ (35 nm) /water and amorphous carbonic (20 nm)/water nanofluids with 3% nanoparticle volumetric fractions. Constant wall heat flux boundary condition was applied for both laminar and turbulent flow regimes. The results showed that turbulent flow experiences more heat transfer coefficient enhancement than laminar flow and Al₂O₃ (35 nm) /water nanofluid has more enhancement than amorphous carbonic (20 nm)/water. It was noted that there exists abnormal heat transfer enhancement which means heat transfer coefficient increment is higher than thermal conductivity enhancement only. Reynolds number

was selected as the comparison parameter. The heat transfer coefficient results of this study are compared with the current study in Chapter 4.

Lai et al. [75] conducted experiments on Al_2O_3 (20 nm) /water nanofluids in the laminar flow regime. Reynolds number interval for the experiments was 30-300 and the comparison criterion was selected as the constant volumetric flow rate (or constant velocity). For the nanoparticle concentrations from 0.5% to 1%, the maximum enhancement was found for 1% concentration nanofluid. Moreover, it was mentioned that the enhancement increases with increasing velocity. Thermal conductivity and Prandtl number increment increases the heat transfer coefficient but there is still an additional unexplained heat transfer enhancement. They attributed the abnormal enhancement to flattened velocity profile suggested by Mills and Snabre [76], who studied the nanoparticle distribution in nanofluids.

Chandrasekar et al. [77] carried out experimental study on heat transfer behavior of Al_2O_3 /water nanofluid under laminar flow with and without wire coil inserts. 0.1% volume concentration of the nanofluid was used in the Reynolds number range 600 – 2275 and heat transfer enhancement increase with Reynolds number was observed. Moreover, the enhancement was higher with wire coil inserts.

Chandrasekar et al. [36] reviewed the literature on experimental studies of convective nanofluid heat transfer. They presented experiments of 18 straight pipe and 12 modified tube geometries and stated that the experimental researchers generally claim abnormal heat transfer enhancement due to dispersion, particle migration, turbulence intensification, and Brownian diffusion.

Conclusively, experimental researchers found generally higher Nusselt number compared to the pure fluid, at a constant Reynolds number or velocity. This additional heat transfer enhancement beyond that of thermal conductivity may be caused by any other mechanisms that do not exist in conventional fluid flows; such as thermophoresis, thermal dispersion or variable thermal conductivity. Slip flow of nanoparticles in nanofluid flow provide enhanced heat transfer by increasing the Nusselt number.

The results of Kim et al.'s [74] and Rea et al.'s [71] experimental studies are compared with the current study in Section 2 of Chapter 4.

3.2.2. Theoretical Studies and Empirical Correlations

Theoretical studies to estimate the abnormal enhancement in convective nanofluid heat transfer exist in the literature. The researchers proposed several mechanisms to provide an explanation to this abnormal enhancement and some of them proposed new correlations or numerical methods to estimate nanofluid heat transfer phenomena.

Pak and Cho [16] proposed a correlation from their experiments for 0-3% volumetric fraction Cu/water nanofluids in the 10^4 - 10^5 Reynolds number range. They did not take into account the particle size, volumetric fraction and type. It is considered that the following correlation represents a very narrow portion of the nanofluid heat transfer phenomena.

$$Nu_{nf} = 0.021Re_{nf}^{0.8}Pr_{nf}^{0.5} \quad (26)$$

In this equation, Re_{nf} is the Reynolds number and Pr_{nf} is the Prandtl number of the nanofluid, defined as:

$$Re_{nf} = \frac{v_m \cdot D \cdot \rho_{nf}}{\mu_{nf}} \quad (27)$$

$$Pr_{nf} = \frac{\mu_{nf} C_{nf}}{k_{nf}} \quad (28)$$

Here, v_m is the mean fluid velocity in channel, and D is the pipe diameter.

Xuan and Roetzel [78] developed a heat transfer correlation for nanofluids because they noted that the heat transfer phenomena of nanofluids cannot be explained by conventional theories developed for single phase heat transfer. From the experimental studies, it was concluded that the Nusselt number for the nanofluid flow depends on the Reynolds number, Prandtl number, thermal conductivity, specific heat and

densities of the base fluid and particle, nanoparticle volumetric fraction, particle size and shape, and flow structure as stated below:

$$Nu_{nf} = f(Re_{nf}, Pr_{nf}, \frac{k_p}{k_f}, \frac{\rho C_p}{\rho C_f}, \phi, d_p, \text{shape of part.}, \text{flow structure}) \quad (29)$$

It was considered that the abnormal heat transfer enhancement excluding the thermal conductivity enhancement was caused by thermal dispersion of the nanoparticles. Thermal dispersion is the chaotic movement of the solid particles in the fluid matrix. Consequently, a thermal dispersion model which explains the abnormal heat transfer was suggested as below:

$$k_d = c_{11} \rho C_{nf} v d_p r_0 \phi \quad (30)$$

Here, k_d , c_{11} , v , r_0 are thermal dispersion conductivity to be added to thermal conductivity, empirical constant, local or mean velocity depending on the modeling of heat transfer and radius of the pipe, respectively. This definition takes place near the thermal conductivity in the differential equation of energy.

Li and Xuan [66] suggested new correlations in the laminar and turbulent flow regime for Cu/water nanofluid, which predicts the Nusselt number depending on the particle conductivity, volumetric fraction and particle diameter including flow and base fluid properties. It is beneficial to present a correlation to estimate the nanofluid heat transfer because a comparison with the other experiments can be easily made and the correlation can be improved for all cases of nanofluid flow and heat transfer using the experimental data. On the other hand, there was no thermophysical property measurement or estimation in that study; thus, the validity of the correlations may be narrow because of usage of different thermal conductivity and viscosity models in different studies. The correlations suggested for laminar and turbulent flow are presented below, respectively.

$$Nu_{nf} = 0.4328 \left(1 + 11.285 \phi^{0.754} Pe_d^{0.218} Re_{nf}^{0.333} Pr_{nf}^{0.4} \right) \quad (31)$$

$$Nu_{nf} = 0.0059 \left(1 + 11.285\phi^{0.6886} Pe_d^{0.001} Re_{nf}^{0.9238} Pr_{nf}^{0.4} \right) \quad (32)$$

$$Pe_d = \frac{u_m d_p}{\alpha_{nf}} \quad (33)$$

Here, Pe_d is the nanoparticle Peclet number.

Anoop et al. [72] proposed a correlation using their experimental results for Al_2O_3 nanofluids. The conditions were constant wall heat flux, laminar flow and thermally developing region. The correlation shown below takes particle diameter effect into account as well. The correlation is based on thermal dispersion and migration of nanoparticles.

$$Nu_{nf,x} = 4.36 + c_{12} x^{+c_{13}} \left(1 + \phi^{c_{14}} \exp^{-c_{15}x^{+}} \right) \left(1 + c_{16} d_p/100 \right)^{-c_{17}} \quad (34)$$

Here, c_{12} , c_{13} , c_{14} , c_{15} , c_{16} and c_{17} are experimental constants. x^{+} is equal to $x/D \cdot Re \cdot Pr$ where x is the distance in the axial direction, D is pipe diameter, Re is Reynolds number and Pr is Prandtl number.

Buongiorno [18] prepared a comprehensive study on nanofluid convective heat transfer which shows the nanoparticle dependence of turbulence and reasons of particle migration. Firstly, it was stated that intensification of turbulence by nanoparticles in a base fluid is not possible by making a turbulent scale analysis. In a cylindrical channel, large turbulent eddies are on the order of the diameter of the pipe and according to Kolmogorov's scaling laws [79], nanoparticles are carried by the turbulent eddies. It means that there is no relative velocity of particles in the fluid, which causes turbulence intensification.

Secondly, seven possible reasons of particle migration which cause relative (on slip) velocity between a particle and the fluid were discussed and an order of magnitude analysis for each of them was performed. Five of these effects, inertia, diffusiophoresis, magnus, fluid drainage, and gravity were due to several reasons (see [18] for detail). On the other hand, two mechanisms, Brownian diffusion and

thermophoresis were found effective when the turbulent eddies are absent (in laminar flow). The conclusion from this study was the importance of these effects and solution method of governing equations. It was mentioned that continuity equation for the nanofluid, continuity equation for the nanoparticles, and momentum and energy equations should be solved as coupled by including these two additional effects in order to reach a reliable result.

The resultant situation from the suggestions of Buongiorno is to solve these equations by taking the thermophysical properties, especially thermal conductivity and viscosity as variable with temperature because of the temperature dependency of nanofluid property and thermophoresis effect.

Additionally, nanofluid heat transfer enhancement in turbulent flow was explained by thermophoresis and temperature gradient effect on nanofluid properties in the laminar sublayer. The following equation adapted from the Gnielinski correlation [80], was proposed for turbulent flow heat transfer.

$$Nu_{nf} = \frac{f/8 \operatorname{Re}_{nf} - 1000 \operatorname{Pr}_{nf}}{1 + \delta_v^+ f/8^{1/2} \operatorname{Pr}_v^{2/3} - 1} \quad (35)$$

where δ_v^+ is dimensionless thickness of laminar sublayer and Pr_v is Prandtl number in laminar sublayer.

Sarkar [81] reviewed correlations of convective heat transfer with nanofluids. The study concluded that friction factor of nanofluids are closely predicted by conventional theories while their heat transfer coefficient cannot be predicted in a similar approach. The mechanisms behind nanofluid heat transfer enhancement should be determined and a comprehensive correlation which covers all cases of nanofluids should be created.

Kakaç and Pramuanjaroenkij [82] reviewed both experimental and theoretical studies convective heat transfer of nanofluids. The most of the experimental studies stated there is abnormal heat transfer enhancement which cannot be explained by only

enhanced thermal conductivity of nanofluids. The aim of the theoretical studies was to estimate experimental studies accurately. The authors extended thermal dispersion theory and defined an apparent thermal diffusivity in the energy equation of nanofluids. The definition was composed using the thermal diffusivity of the fluid and additional diffusivity coming from thermal dispersion in the flow.

3.2.3. Numerical Studies

Maiga et al. [46] numerically investigated $\text{Al}_2\text{O}_3/\text{water}$ and $\text{Al}_2\text{O}_3/\text{EG}$ nanofluids in the nanoparticle volumetric fraction range 1-10% in both laminar and turbulent flow using a straight long pipe. It was assumed that the base fluid and nanoparticles are perfectly mixed and can be treated as a mixture. This approach was called as single phase approach in the literature. After implementing thermophysical properties of nanofluids to fundamental equations, the results showed that the nanofluid heat transfer enhancement increases with volumetric fraction of nanoparticles and along the channel. In addition, the enhancement was more dependent on Reynolds number in turbulent flow and increases with increasing Reynolds number. Finally, $\text{Al}_2\text{O}_3/\text{EG}$ enhancement was found to be higher than $\text{Al}_2\text{O}_3/\text{water}$ nanofluid enhancement.

Maiga et al. [83] extended their investigation on nanofluid heat transfer with the same nanofluids but two different geometries. The first geometry was a uniformly heated straight long pipe and the second was radial channel between heated disks. Similar results found in the previous study were obtained. The volumetric fraction of the nanoparticles was the key parameter in heat transfer enhancement. The higher viscosity of nanofluids was mentioned and possible practical limitations of higher volumetric fraction were noted.

Raisee and Moghaddami [84] studied both constant wall heat flux and constant wall temperature boundary conditions in laminar flow for nanofluid heat transfer. They used two different thermal conductivity and viscosity models where one set was traditional and the other was Brownian motion based models. Fraction of nanoparticles increases heat transfer enhancement but the results were different for two different cases. Along the straight channel, heat transfer enhancement increased

along the channel by using the Brownian based models but decreased by using conventional type models. This was caused by elevated temperature, which causes higher thermal conductivity for the Brownian motion based model. Their approach was also the single phase approach.

Bianco et al. [85] studied heat transfer phenomena in nanofluid flow in circular tube with laminar flow, numerically. Both single and two phase approaches were investigated using a numerical method. Single phase is the direct application of momentum and energy equations. On the other hand, two phase approach takes into account interaction between the base fluid and nanoparticles. Actually, there are numerous effects that influence fluid flow and heat transfer in different order of magnitudes for various types of flows. In this study, two phase approach was based on forces that are created by rotation, Brownian and thermophoretic effects. A comparison between the results of single and two phase approaches was made. It was mentioned that there exists a slight difference and two phase approach gives higher values. Heat transfer coefficient increment with increasing volumetric fraction was observed for both situations. The difference between the two approaches is smaller for higher nanoparticle volumetric fractions.

3.3. Modeling of the Nanofluid Convective Heat Transfer in a Pipe

According to literature, and as mentioned in the previous section, there are two ways of modeling convective heat transfer of nanofluids; these are single phase modeling and two phase modeling. Single phase modeling assumes base fluid and nanoparticles mix homogeneously, there is no additional mechanism to contribute to heat transfer other than existing mechanisms for pure fluids. Two phase modeling states that there are other mechanisms caused by the relative motion between the base fluid and the nanoparticles; such as thermophoresis and thermal dispersion.

In the current study, single phase modeling of the convective heat transfer of nanofluid is performed. However, there are still several differences from conventional theories or correlations used to estimate convective heat transfer, which may affect heat transfer performance of nanofluids. In addition, the single phase modeling is

relatively simpler approach and there is not too much difference between the two approaches especially for higher nanoparticle volumetric fractions as used in the current study according to Bianco et al. [85]. When the literature survey of thermophysical properties and convective heat transfer sections are investigated, the most important issues observed are the followings.

- i) Relative viscosity ($\mu_r = \mu_{nf}/\mu_f$), density, and specific heat of nanofluid nearly does not change with temperature,
- ii) Relative thermal conductivity of nanofluids significantly changes with temperature,
- iii) Brownian motion of nanoparticles affects nanofluid heat transfer phenomenon.

In light of this information, modeling of forced convection heat transfer of nanofluids in a cylindrical pipe is performed with fundamental governing equations using numerical methods as an original study, in the current work.

Since a complete understanding of the enhanced heat transfer of nanofluids is aimed, geometry of the problem should be as simple as possible so that fundamental procedures can be applied and any parameter that provides heat transfer enhancement can easily be recognized. Therefore, a straight pipe is the most proper instrument for this study.

Figure (12) describes the geometry of the problem used in the numerical work. This is a pipe which has diameter D and length L . The flow goes through the pipe from left to right. Heating of the pipe starts just after the flow becomes hydrodynamically fully developed. Boundary condition of the wall is applied in two ways: first is constant wall temperature (T_w) and second is constant wall heat flux (q_w''). “ x ” is axial and “ r ” is radial direction while “ v ” represents the local velocity of fluid.

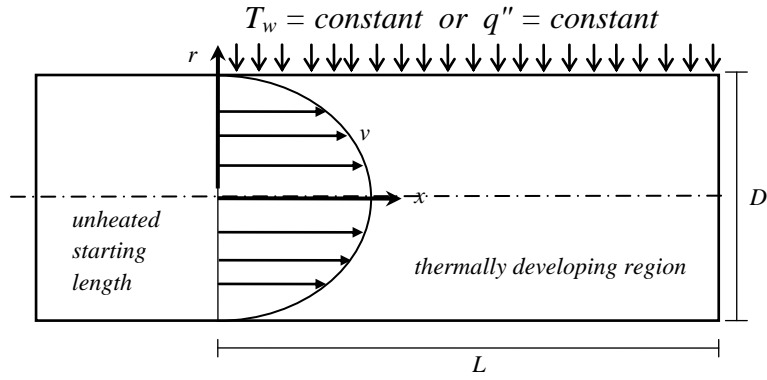


Figure 12 Geometry of the convective heat transfer problem

Thermally developing region of the nanofluid flow is investigated, thus; modeling and solution of flow and heat transfer in this domain is to be performed.

3.3.1. Governing Equations of the Problem

Governing equations for continuity, momentum and energy are available from the literature. They are extracted from mass conservation, Newton's Second Law of Motion and First Law of Thermodynamics, respectively. These fundamental equations are available in classical textbooks, such as Convective Heat Transfer by Kakaç and Yener [86] or Convection Heat Transfer by Bejan [87].

The primitive continuity equation with variable density and time varying conditions is given in vector notation as [86]:

$$\frac{D\rho}{Dt} + \rho \nabla \cdot \mathbf{V} = 0 \quad (36)$$

Here \mathbf{V} is velocity vector, t is time, and ρ is density. The total differential, D/Dt , defined as

$$\frac{D}{Dt} = \frac{\partial}{\partial t} + v_r \frac{\partial}{\partial r} + \frac{v_\phi}{r} \frac{\partial}{\partial \phi} + v_x \frac{\partial}{\partial x} \quad (37)$$

Here, φ , r , and x are angular, radial and axial directions, and their subscripts show the direction of velocity, respectively.

The continuity equation can be reduced to the following form by assuming steady and incompressible flow:

$$\frac{\partial v_r}{\partial r} + \frac{v_r}{r} + \frac{1}{r} \frac{\partial v_\varphi}{\partial \varphi} + \frac{\partial v_x}{\partial x} = 0 \quad (38)$$

When the problem is considered as seen in Figure (12), it is realized that the flow does not experience any change in x direction because this is a hydrodynamically developed flow. Besides, this is an axisymmetric flow which means there is no variation in the φ direction. Therefore, the final form of the continuity equation is:

$$\frac{\partial v_r}{\partial r} + \frac{v_r}{r} = 0 \quad (39)$$

It is known that $v_r = 0$ at $r = r_0$. Thus, solution of the separable differential equation, Equation (39), with this boundary condition gives the following result:

$$v_r = 0 \quad (40)$$

At this point it is important to mention the viscosity of nanofluids. As it was mentioned, the viscosity variation does not significantly change with temperature. Therefore, it is reasonable to assume constant viscosity.

The momentum equations of the problem with constant viscosity assumption can be written for cylindrical coordinates in vectorial notation as [86]:

$$\rho_{nf} \frac{D\mathbf{V}}{Dt} = -\nabla P + \mu_{nf} \nabla^2 \mathbf{V} + \mathbf{F} \quad (41)$$

where P is pressure, μ_{nf} is viscosity, and \mathbf{F} is the body force vector.

Since the flow is axisymmetric, derivative terms including φ can be eliminated. Furthermore, $v_r = 0$ condition was obtained from the continuity equation. The momentum equations reduce to the following equations with additional steady state ($\partial/\partial t = 0$), hydrodynamically developed flow ($\partial/\partial x = 0$ for velocity terms) and no body force ($\mathbf{F} = 0$) assumptions,

$$\rho \frac{v_\varphi^2}{r} = -\frac{\partial P}{\partial r} \quad (42)$$

$$0 = \frac{\partial}{\partial r} \frac{1}{r} \frac{\partial}{\partial r} r v_\varphi \quad (43)$$

$$0 = -\frac{1}{r} \frac{\partial P}{\partial x} + \mu_{nf} \frac{1}{r} \frac{\partial}{\partial r} r \frac{\partial v_x}{\partial r} \quad (44)$$

Boundary conditions of hydrodynamic flow, which are applied to simplified momentum equations are as follows:

$$v_\varphi = 0 \text{ at } r = r_0 \quad (45)$$

$$v_x = 0 \text{ at } r = r_0 \quad (46)$$

$$\frac{\partial v_x}{\partial r} = 0 \text{ at } r = 0 \quad (47)$$

Solution of the simplified momentum equations with the boundary conditions of the flow gives the following equations after mathematical calculations. Therefore, the profile of velocity is shown in Equation (49).

$$v_\varphi = 0 \quad (48)$$

$$v_x = 2v_m \left(1 - \frac{r^2}{r_0^2} \right) \quad (49)$$

Here, v_m is the mean velocity of the fluid in the channel.

Energy equation of the system can be written in the vector form as [86]:

$$\rho C_{nf} \frac{DT}{Dt} = -\nabla P + \nabla \cdot k_{nf} \nabla T + q''' + \Phi \quad (50)$$

Here q''' is the volumetric heat generation and Φ is viscous dissipation.

The energy equation can be simplified by considering steady and hydrodynamically developed flow as in the equation shown below by implementing the velocity profile in Equation (49).

$$\rho C_{nf} \cdot v_x \frac{\partial T}{\partial x} = \frac{1}{r} \frac{\partial}{\partial r} \left(k_{nf} r \frac{\partial T}{\partial r} \right) + \frac{\partial}{\partial x} \left(k_{nf} \frac{\partial T}{\partial x} \right) + \mu_{nf} \frac{\partial v_x}{\partial r}^2 \quad (51)$$

As seen above, the thermal conductivity of the nanofluid depends on nanofluid local temperature. This approach is preferred because the thermal conductivity of nanofluids is strongly dependent on temperature, as mentioned earlier.

Once the final form of the energy equation is obtained, it can be converted to a dimensionless form, which provides an easier solution. The equations shown below are non-dimensionalization both for constant wall heat flux and constant wall temperature boundary conditions. However, Brinkman number defined as the parameter which determines viscous dissipation effect, and temperature non-dimensionalization terms are different for each.

Equation (54), which shows dimensionless thermal conductivity, was previously used in Özerinç's study [88]. Dependency of thermal conductivity on temperature is described with ratio of local thermal conductivity to bulk thermal conductivity. Local thermal conductivity is calculated with local temperature value while bulk thermal conductivity is calculated with average temperature of inlet and outlet mean temperature values, shown in Equation (57).

$$x^* = \frac{x}{r_0} \quad (52)$$

$$r^* = \frac{r}{r_0} \quad (53)$$

$$k^* = \frac{k_{nf,T}}{k_{nf,b}} \quad (54)$$

$$v_x^* = \frac{v_x}{v_m} \quad (55)$$

$$Pe_{nf,b} = \frac{v_m d}{\alpha_{nf,b}} \quad (56)$$

$$T_{m,b} = \frac{T_{m,i} + T_{m,o}}{2} \quad (57)$$

In the Equations (54)-(57), the subscript “ nf,b ” refers to nanofluid property calculated with bulk mean fluid temperature, $T_{m,b}$, where $T_{m,i}$ and $T_{m,o}$ are inlet and exit mean fluid temperatures of the fluid. The subscript “ nf,T ” describes nanofluid property calculated at local temperature. Pe_{nf} is the bulk Peclet number of the flow where $\alpha_{nf,b} = k_{nf,b} / \rho C_{nf,b}$ is the thermal diffusivity with bulk mean temperature.

3.3.2. Boundary Conditions

3.3.2.1. Constant Wall Temperature

Dimensionless temperature and Brinkman number definitions are given in following equations for constant wall temperature condition.

$$\theta = \frac{T - T_w}{T_i - T_w} \quad (58)$$

$$Br_{nf} = \frac{\mu_{nf,b} v_m^2}{k_{nf,b} (T_i - T_w)} \quad (59)$$

Here, Brinkman number Br_{nf} shows the importance of viscous dissipation in flow. The non-dimensional energy equation is:

$$\frac{Pe_{nf}}{2} v_x^* \frac{\partial \theta}{\partial x^*} = \frac{1}{r^*} \frac{\partial}{\partial r^*} k^* r^* \frac{\partial \theta}{\partial r^*} + \frac{\partial}{\partial x^*} k^* \frac{\partial \theta}{\partial x^*} + Br_{nf} \frac{\partial v_x^*}{\partial r^*}^2 \quad (60)$$

Boundary conditions of the energy equation with constant wall temperature are,

$$\theta = 0 \text{ at } r^* = 1 \quad (61)$$

$$\frac{\partial \theta}{\partial r^*} = 0 \text{ at } r^* = 0 \quad (62)$$

$$\theta = 1 \text{ at } x^* = 0 \quad (63)$$

3.3.2.2. Constant Wall Heat Flux

Non-dimensionalization of temperature and Brinkman number for this boundary condition is given below. The dimensionless energy equation is the same as in Equation (60). In addition, values of dimensionless boundary conditions are shown in Equations (66) and (67).

$$\theta = \frac{k_{nf,b} T - T_i}{q_w'' r_0} \quad (64)$$

$$Br_{nf} = \frac{\mu_{nf,b} v_m^2}{q_w'' r_0} \quad (65)$$

$$\frac{\partial \theta}{\partial r^*} = 0 \text{ at } r^* = 0 \quad (66)$$

$$\theta = 0 \text{ at } x^* = 0 \quad (67)$$

3.3.3. Numerical Method to Solve the Energy Equation

The numerical method is prepared and a computer code is created in the commercial program MATLAB® to solve the obtained matrix. Post processing of the data is also made using the same program.

3.3.3.1. Finite Difference Method

There are mainly three numerical methods, finite difference, finite volume and finite element, to solve flow and heat transfer problems. Finite difference is the origin of methods and can be easily applied to simple geometries. On the other hand, finite volume and finite element methods provide a wide range of applicability and stability although their preparation is difficult compared to the finite difference method. It is suitable to use the complicated methods for complex geometries and flow conditions. However, solution of the problem for the geometry shown in Figure (12) is relatively simple. Moreover, the aim of this study is not to test the performance of a method, but to be able to make comments on the accuracy of nanofluid heat transfer estimation with single phase variable thermal conductivity assumption and magnitude of heat transfer enhancement of nanofluids.

After determining the numerical method, discretization of the differential energy equation should be obtained. It is different for interior and boundary nodes because of known or unknown temperature values and other conditions. Before performing discretization, it is suitable to mention nodes and the solution domain, shown in Figure (12). The axisymmetric problem of the flow in the cylindrical pipe is modeled as half of the pipe, from center to wall, because of the symmetry, hence; a reduction in the number of the nodes is achieved to give a faster solution without sacrificing accuracy. The section marked as 1 represents the inlet portion of the problem which has a parabolic velocity profile (Eq. 49) and constant temperature. The section 2 is the wall condition, which is either constant wall temperature or constant wall heat flux. The section 3 is the center of the pipe ($r=0$), therefore; the symmetry condition is applicable. Finally, the section 4 is the exit condition.

The terms Δx and Δr in Figure (13) are the distance between two nodes in the corresponding direction while “ i ” and “ j ” represents the node number in axial and radial direction, respectively. These are equally distributed nodes over the domain.

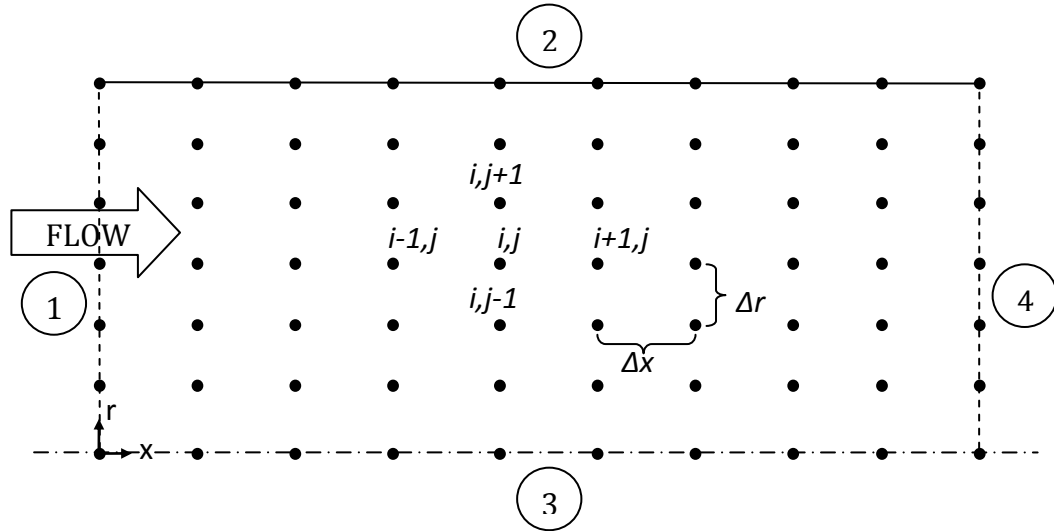


Figure 13 The problem geometry and nodes used in numerical solution, number of nodes is shown arbitrarily.

3.3.3.2. Discretization of Interior Nodes

The main body of the problem is the interior nodes because it includes all nodes except inlet, center and wall conditions. The energy equation is discretized by considering stability, accuracy and solution time issues. In order to have a higher accuracy, second order finite difference terms are mostly preferred.

The convection term is second order backward difference. It is chosen as backward difference because stability is not provided by central or forward difference. This is called as upwind method [89]. The equation is given as:

$$\frac{Pe_{nf}}{2} v_x^* \frac{\partial \theta}{\partial x^*} = \frac{Pe_{nf}}{2} v_{xj}^* \frac{3\theta_{i,j} - 4\theta_{i-1,j} + \theta_{i-2,j}}{2\Delta x^*} \quad (68)$$

Other terms, axial conduction and radial conduction, are selected as second order central difference. The challenging issue on these terms is variable conductivity value.

Actually, there are two ways of discretizing variable property conduction terms. The first one is the non-conservative approach, where all simplifications are applied to the term and the final form of this is discretized. The second one is the conservative approach, chosen in this study, involving simultaneous discretizations of complex derivatives. Discretization of the second derivative of the radial convection term is shown in Equation (69). As seen, middles of the two nodes are referenced for the first discretization. A second discretization is needed in order to eliminate left differential terms. After it is performed, Equation (70) is obtained as the final form of the radial conduction term is obtained. Axial conduction term can be discretized in the same manner.

$$\frac{1}{r^*} \frac{\partial}{\partial r^*} k^* r^* \frac{\partial \theta}{\partial r^*} = \frac{1}{r_j^* \Delta r^*} k^* r^* \frac{\partial \theta}{\partial r^*} \Big|_{i,j+1/2} - k^* r^* \frac{\partial \theta}{\partial r^*} \Big|_{i,j-1/2} \quad (69)$$

$$\begin{aligned} \frac{1}{r^*} \frac{\partial}{\partial r^*} k^* r^* \frac{\partial \theta}{\partial r^*} &= \frac{1}{4r_j^* \Delta r^{*2}} \theta_{i,j+1} k_{i,j+1}^* + k_{i,j}^* r_{j+1} + r_j \\ &- \theta_{i,j} k_{i,j+1}^* + k_{i,j}^* r_{j+1} + r_j + k_{i,j}^* + k_{i,j-1}^* r_j + r_{j-1} \\ &+ \theta_{i,j-1} k_{i,j}^* + k_{i,j-1}^* r_j + r_{j-1} \end{aligned} \quad (70)$$

Because the velocity profile in radial direction is extracted analytically, velocity derivative with respect to radial direction in viscous dissipation term can be discretized with centered difference.

Only the second column in the x direction (j=2) requires first order differencing because there is no node corresponding to “j=0”. First order derivative is applied in this column.

3.3.3.3. Discretization of Boundary Nodes

The inlet condition of the problem shown in Figure (13) marked as number 1 is constant fluid temperature. Therefore, it can be directly equated to the known temperature.

The wall boundary, number 2, has two different cases; one of them is constant wall temperature and the second is constant wall heat flux. In constant wall temperature, it is enough to equate the temperature value of the node to the known boundary condition. In constant wall heat flux, the equation shown below is discretized with second order backward differencing.

$$\frac{q''r_0}{k_{nf,b}} = k^* \frac{\partial \theta}{\partial r^*} \quad (71)$$

The center of the pipe, number 3, has symmetry so that the temperature derivative with respect to direction r is zero. The “ $\partial \theta / \partial r^* = 0$ ” equation can be discretized using a second order backward difference.

After obtaining all equations in numerical form, a matrix is obtained that includes all temperature nodes in it. It is solved with known boundary values and temperature distribution in the domain is obtained. Because the thermal conductivity of the nanofluid is temperature dependent, an iterative solution procedure is needed. In addition, calculation of thermal conductivity is made with dimensional temperature values while solution procedure of the matrix is made with dimensionless temperature values. Detailed information about the structure of the code is provided in Appendix A.

3.3.4. Verification of the Numerical Study

A verification analysis is crucial for an efficient and accurate solution in numerical studies. There are mainly two parts of this analysis. The first one is mesh dependency analysis of the code. It must be analyzed for an optimum solution mesh. A mesh having lower number of nodes in its structure may provide inaccurate results while

one having higher number of nodes causes a long computational time to obtain a solution. Therefore, there is an optimum value for the best solution of the problem in terms of accuracy and solution time. In addition, because the procedures are very similar for both boundary conditions of the energy equation, it is reasonable to present verification of the numerical study with only one boundary condition, constant wall heat flux. The second one is code validation with literature for pure water. It is expected to have the same results with the conventional theories for pure water case such as Graetz solution for thermally developing region [86].

3.3.4.1. Mesh Dependency Analysis

Nodes on x and r directions have different relative importance. At first, x direction requires more nodes for computation. An analysis is performed on node number relationship between x and r direction and it is decided that node numbers on x direction should be 2 times larger than node number of r direction.

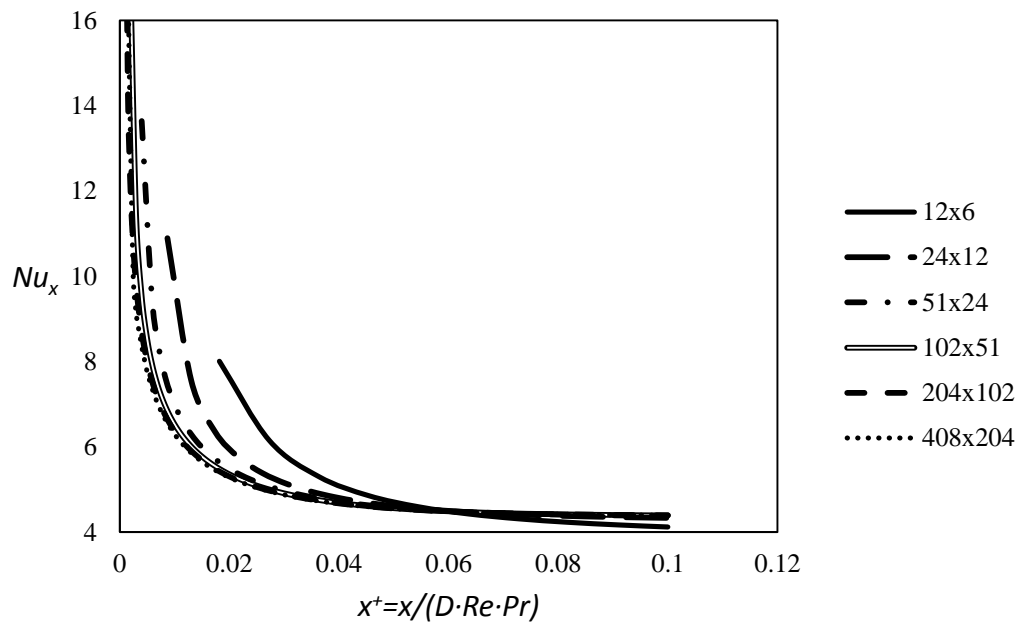


Figure 14 Mesh sensitivity analysis of the numerical study at Peclet number 2000 with pure water as a function of 2nd dimensionless axial length (Nu_x is Nusselt number and $x^+ = x / (D \cdot Re \cdot Pr)$ the reverse of Graetz number.)

After determining the situation mentioned above, size of the node is determined for optimum node numbers with minimum computational effort and maximum accuracy. Nusselt numbers for laminar flow with pure water are obtained with different node sizes are compared in Figure (14). As seen, nodes with 12 in x-direction and 6 in r-direction (12x6) is the worst scenario. Although it reflects a similar trend with the other solutions, it cannot predict the result well. Other results are converging to a certain fully developed Nusselt value by increasing the grid resolution. There is no more difference on results after the solution with 204x102 nodes. The difference between 102x51 and 204x102 is lower than 1% for the complete domain. Therefore, the results stated on this study generated by using 204x102 nodes for constant wall heat flux case. In addition, because constant wall temperature has relatively difficult convergence, its optimum grid is selected as 204x204.

3.3.4.2. Validation of the Code with Pure Water

The numerical study should be checked by using conventional and well documented theories before performing the nanofluid heat transfer analyses. The numerical work must give accurate results for pure water compared to analytical solutions.

Solution of constant property energy equation for single phase fluids with the current geometry is known as the Graetz solution [86]. This solution is extracted from the energy equation through a theoretical approach making an analytical study. On the other hand, there are various correlations which are easier to apply a problem derived from the Graetz solution. One such correlation is shown in Equation (72) [90] and its error compared to Graetz solution is below 1%. A comparison is made between this correlation and the current numerical study, as shown in Figure (15). As it is seen, there is an excellent match. It is important to note that this comparison made by assuming the thermal conductivity is constant over the domain because of the requirements of Graetz solution. Dimensionless thermal conductivity, k^* , is equated to one to apply this assumption.

$$Nu_x = 4.364 + 0.263 \frac{1}{x^+}{}^{0.506} \exp -41x^+ \quad (72)$$

Here, x^+ is the dimensionless distance and reverse of the Graetz number.

$$x^+ = \frac{x/D}{Re_{nf} Pr_{nf}} \quad (73)$$

Here, D is the channel diameter.

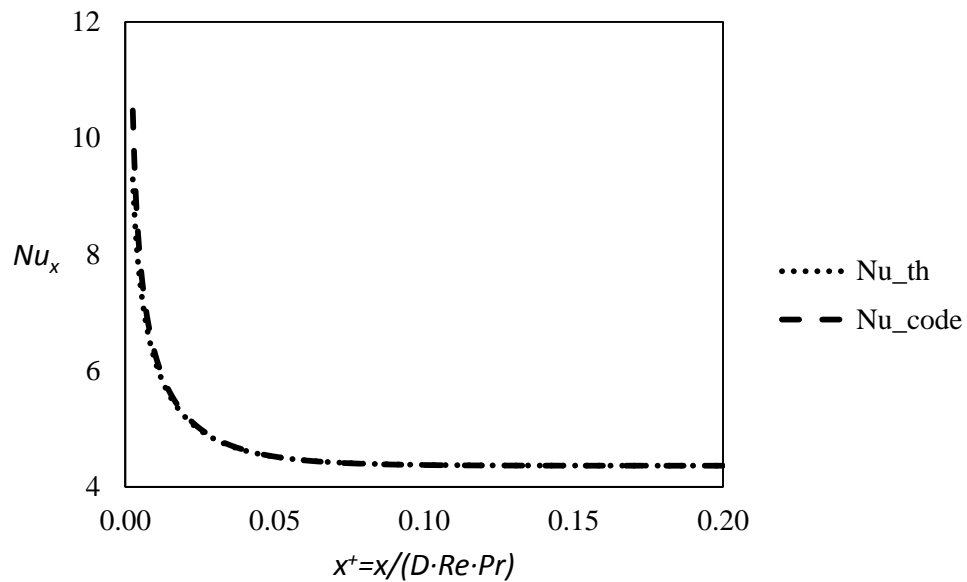


Figure 15 Validation of the code with Equation (72) [90] for pure water solution at Peclet number 1000

3.3.5. Demonstrative Parameters

After obtaining temperature distribution in the flow domain, Nusselt number and heat transfer coefficient which are two important parameters for heat transfer evaluation, can be obtained. Local Nusselt number for constant wall temperature and constant wall heat flux boundary conditions can be obtained from the following equations [86], respectively.

$$Nu_x = \frac{2}{\theta_m} \frac{\partial \theta}{\partial r^*} \Big|_{r^*=1} \quad (74)$$

$$Nu_x = \frac{2}{\theta_w - \theta_m} \quad (75)$$

Here, θ_w and θ_m are dimensionless local wall and local mean temperature are shown as:

$$\theta_w = \frac{k_{nf,b} T_w - T_i}{q_w'' r_0} \quad (76)$$

$$\theta_m = \frac{\int_0^1 \theta x^*, r^* v^* r^* dr^*}{\int_0^1 v^* r^* dr^*} \quad (77)$$

respectively.

Heat transfer coefficient is given as:

$$h_{nf} = \frac{Nu_{nf} k_{nf}}{D} \quad (78)$$

A heat transfer enhancement ratio definition is introduced in order to understand the benefit of usage of nanofluids instead of a base fluid.

$$h_r = \frac{h_{nf}}{h_f} \quad (79)$$

Different analyses are performed and presented in Chapter 4 using the formulation in Chapter 3. The estimation of the nanofluid heat transfer is important in evaluation of heat transfer performance according to pumping power considerations as it is done in Chapter 5.

CHAPTER 4

RESULTS OF THE NUMERICAL STUDY AND DISCUSSION

4.1. Introduction

In this chapter, a detailed investigation on convective heat transfer of nanofluids is provided using the modeling approach and created code explained in Chapter 3. First, a comparison with experimental results is presented to evaluate how the numerical study is successful in estimation of convective nanofluid heat transfer. Second, boundary conditions and the difference on heat transfer enhancement between the two conditions are presented and discussed. Third, other effects that significantly change heat transfer coefficient and Nusselt number are also discussed.

While doing the analyses, a variable thermal conductivity with Corcione model [28], using Al_2O_3 ($d_p = 20$)/water and inlet temperature $21\text{ }^\circ\text{C}$, Peclet number (Eq. 56) 2000 are used unless another condition is stated. Moreover, only constant wall heat flux boundary condition is used for several analyses because constant wall temperature (CWT) and constant wall heat flux (CHF) analyses give similar trends.

4.2. Comparison with Experimental Results

There are numerous experimental studies on convective heat transfer of nanofluids in laminar flow with constant heat flux boundary condition while there are a limited number of experiments with constant wall temperature boundary condition. Because of this reason, it is assumed that comparison with the experimental study for constant

wall heat flux boundary will be sufficient to comment on the accuracy of the numerical results. Furthermore, Corcione thermal conductivity model [28] shown in Equation (19) is used as a thermal conductivity model in comparison.

As mentioned in Section 2 of Chapter 3, Kim et al. [74] conducted experiments with constant wall heat flux boundary condition for both laminar and turbulent flow. Their study is reviewed and the same geometrical and flow boundary conditions are applied to the code. The diameter and length of the pipe are 4.5 mm and 2 m, respectively. Inlet temperature of the nanofluid is 22 °C for all cases. The nanofluid is Al₂O₃/water with averaged nanoparticle size 35 nm and its volumetric fraction is 3%.

The results of the experimental study and current numerical study results are plotted in Figure (16). The only available local heat transfer coefficient data along the channel from the experiment is for Reynolds number 1460. As seen, there is a very good agreement between Kim et al.'s study and the current study.

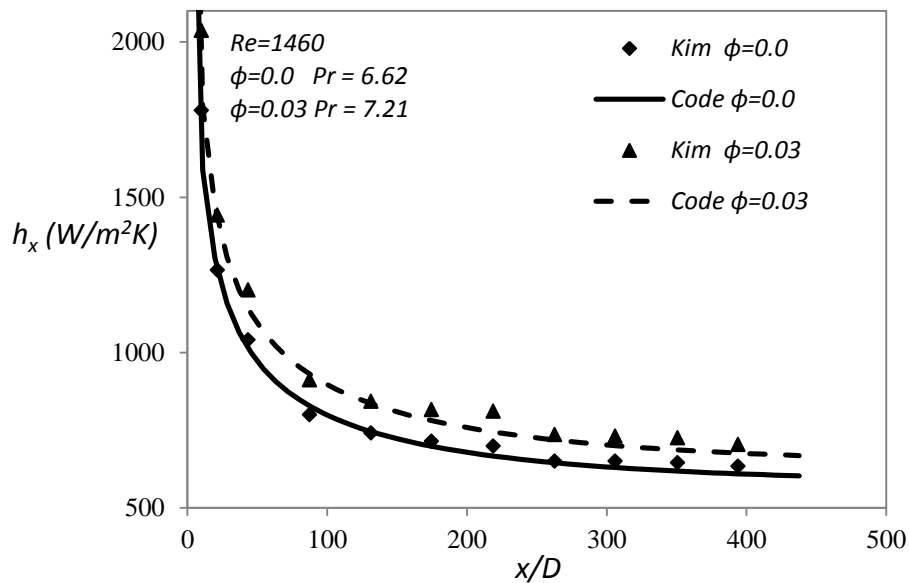


Figure 16 Comparison of the local heat transfer coefficient from the current study with experimental data from Kim et al. [74] for pure water and Al₂O₃/water nanofluid using Corcione's thermal conductivity model

In addition to the comparison with Kim et al.'s experimental data [74], a comparison with Rea et al.'s study [71] is also made. Rea et al. performed experiments with constant wall heat flux boundary condition for laminar flow in a straight pipe as mentioned in Section 2 of Chapter 3. The diameter and length of the pipe are 4.5 mm and 1.01 m, respectively. Inlet temperature and Peclet number of the nanofluid is taken 21 °C and 1000, respectively. The information of temperature difference is also taken account, which was given as 10 °C in Rea et al.'s study [71]. It is found that there is also good agreement between the data for local Nusselt number for the volumetric fraction 3% as given in Figure (17).

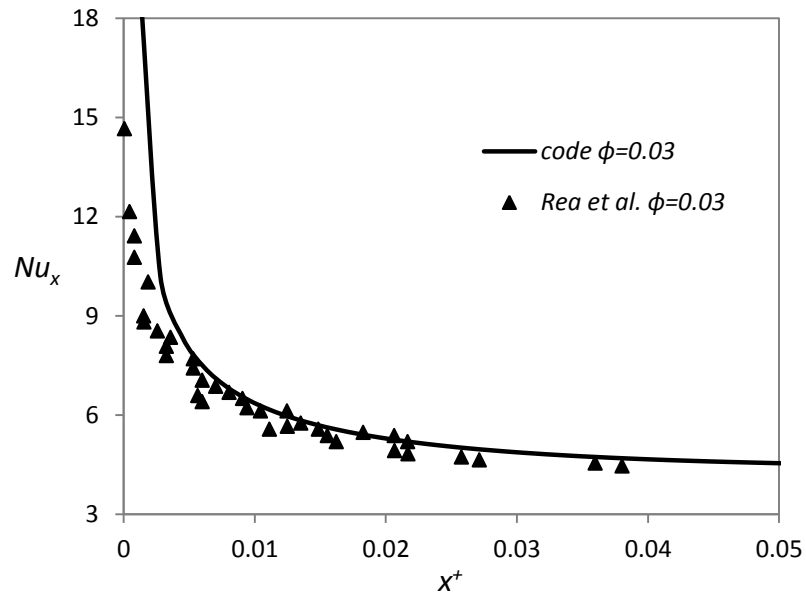


Figure 17 Comparison of the local heat transfer coefficient from the current study with experimental data from Rea et al. [71] for pure water and $\text{Al}_2\text{O}_3/\text{water}$ nanofluid using Corcione's thermal conductivity model

4.3. Comparison of Five Different Thermal Conductivity Models for the Two Boundary Conditions

4.3.1. Constant Wall Temperature

The literature survey of thermal conductivity of nanofluid shows that there are many thermal conductivity models for nanofluids. On the other hand, there are disagreements about enhancement mechanisms of conductivity. Therefore, it is suitable to investigate different theory based models for the same conditions with the constant wall temperature boundary condition (CWT) and decide which ones are widely used in the literature or close to experimental data. The models are selected as Hamilton Crosser [23], Koo and Kleinstreuer [25], Sitprasert [26], Chon [31], and Corcione [28] which have all been introduced earlier, in Section 2 of Chapter 2. Hamilton Crosser is the primitive model and has been widely used in comparison with theory in experimental studies and estimation of heat transfer in numerical studies. Koo and Kleinstreuer is a theoretical model based on Brownian motion. Sitprasert is another theoretical model which was proposed considering nanolayering around nanoparticles. Chon and Corcione models are empirical models and the latter one has been created using extensive data.

The dimensional values for the analyses affect the results because of the temperature dependency of the nanofluid thermal conductivity. The channel geometry and dimensional boundary conditions for the analyses in Section 3 of Chapter 4 are given in Appendix B, Table 4.

Figures (18) and (19) show local heat transfer coefficient values of nanofluids with the five thermal conductivity models at nanoparticle volumetric fractions 1% and 4%, respectively. There is not much difference in the result for fraction 1% but the models estimate different values for fraction 4%; the differences can be as large as 15%. Hamilton Crosser model gives the lowest value as expected while Koo Kleinstreuer, Chon, and Corcione models give similar results. Sitprasert model has the highest values. Because Corcione results are compared with experimental studies in the previous section, it is concluded that it should provide the most accurate results.

Therefore, it can be said that Sitprasert model overpredicts and Hamilton Crosser model underpredicts heat transfer coefficient values.

Figures (20) and (21) are also provided to see how much enhancement ($h_r = h_{nf}/h_f$) is achieved using nanofluids instead of pure water. For the volumetric fraction 1%, the difference among the models and enhancements are relatively low. There is not much change in the enhancement value along the axial direction. However, in Figure (21), there are large differences among models. Hamilton Crosser gives constant, 12%, enhancement while Koo Kleinstreuer gives constant, 21%, enhancement in heat transfer coefficient. Chon and Corcione models give nearly the same values, increasing from 22% to 27%. Sitprasert model enhancement increases with increasing axial location as well. This is caused by temperature dependency of these models because temperature increases along the channel in heating application of pipes. If a cooling application was implemented, the reverse of this behavior would be observed. This phenomenon, increment of heat transfer enhancement with temperature, is especially important for high nanoparticle volumetric fraction and high temperature variation applications.

Actually, average of the heat transfer coefficient of the nanofluid through the channel is important for constant wall temperature boundary condition, thus; enhancement at near inlet of the pipe is more important because heat transfer coefficient is always higher in this region. It is desired to have higher heat transfer enhancement ratio in the high heat transfer coefficient region because this case gives higher average heat transfer coefficient for nanofluids.

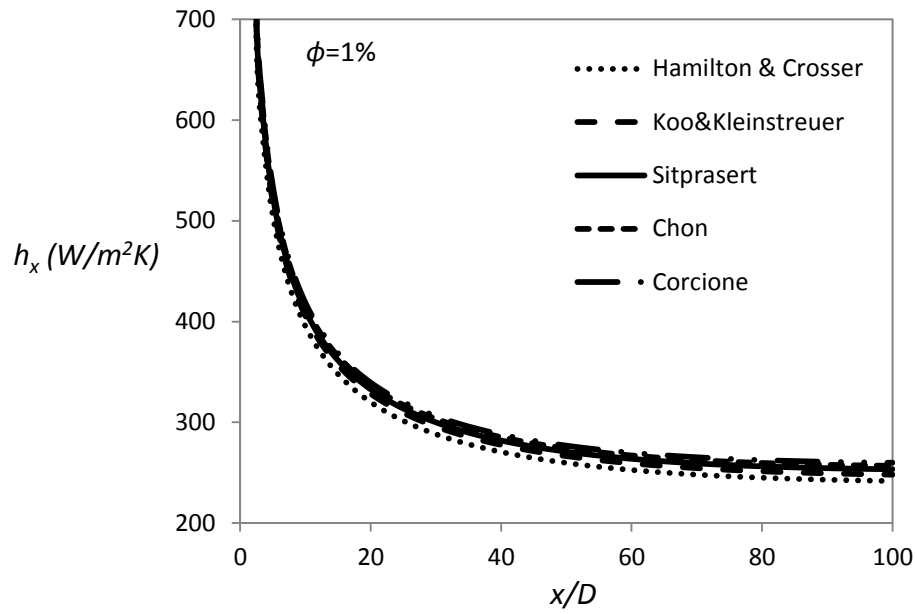


Figure 18 Local heat transfer coefficient of Al_2O_3 (20 nm) /water nanofluent at Peclet number 2000 by using the five conductivity models ($\phi=1\%$) for CWT

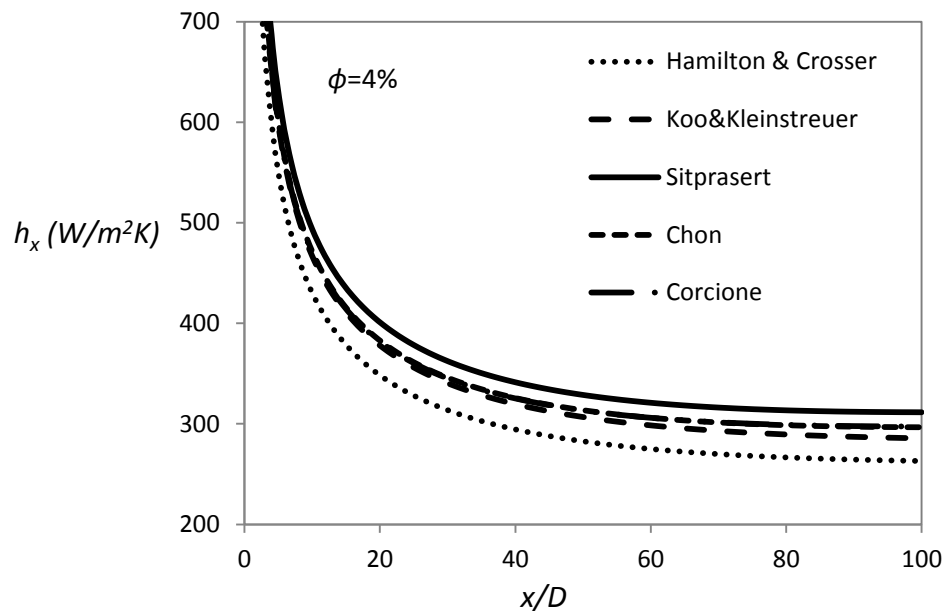


Figure 19 Local heat transfer coefficient of Al_2O_3 (20 nm) /water nanofluent at Peclet number 2000 by using the five conductivity models ($\phi=4\%$) for CWT

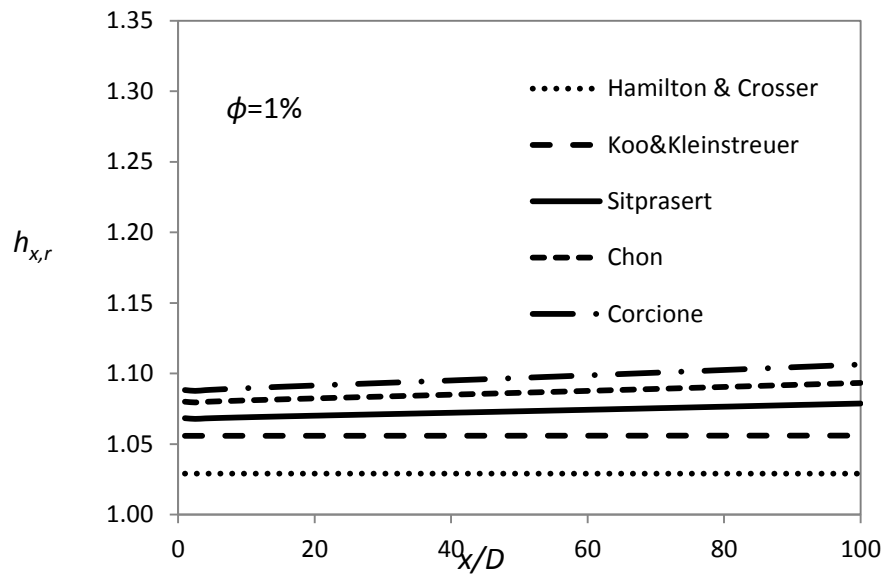


Figure 20 Local heat transfer enh. of Al_2O_3 (20 nm) /water nanofluid at Peclet number 2000 by using the five conductivity models ($\phi=1\%$) for CWT condition

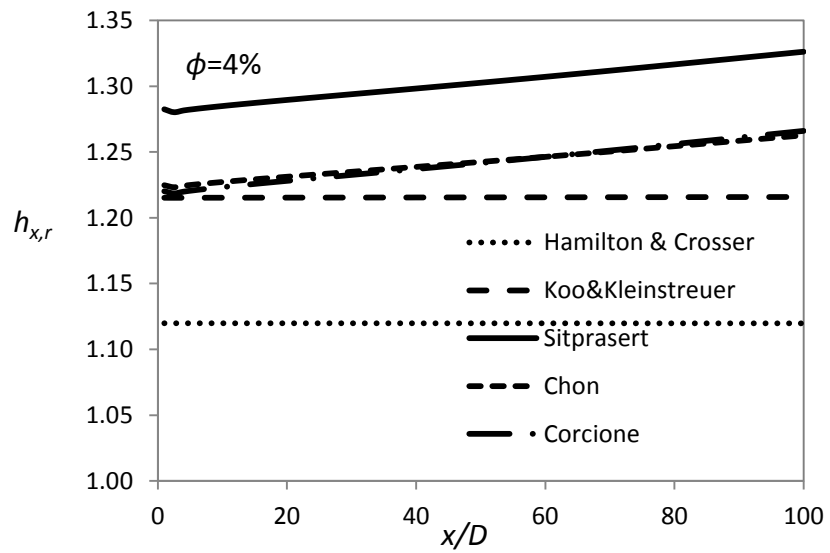


Figure 21 Local heat transfer enh. of Al_2O_3 (20 nm) /water nanofluid at Peclet number 2000 by using the five conductivity models ($\phi=4\%$) for CWT condition

4.3.2. Constant Wall Heat Flux

Similar to the previous case, constant wall heat flux boundary condition local heat transfer coefficient results are provided in Figure (22) and (23) for volumetric fractions 1% and 4%. There is a similar trend in curves for different thermal conductivity models with CWT boundary condition. Heat transfer enhancement values in Figures (24) and (25) also have similar behavior but the range between inlet and exit values is higher. For example, for the Corcione model, the enhancement increases from 14% to 23% along the channel.

Moreover, the variation of heat transfer enhancement along the channel is more important in CHF condition because it is not proper to use an average heat transfer coefficient or average heat transfer enhancement definition for this boundary condition. Local heat transfer coefficient always reserves its vitality because it directly affects heat transfer performance. The most important location is the exit region because the maximum wall temperature occurs at this region (undesired situation), therefore; it is desired to have the highest heat transfer coefficient at the exit region. This issue is discussed in detail in Chapter 5.

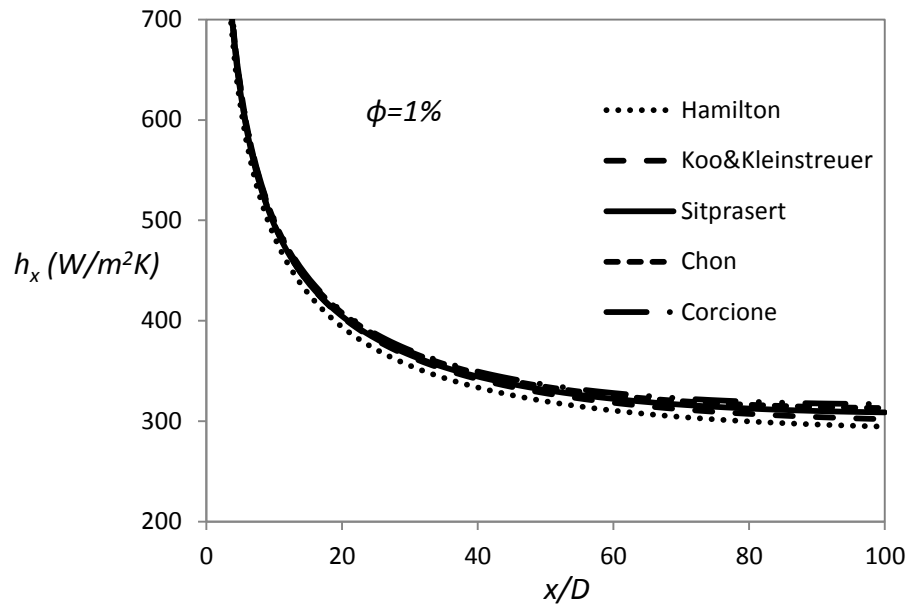


Figure 22 Local heat transfer coefficient of Al_2O_3 (20 nm) /water nanofluid at Peclet number 2000 by using the five conductivity models ($\phi=1\%$) for CHF

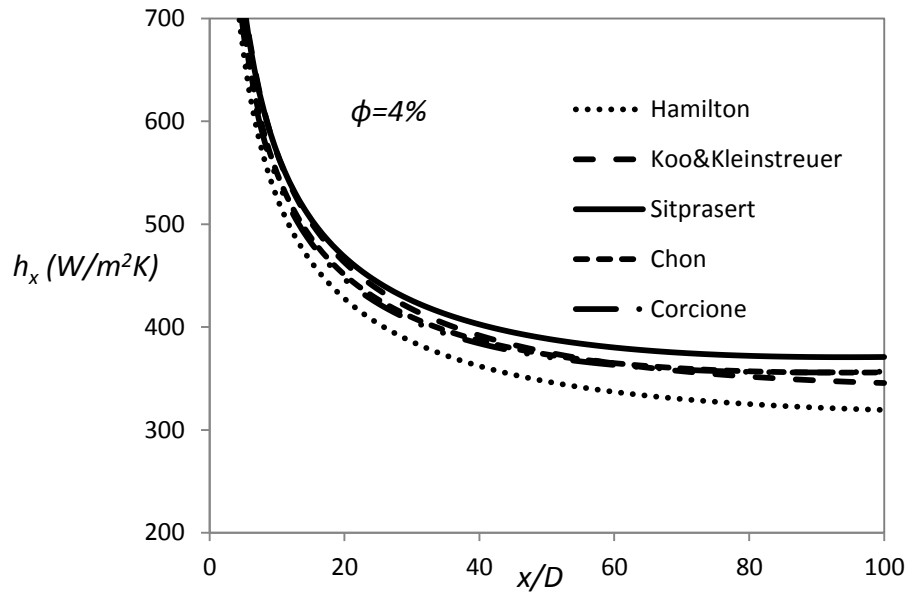


Figure 23 Local heat transfer coefficient of Al_2O_3 (20 nm) /water nanofluid at Peclet number 2000 by using the five conductivity models ($\phi=4\%$) for CHF

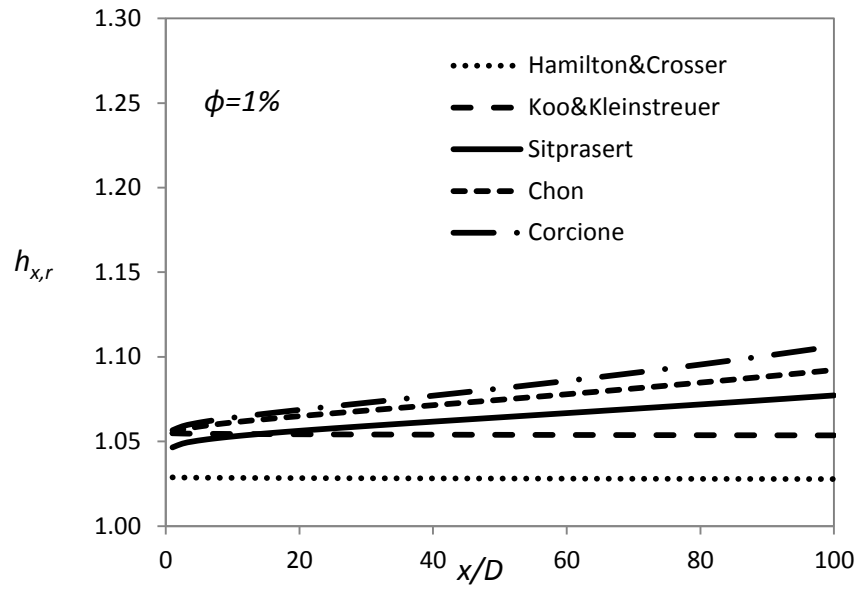


Figure 24 Local heat transfer enh. of Al_2O_3 (20 nm) /water nanofluent at Peclet number 2000 by using the five cond. models ($\phi=1\%$) for CHF condition

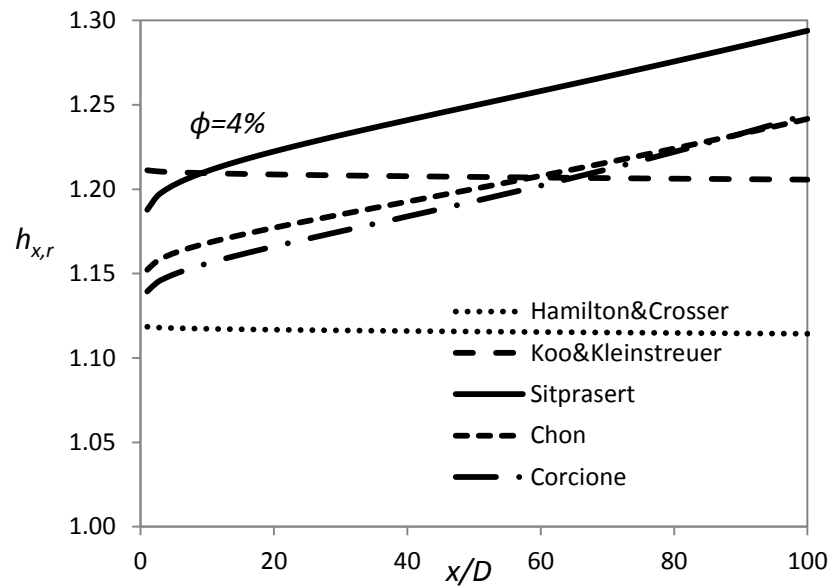


Figure 25 Local heat transfer enh. of Al_2O_3 (20 nm) /water nanofluent at Peclet number 2000 by using the five conductivity models ($\phi=4\%$) for CHF condition

4.4. Nusselt Number of the Two Boundary Conditions

In this analysis, pure water and Al_2O_3 (20nm)/water nanofluid with 4% nanoparticle volumetric fraction heat transfer analyses are performed using the Corcione model for the thermal conductivity. The Nusselt number results for the pure water with CWT, the nanofluid with CWT, the pure water with CHF, the nanofluid with CHF are plotted in Figure (26). The analyses are done by taking into account the temperature dependent variable conductivity.

Figure (26) shows local Nusselt number values along axial direction with dimensionless axial distance defined as $x^+ = x / D \cdot Re_{nf} Pr_{nf}$ in Equation (73) for both boundary conditions (CWT and CHF). For the CWT case, Nusselt number for the nanofluid with volumetric fraction 4% is higher than pure water in the thermally developing region and the difference between them is continuously decreasing. This behavior can be explained by dimensional temperature values of the problem. When the flow goes through the channel and approach as the fully developed region, dimensional values of temperature are closer at an axial location. Therefore, abnormal enhancement caused by temperature difference along the radial direction diminishes.

On the other hand, it is seen that the difference in Nusselt number between pure water and nanofluid always exists for the CHF case although it is very small. This is also caused by nearly constant slope of the dimensional temperature profile in the radial direction which does not change with axial direction.

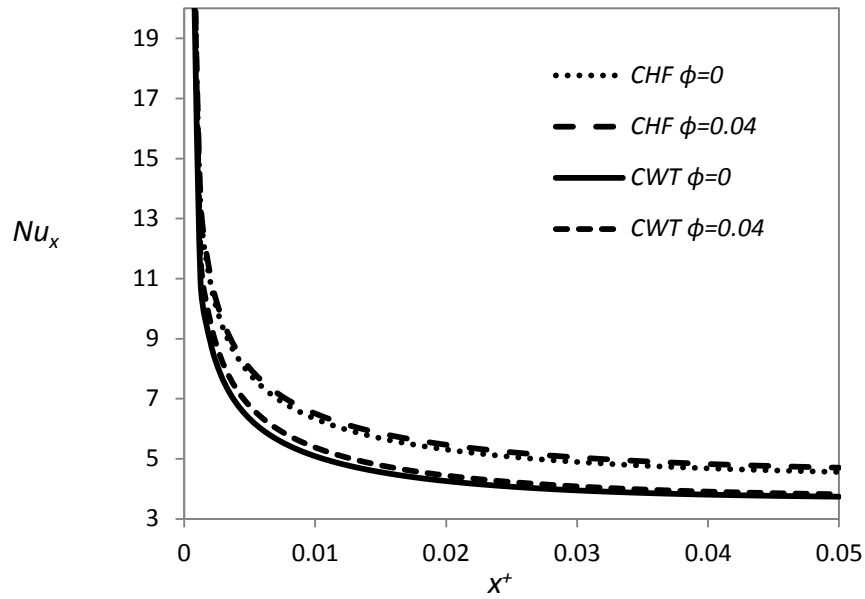


Figure 26 Local Nusselt number along the channel for the Al_2O_3 (20 nm) /water nanofluid at $\phi=4\%$ and the pure water using Corcione model with CWT and CHF boundary conditions at Peclet number 2000

4.5. Other Affecting Parameters

4.5.1. Temperature Dependent Variable Thermal Conductivity

The effect of temperature dependent thermal conductivity modeling as stated in Equations (54) and (60) is investigated in this section. As stated in Section 3.3.1, according to these equations, temperature dependent thermal conductivity is taken into account if the term $k^* = k_{nf,T}/k_{nf,b}$ is calculated by estimating local thermal conductivity at local temperature and average thermal conductivity at bulk temperature. On the other hand, the term k^* is equated to 1 for constant thermal conductivity modeling. Namely, the difference between temperature dependent variable and constant thermal conductivity is investigated in terms of Nusselt number and heat transfer enhancement ratio.

The analyses are performed using water and Al_2O_3 (20 nm)/water nanofluid with volumetric fraction 4% similar to the previous cases. Both variable and constant thermal conductivity analyses are done for both the pure water and the nanofluid. Because the basic idea is similar, only CHF boundary condition is performed in this section. The thermal conductivity model is the Corcione model.

The variation of thermal conductivity with changing temperature affects heat transfer coefficient in two ways. The first one is caused by directly the thermal conductivity value while the second one is the variable thermal conductivity effect on Nusselt number. In fact, solving the energy equation with variable thermal conductivity as stated in the previous chapter provides a result which is higher than the conventional solution. CHF boundary condition is used in this section.

Figure (27) shows Al_2O_3 (20 nm)/water nanofluid with nanoparticle volumetric fraction 4% and pure water local Nusselt numbers along the axial direction. There are two curves for each fluid, which describe the analyses of heat transfer with variable conductivity and constant conductivity models. As seen, constant thermal conductivity which does not change with local temperature values cases for pure fluid and nanofluid give exactly the same Nusselt number values. However, Nusselt number with variable conductivity is higher for the nanofluid than for the pure fluid. When the nanofluid is considered, there is a 5% difference between variable and constant cases at the exit of the pipe. If heat transfer enhancement ratio range, 10%-35%, is considered, it can be said that using a temperature dependent thermal conductivity approach with a temperature dependent model (e.g. Corcione model) is important.

As stated at the beginning of this section, another important issue in variable conductivity is directly thermal conductivity variation in heat transfer coefficient. When both mechanisms that create this situation are considered, it is suitable to demonstrate a heat transfer enhancement figure which shows the difference between variable and constant conductivity assumptions. Figure (28) which shows the heat transfer enhancement ratio for both constant conductivity and temperature dependent conductivity assumptions is prepared from the analysis of the energy equation with

the Corcione model. The importance of variable conductivity is well understood from this figure because the maximum difference between the two cases is 10%.

A detailed table of fully developed Nusselt number and heat transfer coefficient values of CWT and CHF boundary conditions with variable and constant thermal conductivity are given along with the geometrical conditions used in analyses in Appendix B, Table 5. In this table, the analyses are done for Al_2O_3 (50 nm, $\phi=5\%$) /water nanofluid and pure fluid. As seen, there is a significant difference between constant conductivity and temperature dependent variable conductivity cases especially for the nanofluids at Peclet number 1000 case. This is caused by the increased temperature of the fluid.

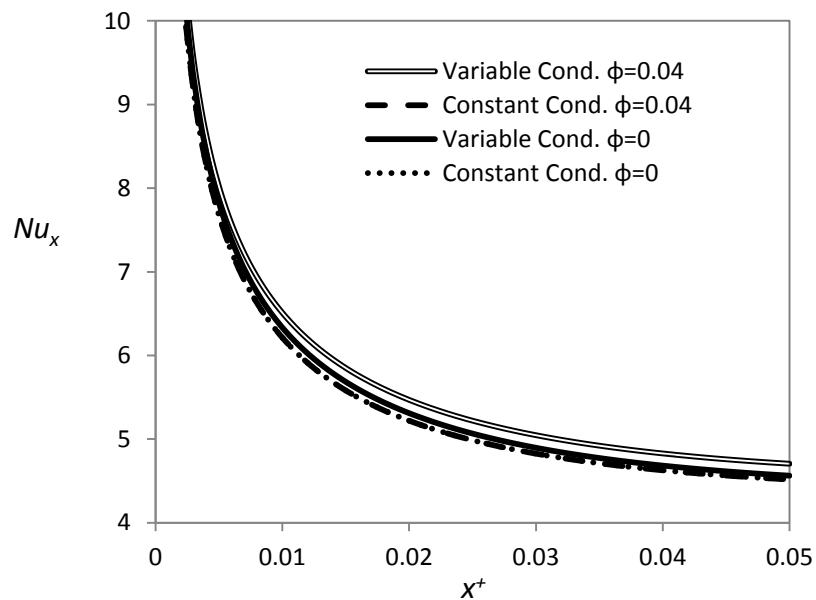


Figure 27 Local Nusselt number with variable and constant thermal conductivity assumptions for Al_2O_3 (20 nm) /water nanofluid at $\phi=4\%$ and pure water at Peclet number 2000 using Corcione model (CHF condition is applied)

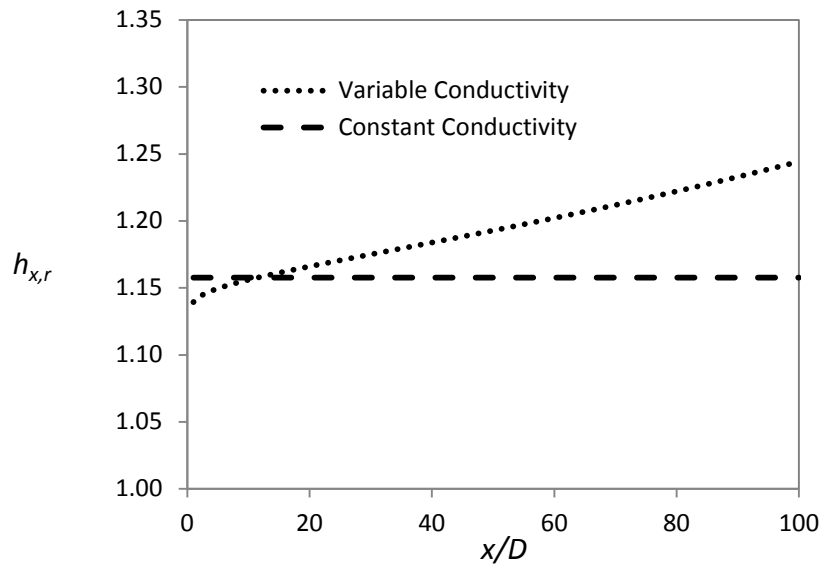


Figure 28 Local heat transfer enh. along the channel for Al_2O_3 (20 nm) /water nanofluent at $\phi=4\%$ with variable cond. and constant cond. assumptions at Peclet number 2000 using Corcione model (CHF condition is applied)

4.5.2. Peclet Number

In this section, the analyses are performed using water and Al_2O_3 (20 nm)/water nanofluent with volumetric fraction 4% which is similar to the previous cases. The boundary condition is selected as CHF and the thermal conductivity model is the Corcione model used in the analyses.

In the thermal dispersion model to estimate nanofluent heat transfer, a significant role is attributed to Peclet or Reynolds number. As stated in Section 3.2.2, thermal dispersion was proposed as an enhancement mechanism that increases the Nusselt number of the nanofluent flow [78]. On the other hand, once single phase assumption is made, the energy equation (Eq. 60) affected by the magnitude of Peclet number is limited only to thermophysical property change. The thermophysical property change is caused by bulk mean temperature change of the fluid. In other words, the flow

cannot be the same bulk temperature with the lower Peclet number case if Peclet number shown in Equation (60) is increased.

This effect is shown in Figure (29) for the nanofluid under CHF boundary condition varying heat transfer enhancement along the channel with different Peclet numbers. The enhancement starts from the same point but its slope is lower for higher Peclet numbers because, temperature of higher Peclet number flow increases slowly.

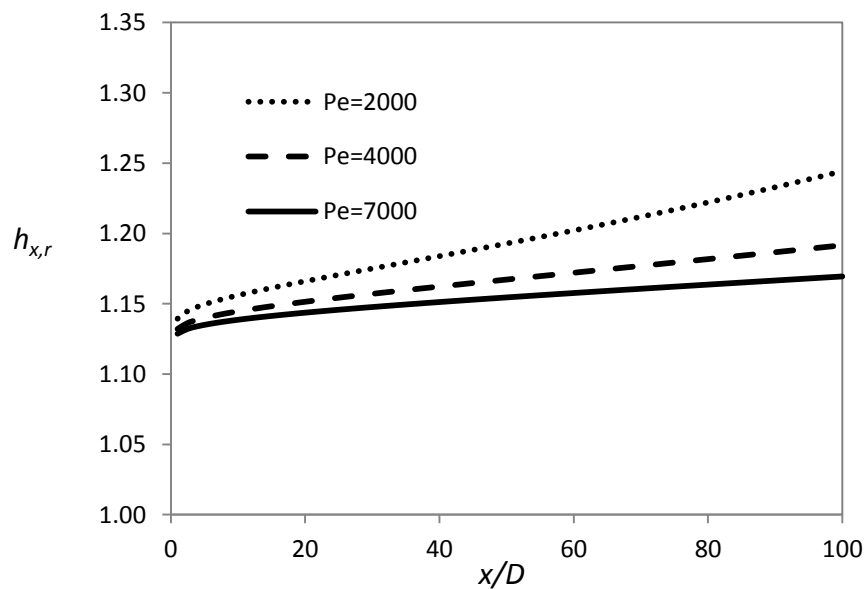


Figure 29 Local heat transfer enhancement along the channel for different Peclet numbers for Al_2O_3 (20 nm) /water nanofluid at $\phi=4\%$ using Corcione model (CHF condition is applied)

4.5.3. Particle Size

In this section, the analyses are performed using water and Al_2O_3 (20 nm)/water nanofluid with volumetric fraction 4%. The boundary condition is selected as CHF

and the thermal conductivity model is the Corcione model which takes into account the particle size effect.

Particle size effect on thermal conductivity is discussed in literature survey of thermal conductivity section in Chapter 2. As stated, the smaller particle size causes an increment in the thermal conductivity of the nanofluid due to Brownian motion. As particle size decreases, heat transfer coefficient and heat transfer enhancement increases similar to thermal conductivity. The difference among to the results below 40 nm particle diameter is much more significant as seen in Figure (30). This result is consistent with literature.

In practical applications, it may be advantageous to use smaller nanoparticle sizes according to this investigation.

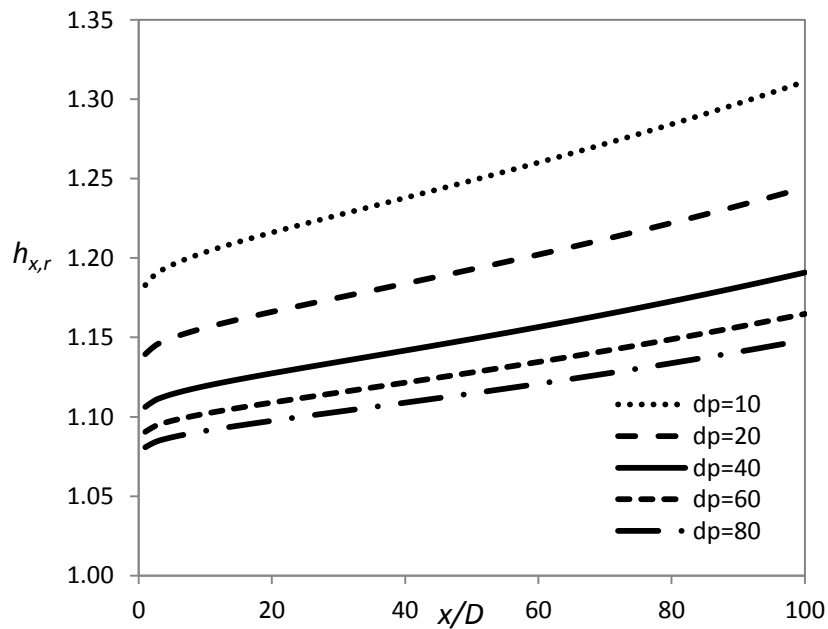


Figure 30 Local heat transfer enhancement along the channel for Al_2O_3 /water with different nanoparticle diameters nanofluid at $\phi=4\%$ using Corcione model (CHF condition is applied)

4.5.4. Axial Conduction

Axial conduction is generally negligible when the working fluid of heat transfer medium is water because Peclet number below 10 is required for significant effect of axial conduction as can be seen in the energy equation (Eq. 60). However, Peclet number is mostly far above 10 for water since low Peclet number refers to a very low mean velocity for a flow which is not practical. This notion can be understood by looking at the differential equation of energy.

On the other hand, a study on axial conduction effect on convective heat transfer of nanofluid provides knowledge on this issue. It helps to observe whether temperature dependent nature of the nanofluid thermal conductivity alters the phenomenon or not.

Figure (31) presents Nusselt number values for nanofluid at nanoparticle volumetric fraction 5% and pure water. The conditions are the same in terms of Peclet number ($Pe = 10$). When axial conduction term is taken into account in the energy equation, it is called “ON” case while when it is neglected; it is called “OFF”. As seen, axial conduction affects the results especially in the thermally developing region. The effect gradually decreases along the axial direction. However, there is no difference between water and nanofluid cases for the ON condition. In fact, the effect of axial conduction on nanofluid heat transfer is the same as pure water heat transfer.

Axial conduction effect on fully developed region is also shown in Appendix B, Table 6 for both CWT and CHF conditions for pure water and Al_2O_3 (50 nm, $\phi=5\%$) /water nanofluid. As seen, the results for both the pure fluid and the nanofluid nearly do not change with the addition of axial conduction effect into the solution.

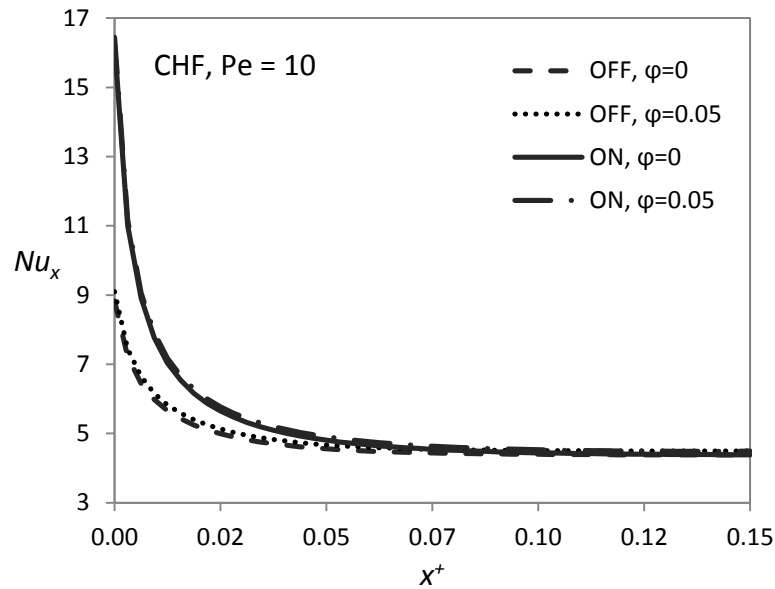


Figure 31 Local Nusselt number along the channel with and without the axial conduction term in Eq. 60 assumptions for pure water and Al_2O_3 (20 nm) /water nanofluid at $\phi=5\%$ using Corcione model ,(CHF condition is applied), (ON:axial conduction considered, OFF:axial conduction neglected)

4.5.5. Viscous Dissipation

Viscous dissipation is defined as “the rate at which the viscous forces do irreversible work on the fluid [86]”. Viscous forces are especially important for high viscosity fluids such as oil, hence; viscous dissipation is higher for these types of fluids. Actually, the order of magnitude of effect of viscous dissipation can be predicted by looking at Brinkman number shown in Equation (59) or (65). At a constant Peclet number, viscous dissipation is higher for nanofluids than pure fluids because it is known that the viscosity of nanofluids is higher.

If a significant viscous dissipation exists in a nanofluid heat transfer system, this becomes a drawback of nanofluids because it reduces the Nusselt number and heat transfer coefficient. Figure (32) presents the Nusselt number of pure water and nanofluid at Peclet number 4000. Similar to axial conduction case, “ON” term implies that viscous dissipation is taken into consideration while “OFF” case not. The results

show that Nusselt number is the same for water and nanofluid in the OFF case. However, it differs when viscous dissipation is ON. The decrease in Nusselt number is especially higher for the nanofluid because it has a higher Brinkman number when Peclet number is taken as constant. This is caused by increased viscosity of nanofluids compared to the base fluids as stated above.

Figure (33) is also about the viscous dissipation effect on Nusselt number. However, unlike other figures, it shows fully developed values of Nusselt number in different analyses with different channel diameters. As seen, when the diameter of the pipe is below about 0.5mm, viscous dissipation causes a dramatic decrease in Nusselt number. Moreover, it is worse for nanofluid heat transfer.

This phenomenon creates the idea that usage of nanofluids in microchannels may be disadvantageous under certain conditions. In fact, values of boundary conditions of the fluid are especially important for this situation because Brinkman number definition includes dimensional boundary conditions; such as dimensional heat flux value for CHF condition.

Viscous dissipation effect on fully developed region is also shown in Appendix B, Table 7 for both CWT and CHF conditions for pure water and Al_2O_3 (50 nm, $\phi=5\%$) /water nanofluid. As seen, the difference between viscous dissipation neglected (OFF) and not neglected (ON) cases is more significant in CHF condition. This is caused by the dimensional value of the wall temperature in CWT condition and dimensional value of the wall heat flux in CHF condition.

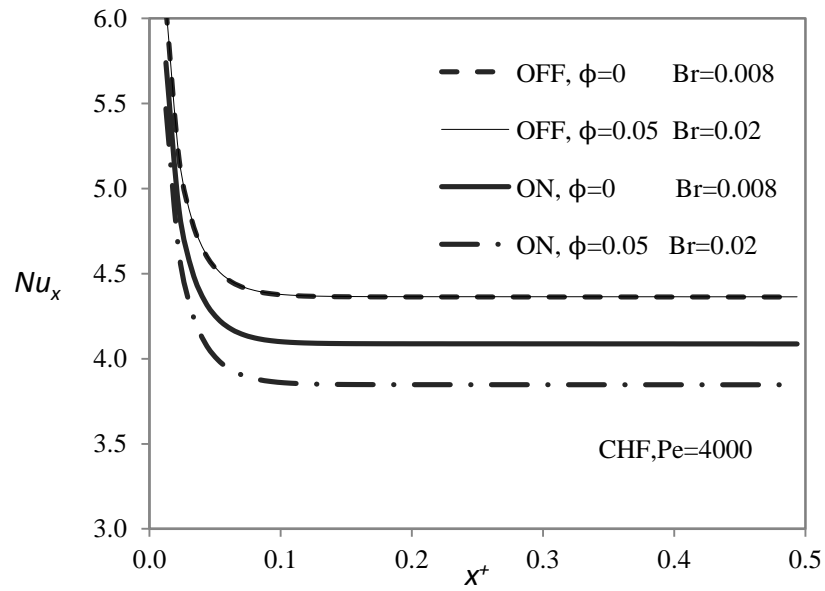


Figure 32 Local Nusselt number along the channel with and without negligible viscous dissipation assumptions for pure water and Al_2O_3 (20 nm) /water nanofluid, (CHF condition is applied), ($\phi=5\%$, ON: viscous dissipation conduction considered, OFF:not considered)

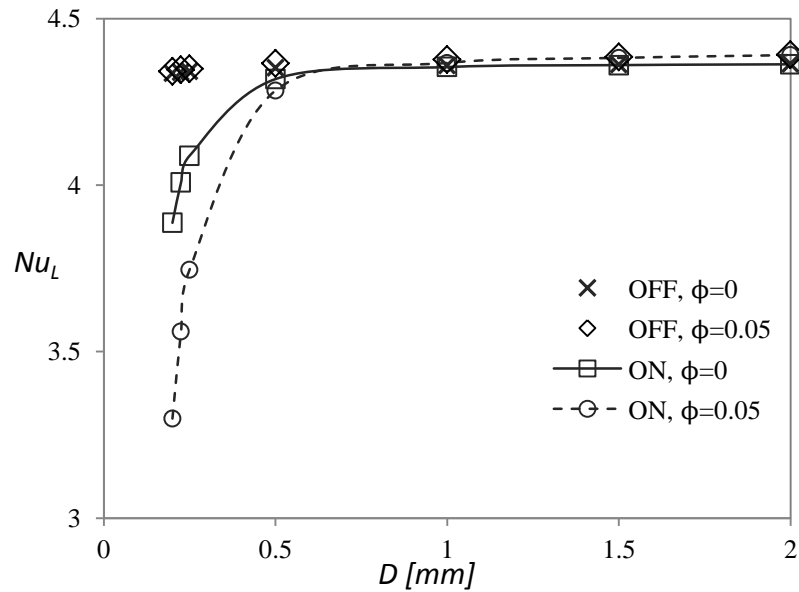


Figure 33 Fully developed Nusselt number with varying channel diameter with and without negligible viscous dissipation assumptions for pure water and Al_2O_3 (20 nm) /water nanofluid, (CHF condition is applied), ($\phi=4\%$, ON: viscous dissipation conduction considered, OFF:not considered)

4.6. Conclusion

In this Chapter, forced convective heat transfer of nanofluids is investigated considering only the heat transfer coefficient and the Nusselt number enhancement at constant Peclet number.

The numerical analyses are performed using the five thermal conductivity models presented and selected in Chapter 2, and it is concluded that the Corcione model is the most suitable alternative. The two boundary conditions, constant wall temperature and constant wall heat flux, are investigated and it is seen that there is a slight difference in results. Other effects on the heat transfer coefficient and Nusselt number enhancement are also investigated. Finally, it is concluded that the heat transfer coefficient for a nanofluid is enhanced with respect to the base fluid at a constant Peclet number. This enhancement comes from the thermal conductivity and Nusselt number enhancements.

On the other hand, the usage of nanofluids depends also on the pumping power performance of nanofluids. In this Chapter, the estimation of the nanofluid heat transfer is achieved. The constant Peclet number analyses help understand the nanofluid heat transfer value deviation from the conventional theories. However, the enhancement values do not show the absolute enhancement because the pumping power also increases due to constant Peclet number.

Therefore, it is required to investigate pumping power behavior of the nanofluids and a comparison between the base fluids and nanofluids is also needed to understand the performance enhancement as performed in Chapter 5. The performance comparison between the nanofluids and the base fluids is actually more important than the heat transfer estimation because this issue determines whether the nanofluid should be used instead of the base fluid. The heat transfer estimation is only a parameter that affects the heat transfer/pumping power considerations.

CHAPTER 5

HEAT TRANSFER PERFORMANCE EVALUATION OF NANOFLUIDS WITH PUMPING POWER CONSIDERATION

5.1. Introduction

Up to now, prediction of thermophysical properties and convective heat transfer of nanofluids have been discussed. They are vitally important for robust and reliable heat transfer application design and operational conditions. On the other hand, it is not sufficient to explain how beneficial nanofluids are for an application. In other words, it cannot be decided by looking at only thermal conductivity and heat transfer coefficient increment at a constant parameter such as Reynolds or Peclet number whether nanofluids should be used or not.

This situation may seem confusing because it is a fact that heat transfer coefficient of a system increases using a nanofluid instead of using the base fluid, its substitute. However, there are other crucial parameters that affect heat transfer performance of systems. Even though the thermal conductivity of the system always increases by changing its working medium to nanofluid, it also requires more pumping power to be circulated in the system because of increased viscosity of the fluid.

Increment in the pumping power is caused by increment in fluid viscosity due to addition of nanoparticles in it. Therefore, the pressure drop/pumping power

(hydrodynamic) behavior of the nanofluid in addition to heat transfer behavior should be investigated to comment on the absolute benefit of nanofluids.

On the other hand, it is seen that constant Reynolds (or Peclet) number comparisons among different types of nanofluids and base fluids are preferred in convective heat transfer studies in the literature and as demonstrated in Chapter 4. This approach is acceptable while evaluating the method of prediction of nanofluid heat transfer and searching for any abnormal enhancement but may be misleading when heat transfer performance of the nanofluid compared to the base fluid is considered.

This chapter explains why constant Reynolds number analyses are not sufficient to determine the heat transfer performance of nanofluids and what other methods to evaluate the performance may be.

Actually, the evaluation of nanofluid heat transfer performance considering pumping power is more important than the only heat transfer coefficient enhancement at a constant parameter. Therefore, the results obtained from Chapter 5 will be more important than the only heat transfer coefficient estimation in Chapter 4. This is the most significant contribution of the current study.

5.2. Survey of the Performance of Nanofluids in Literature

Choi and Eastman [22] investigated nanofluid thermal conductivity and feasibility of the use of nanofluids in heat transfer systems. They compared pumping power ratio and heat transfer coefficient ratio based on a reference state. This may seem to be logical, but the authors took the thermophysical properties except thermal conductivity as constant because of the lack of information. This does not reflect the real situation. Moreover, heat transfer coefficient does not show the whole picture because the heat transfer depends on other parameters such as specific heat and density.

Garg et al. [58] measured thermal conductivity and viscosity of copper - ethylene glycol nanofluids and suggested an evaluation criterion for nanofluid heat transfer performance. At first, they made an order of magnitude analysis on thermal

conductivities of the base fluid and the nanoparticles and showed that k_f/k_p ratio is nearly zero. With the aid of this information, Maxwell model (Eq. 8 in Ch. 2), of conductivity is reduced into the form as follows:

$$\frac{k_{nf}}{k_f} = 1 + c_{18}\phi \quad (80)$$

Here, c_{18} is the constant for thermal conductivity enhancement (Eq. 80) and may be different for different type of nanofluids. The authors reduced the Einstein model (Eq. 21) for the nanofluids to the following form:

$$\frac{\mu_{nf}}{\mu_f} = 1 + c_{19}\phi \quad (81)$$

Here, c_{19} is the constant for viscosity increment for nanofluids.

After these definitions, a performance comparison criterion between the base fluid and nanofluid is suggested as:

$$\eta = \frac{\text{heat removed}_{nf} / \text{pumping power}_{nf}}{\text{heat removed}_f / \text{pumping power}_f} \quad (82)$$

Chiesa et al. [91] investigated thermal conductivity of water-in-oil nanoemulsions. Although this is not the main subject of the current study, the method of the evaluation of the heat transfer fluid is interesting. They suggest the methodology in Nuclear Engineering Handbook by Etherington [92] which states that a certain heat removal aim (maximum temperature, heat transfer rate etc.) should be accomplished with a lower pumping power. This method is called as efficacy and should be higher than 1 for a better performance:

$$\epsilon = \frac{P_f}{P_{nf}} \quad (83)$$

Here, ϵ is the efficacy, P_f is the pumping power for the base fluid and, P_{nf} is the pumping power for the nanofluid.

Singh et al. [93] studied entropy generation of nanofluid flow and heat transfer. They stated that the evaluation of the heat transfer performance is proper with comparison of the entropy generation of nanofluid and base fluid flows. They made analyses with entropy generation expressions by Bejan [94] for different cases and entropy generation rate ratio was defined as the ratio of entropy generation rate of nanofluid flow to entropy generation rate of base fluid at constant mass flow rate. Both laminar and turbulent flows were examined in a microchannel (0.1 mm), minichannel (1 mm) and conventional channel (10 mm). Thermophysical properties of nanofluids were represented by two models. Model 1, which is the theoretical one, includes $c_{18} = 3$ (Eq. 80) and $c_{19} = 2.5$ (Eq. 81) and the Model 2, which is the experimental one, includes $c_{18} = 4$ and $c_{19} = 10$. The heat transfer enhancement coming from the two phase flow effects is neglected for simplicity. However, addition of this effect would give more realistic results if a different model had been defined as Model 3 with this approach. Different conclusions were obtained for different channels and flow regimes. According to Singh et al. [93], it is disadvantageous, may be advantageous or disadvantageous and, is advantageous to use the nanofluids in laminar flow with microchannels, minichannels, and conventional channels, respectively. For the turbulent flow, nanofluid usage in a microchannel is always advantageous while the advantage of use of nanofluid with minichannel or conventional channel depends on the thermophysical properties.

Liu et al. [95] investigated the impact of nanofluid heat transfer enhancement on the performance of heat exchangers theoretically in laminar and turbulent flow regimes. At first, water and ethylene glycol based nanofluid thermophysical properties and resulting heat transfer coefficient values for pure fluids and nanofluids were presented. However, Einstein viscosity model which underestimates the viscosity is used and conventional Nusselt number correlations are used to calculate the Nusselt number. After calculating the heat transfer enhancement at constant pumping power, heat exchanger performance improvement is observed. Enhancement in number of

transfer units (NTU) and resulting enhancement on the heat transfer rate were explained with following equations. It is important to note that the thermal resistance weight (reverse of overall heat transfer coefficient, fraction of thermal resistance of nanofluid in the total thermal resistance of the heat exchanger) of the nanofluid side of the heat exchanger is as important as the heat transfer coefficient enhancement. The maximum heat transfer rate enhancement is presented as 7% when the heat transfer coefficient enhancement is increased by 50% with the nanofluid. In addition, heat transfer area reduction in heat exchangers with the usage of nanofluids was investigated. Detailed information can be found in Reference [95].

The Number of transfer units mentioned above is compared for nanofluid and base fluid as follows:

$$\frac{NTU_{nf}}{NTU} = \frac{UA_{nf}}{UA} \quad (84)$$

Here, U is overall heat transfer coefficient with heat transfer area, A , with previously defined subscripts for nanofluid and base fluid. Heat transfer rate ratio for the same heat exchanger with nanofluid and base fluid cases was also developed in this work [95].

$$\frac{Q_{nf}}{Q} = \frac{1 - \exp \frac{NTU_{nf}^{0.22}}{C_r} \exp -C_r NTU_{nf}^{0.78} - 1}{1 - \exp \frac{NTU^{0.22}}{C_r} \exp -C_r NTU^{0.78} - 1} \quad (85)$$

In this equation, C_r is the specific heat ratio of nanofluid to base fluid as stated in Equation (4).

Falahat [96] made a second law analysis of nanofluid flow in coiled tube under constant heat flux boundary condition. Entropy generation number was found for different volumetric fraction of nanofluid and pure fluid by changing the Reynolds number. It was found that the usage of the nanofluids is advantageous for the flow

with Reynolds number lower than 150000 but it is disadvantageous for higher Reynolds number flows. In addition, a pumping power ratio is defined as the ratio of pumping power to heat transfer rate for a specific flow. Pumping power ratio always increases with increasing volumetric fraction. Actually, this is not surprising because heat transfer rate is constant for constant heat flux condition and pumping power should increase with increasing volumetric fraction.

Routbort et al. [97] experimentally investigated the pumping power required for nanofluid flow. They used 2, 4 and 8% Al_2O_3 /water and 2.2% SiC/ethylene glycol-water (50/50) nanofluids in a flowing system. In the experimental setup, torque which drives the nanofluid flow and volumetric flow rate was measured. After completing the experiments, comparison with the conventional theory which was derived for the single phase flow was made and it was concluded that the flow phenomena of nanofluids can be considered as the single phase flow in a system that consists of piping, elbows, and expansions. Therefore, they stated that the usage of conventional friction factor correlations is suitable for nanofluid flows in the turbulent flow region.

Corcione et al. [98] studied turbulent flow heat transfer of nanofluids with constant pumping power in a straight pipe, theoretically. Assuming traditional correlations for heat transfer are applicable for nanofluids, the heat transfer rate was observed for different types of nanofluids at constant pumping power. They investigated constant wall temperature boundary condition with turbulent flow and obtained maximum heat transfer rate for certain values of nanoparticle volumetric fraction. In other words, they observed optimum volumetric fraction of nanofluids at a specified working temperature, particle diameter and other nanofluid properties, Reynolds number, base fluid and length over diameter ratio of the straight pipe.

Additionally, Li and Kleinstreuer [99], Moghaddami et al. [100], and Shokouhmand et al. [101] made theoretical second law analyses for nanofluids in various channels. They obtained optimum operational conditions for nanofluid flow and heat transfer.

To sum up, the research in this area covers a wide range of methods and approaches. These performance analyses were usually done using conventional thermophysical

properties but this situation cannot provide an accurate solution. At first, accurate thermophysical property models should be properly implemented to the system. Then, a suitable way to evaluate performance can be created.

5.3. Evaluation Criterion and Problem Geometry

Among the research surveyed, two studies attracted attention, which are second law studies and the constant pumping power analysis study by Corcione [98]. Actually, second law analysis studies provide the whole picture of the problem. Namely, irreversibilities due to flow and heat transfer are taken into account. However, relative importance of them should be still determined by taking one of them (heat transfer or flow irreversibility) as constant.

As an alternative, Corcione's [98] study provides an easier and practical way for evaluation of "nanofluid heat transfer energetic efficiency". Heat transfer rate comparison at constant pumping power is chosen as the evaluation criterion in the current work, and is improved for further analyses because of the detailed discussion in this section. This study aims to determine an approximate heat transfer performance increment by using constant pumping power analysis for an existing device. A constant heat transfer rate analysis would also be helpful for nanofluid investigation under the consideration of reducing pumping power and saving electrical energy.

In Chapter 4, the analyses were done considering constant Peclet number and increment on heat transfer coefficient ($h_r = h_{nf}/h_f$) was observed. However, pumping power also increases by taking the Peclet number as a constant because a higher velocity is required to balance the enhanced conductivity (See Eq. 56). Increased velocity due to constant Peclet number and increased viscosity due to addition of nanoparticles causes an increment of pumping power. Similarly, Reynolds number is taken as constant in literature widely, but this situation also causes increment on velocity due to viscosity increment; to keep Reynolds number constant.

The important point is how much enhancement can be achieved at constant pumping power for a heat transfer application with this new type of heat transfer fluid. "Energetic efficiency" term is used to express this notion by Corcione [98].

Parallel to the previous chapter of the current study, flow in a straight long pipe is used as in Figure (12) for the determination of affecting parameters and analyses in laminar flow.

5.4. Pressure Drop and Pumping Power of Nanofluids

As discussed, pressure drop and pumping power of nanofluids were investigated by many researchers [16, 97] and they stated that it is reasonable to apply conventional theories existing for Newtonian fluids to nanofluid flow. Therefore, while calculating pumping power of base fluids and nanofluids, Equations (86)-(90) which are adopted from Incropera [64] are used.

Pressure drop for a flow in a straight circular channel can be explained as:

$$\Delta P_f = f_f \cdot \rho_f \cdot \frac{v_{m,f}^2 L}{2D} \quad (86)$$

Here, L is the length of the pipe, and f is the friction factor, and v_m is the mean velocity in the flow. The Darcy friction factor for laminar flow is as defined as follows:

$$f_f = \frac{64}{Re_f} \quad (87)$$

$$Re_f = \frac{v_{m,f} \cdot D \cdot \rho_f}{\mu_f} \quad (88)$$

In the previous equation, Re_f is the Reynolds number for the base fluid.

Because the critical parameter for this application is pumping power, it must also be defined.

$$P_f = \Delta P_f \cdot \frac{m_f}{\rho_f} \quad (89)$$

Here, m_f is mass flow rate of the system.

$$m_f = v_{m,f} \cdot \rho_f \frac{\pi D^2}{4} \quad (90)$$

It is advantageous to have a Reynolds number dependent pumping power expression for further analysis because it is a dimensionless parameter which gives an idea about the flow regime. Therefore, pumping power of fluids can also be expressed as:

$$P_f = \frac{8\pi L Re_f^2 \mu_f^3}{D^2 \rho_f^2} \quad (91)$$

The Equations from (86) to (91) can also be used to calculate nanofluid pumping power by implementing nanofluid properties to the equations, as stated at the beginning of the section. Then, pumping power of nanofluids can be calculated and shown with the proper subscript, “ nf ” according to [16] and [97] as mentioned above.

The key issue in evaluation of heat transfer performance of nanofluids is the constant pumping power case for the current study. As a result,

$$P_f = P_{nf} \quad (92)$$

Using Equations (91) and (92), a Reynolds number ratio can be obtained as below for further analysis in the following sections of this chapter.

$$Re_r = \frac{Re_{nf}}{Re_f} = \frac{\rho_r}{\mu_r^{3/2}} \quad (93)$$

5.5. Performance Ratio for the Two Boundary Conditions

5.5.1. Constant Wall Temperature

With a constant wall temperature boundary condition for a heating or cooling application, the aim is to obtain heat transfer rate as high as possible. In fact, the problem is to increase heat transfer rate by trying different methodologies. One of them is to increase the heat transfer area, as stated in Chapter 1. A newer way of improving heat transfer rate is the usage of nanofluids.

First of all, it is necessary to define fundamental equations for heat transfer in a pipe under the CWT boundary condition for the base fluid. The first law equation for the system in Figure (12) can be expressed as:

$$Q_f = m_f C_f (T_{m,o,f} - T_{m,i}) \quad (94)$$

where $T_{m,o,f}$ and $T_{m,i}$ are exit and inlet mean temperature of the working base fluid and Q_f is the heat transfer rate along the channel for the base fluid case. Inlet temperature of the fluid is specified for the system but outlet temperature should be estimated using an approach suitable for pure fluid and nanofluid heat transfer. The difference between outlet and inlet mean temperatures can be shown as [64]:

$$T_{m,o,f} - T_{m,i} = (T_w - T_{m,i}) \left[1 - \exp\left(-\frac{\pi DL}{m_f C_f} h_f\right) \right] \quad (95)$$

Here, T_w is the constant wall temperature, and h is the average heat transfer coefficient over the channel and is to be estimated for the base fluids. The Equations (94) and (95) can also be used for nanofluid heat transfer without requiring any additional assumption because these are from the first law of thermodynamics and Newton's law of cooling, respectively. Finally, the heat transfer rate ratio between the nanofluid and the base fluid can be defined as in the following equation by implementing the Equations (94) and (95).

$$Q_r = \frac{Q_{nf}}{Q_f} = \frac{m_{nf} C_{nf} \left(1 - \exp\left[-\frac{\pi DL}{m_{nf} C_{nf}} h_{nf}\right]\right)}{m_f C_f \left(1 - \exp\left[-\frac{\pi DL}{m_f C_f} h_f\right]\right)} \quad (96)$$

It is desired to have Q_r for better heat transfer performance for the nanofluid. Namely, if the nanofluid usage is advantageous, Q_r , which is defined as the heat transfer performance for CWT condition, should be greater than 1.

The Equation (96) should be rewritten considering constant pumping power case with the simplest case. Therefore, the newly suggested heat transfer performance equation for CWT condition can be defined using Equations (78), (88), (90), (92), (93), and (96) as follows:

$$Q_r = \frac{\rho_r C_r}{\mu_r^{1/2}} \frac{1 - \exp\left[-4 \frac{Nu_f}{Re_f \cdot Pr_f} \cdot \frac{L}{D} \cdot \frac{Nu_r}{Re_r \cdot Pr_r}\right]}{1 - \exp\left[-4 \frac{Nu_f}{Re_f \cdot Pr_f} \cdot \frac{L}{D}\right]} \quad (97)$$

In this equation, Nusselt values are average Nusselt number of the flow along the channel. Nu_r and Pr_r are the Nusselt number and Prandtl number ratios of the nanofluid and the base fluid.

$$Nu_r = \frac{Nu_{nf}}{Nu_f} \quad (98)$$

$$Pr_r = \frac{Pr_{nf}}{Pr_f} \quad (99)$$

The methodology for CWT condition is to take pumping power as constant and observe the change in heat transfer rate. This is more meaningful than heat transfer coefficient comparison because the heat transfer rate is also dependent on other parameters than heat transfer coefficient. Moreover, the desired physical phenomenon in this problem is to increase the heat transfer rate as much as possible.

Equation (97) may seem somewhat confusing but it represents a relatively simple phenomenon, which depends on relative thermophysical properties defined in Equations (1)-(4), base fluid Graetz number, base fluid Nusselt number, Nusselt

number ratio (Eq. 98) and Reynolds number ratio (Eq. 93). The Equation (97) can be simplified to a new form with the aid of two newly defined parameters as follows:

$$Q_r = \beta \frac{1 - \exp\left(-4 \frac{Nu_f}{Gz_f} \cdot h_r / \beta\right)}{1 - \exp\left(-4 \frac{Nu_f}{Gz_f}\right)} \quad (100)$$

Here, base fluid Graetz number, β and h_r are shown in the following equations, respectively.

$$Gz_f = Re_f \cdot Pr_f \cdot \frac{L}{D}^{-1} \quad (101)$$

$$\beta = \frac{\rho_r C_r}{\mu_r^{1/2}} \quad (102)$$

$$h_r = Nu_r k_r \quad (103)$$

The Nusselt number in Equation (98) is average Nusselt number for CWT condition.

Graetz number is already known by heat transfer researchers and used in the prediction of Nusselt number of thermally developing region of laminar flow. It is also important to note that the Graetz number in Equation (100) and (101) is for the base fluid. Nanofluid Graetz number automatically takes its value according to Equations (93) and (99). Therefore, the nanofluid heat transfer performance can be explained by three main parameters. The first one, Nu_f/Gz_f , is related with only base fluid flow and not affected by nanofluid conditions. It only depends on base fluid flow and heat transfer conditions and properties. The other two components, β and h_r , include relative properties of the nanofluid (ρ_r, C_r, k_r) and relative Nusselt number (Nu_r) compared with the base fluid. The parameter h_r is actually equal to heat transfer enhancement ratio at constant pumping power.

5.5.2. Constant Wall Heat Flux

This performance ratio is developed by using fundamental equations and with a methodology similar to the one used in the previous section. First of all, it should be understood why it is desired to increase the heat transfer coefficient for a CHF condition in a pipe. Actually, the idea behind higher heat transfer coefficient is to obtain lower temperature on the pipe wall. Decrement of the temperature of the pipe wall may be desired because of material or operational conditions. Outlet of the pipe is especially important and the most critical region because there, the wall has the highest temperature. Increased temperature at the wall is the undesired case due to material considerations, generally.

As a result, for this boundary condition, a heat transfer performance suggestion is made by considering the outlet wall temperature of the pipe for nanofluid and base fluid cases at constant pumping power.

By combining Newton's law of cooling shown in Equation (104) and energy balance between inlet and exit section of the pipe shown in Equation (105), the temperature difference between exit region of the wall and inlet mean fluid temperature can be defined as in Equation (106) for the fluid heating case.

$$q'' = h T_{w,o} - T_{m,o} \quad (104)$$

$$T_{m,o} = T_{m,i} + \frac{q'' \pi DL}{mC} \quad (105)$$

$$\Delta T_{w,o} = T_{w,o} - T_{m,i} = \frac{q'' \pi DL}{mC} + \frac{q''}{h} \quad (106)$$

Here, $\Delta T_{w,o}$ is defined as wall temperature difference and q'' is the constant heat flux along the wall. The wall temperature difference is used for comparison between base fluid and nanofluid cases. The comparison criterion is defined as for the fluid heating (wall cooling) case:

$$\Delta T_r = \frac{\Delta T_{w,o}}{\Delta T_{w,o,nf}} = \frac{T_{w,o} - T_{m,i}}{T_{w,o,nf} - T_{m,i}} \quad (1077)$$

It is desired to have a ΔT_r value higher than 1 for a better heat transfer performance with the nanofluid. In other words, if the nanofluid usage is advantageous, ΔT_r , which is defined as the heat transfer performance for CHF condition, is greater than 1.

Equation (107) can be rewritten using Equations (78), (88), (90), (92), (93), (106), and (107) as follows:

$$\Delta T_r = \frac{\frac{q''D}{Nu_f} + \frac{4q''L}{Re_f Pr_f}}{\frac{q''D}{Nu_f} \frac{1}{Nu_r k_r} + \frac{4q''L}{Re_f Pr_f} \frac{1}{Re_r Pr_r}} \quad (108)$$

Similar to the CWT boundary condition, a simplification can be made by using Nusselt number, Graetz number, γ , and β as in Equation (100); hence Equation (109) is obtained. These equations, Equation (100) for CWT and Equation (109) for CHF case represent very similar trends when they are considered as function of the related parameters as will be described in following sections.

$$\Delta T_r = \frac{1 + 4 \frac{Nu_f}{Gz_f}}{\frac{1}{h_r} + \frac{1}{\beta} 4 \frac{Nu_f}{Gz_f}} \quad (109)$$

In this equation, Nusselt number is the base fluid local Nusselt number for CHF condition. Other parameters were defined in Equations (101), (102), and (103), previously.

For better understanding of the nanofluid evaluation criteria for constant wall temperature and constant wall heat flux boundary conditions, a flow chart that shows the methodology followed using the fundamental flow and energy equations is provided in Appendix C.

5.6. Investigation of Affecting Parameters in Fully Developed Region

5.6.1. The Parameter Nu_f/Gz_f

There are many parameters that affect the heat transfer performance of nanofluids. Therefore, it is reasonable to assume some properties to be constant for better understanding of the effect of parameters, individually. As a first approximation, it is reasonable to assume fully developed flow so that the Nusselt number of the base fluid system, Nu_f , can be considered as constant. In addition, it is assumed that the parameters β and h_r are constant for a certain case. In fact, they are nearly constant for a specific nanofluid if the working fluid temperature does not change very much. In an actual case, the variations of the parameters β and h_r in a flow do have a small impact on performance ratio compared to the effect caused by the variation of the parameter Nu_f/Gz_f . Thus, the only parameter remaining is Graetz number.

According to Equations (100) and (109), performance ratio can be expressed by changing Graetz number as in Figure (34). Both CWT and CHF conditions have a similar behavior as shown in Figure (34). The curve in Figure (34) follows a decreasing trend in Q_r or ΔT_r with increasing Nu_f/Gz_f , which means Graetz number should be kept as high as possible for better heat transfer performance of nanofluids.

When components of the Graetz number are considered (Eq. 101), higher Graetz number means higher Reynolds and Prandtl number for the base fluid, and lower length over diameter ratio for the channel. It can be concluded that high Prandtl number fluids have more potential of nanofluid heat transfer performance enhancement. Reynolds number is between 0-2300 for laminar flow and it gives higher performance for nanofluids with values close to 2300. Finally, length over diameter ratio (L/D) for the pipe should be as low as possible, meaning short pipes with larger diameters will provide better performance with nanofluids. On the other hand, these parameters are usually design criteria and cannot be easily changed for a better heat transfer.

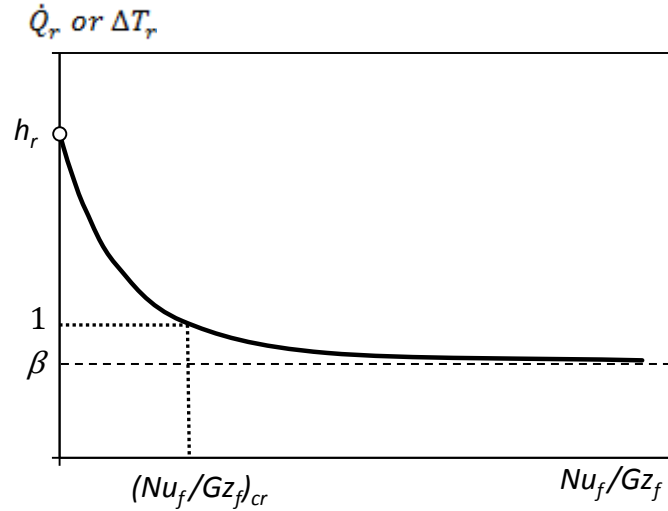


Figure 34 Variation of heat transfer performance ratio with in fully developed region as a function of Nu_f/Gz_f (Eq. 100 or 109)

The trend in Figure (34) is obtained considering $h_r > \beta$ situation which is always valid for nanofluids as will be explained later. As seen, performance ratio is close to h_r value when Graetz number is high although it approaches to β value when Graetz number is low. It means that the performance value is close to h_r if the flow is in thermally developing region and the value is close to β if the flow is far away from the developing region, possibly thermally fully developed.

Additionally, it will be meaningful to define a critical Nu_f/Gz_f value as Nu_f/Gz_f_{cr} , which corresponds to $Q_r = 1$ for CWT boundary condition or $\Delta T_r = 1$ for CHF boundary condition. The nanofluid usage is going to be harmful beyond this point because the performance ratio is smaller than 1 for either boundary condition.

As a result, using high Prandtl number fluids in such systems would be beneficial to increase performance ratio when other variables are considered as constant. Another way of improving performance is to keep high Reynolds number and low length over

diameter ratio. A heat transfer enhancement with nanofluids should be considered when these values are suitable with these conditions. If these conditions are not satisfied, a heat transfer performance lower than 1, lower performance than its base fluid, may be obtained. This situation is caused by the parameter β , which is lower than 1 for nanofluids in this study.

The rest of the analyses in this chapter depend on numerical values of defined parameters β and h_r , and these parameters are related with base fluid and nanoparticle properties.

As stated previously, Graetz number used in the current study is the base fluid Graetz number and it is not constant for the nanofluid that is going to be compared with the base fluid. The nanofluid has its corresponding Graetz number coming from the constant pumping power case.

5.6.2. The Parameter β

The parameter β shown in Equation (102) is clearly dependent on nanofluid properties. Higher relative volumetric heat capacity and lower relative viscosity is desired to obtain a higher β value. Considering Equations (2-5), (7), and (24) by Corcione [28] for the calculation of this parameter, β can be obtained for different type of base fluids with nanoparticles. For comparison, Al_2O_3 , CuO and Cu particles are used with water and ethylene glycol base fluids for the current study. It is observed that the particle selection among the three particles does not change the resultant β value. β values for different volumetric fractions and particle diameters are shown in Figures (35) and (36) for Cu/water and Cu/EG at 20°C, respectively. It is important to note that the variation of β is negligible with changing temperature. However, the trend is not shown, for simplicity.

As seen from the two figures, the values of β decrease with increasing volumetric fraction and particle diameter as expected. On the other hand, it is desired to keep the parameter β as high as possible for a better heat transfer performance. Furthermore, there is no significant difference for different types of nanoparticles, thus; only Cu particle results are presented.

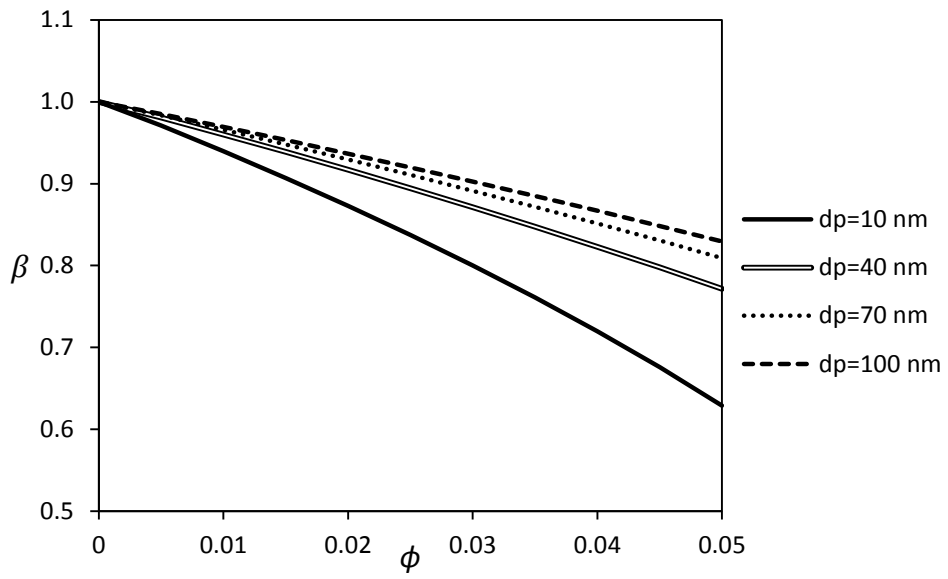


Figure 35 Variation of β parameter with changing volumetric fraction at different particle sizes for Cu/water nanofluid at 20°C (Eq. 5, 7, 24, 102).

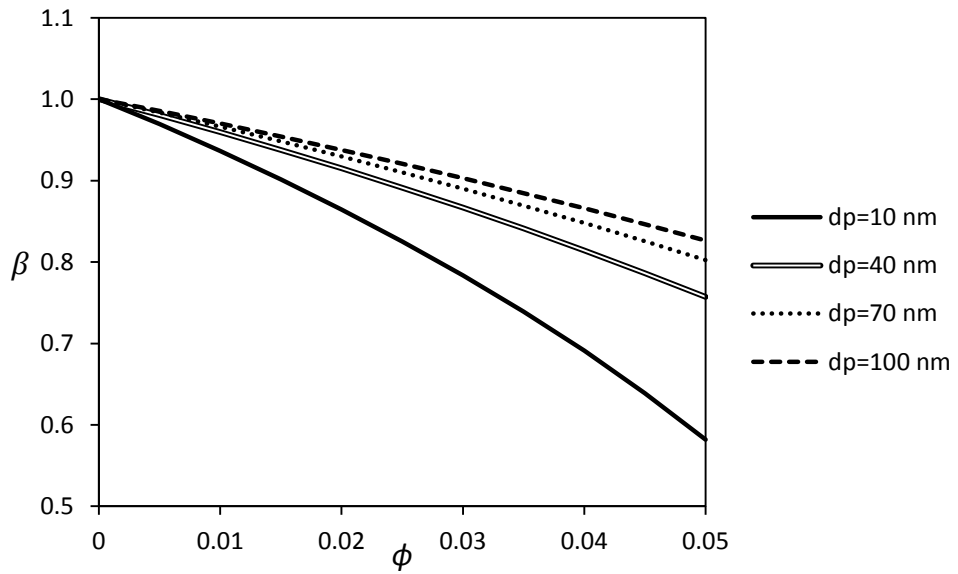


Figure 36 Variation of β parameter with changing volumetric fraction at different particle sizes for Cu/EG nanofluid at 20°C (Eq. 5, 7, 24, 102).

5.6.3. The Parameter h_r

As a first approximation, fully developed region is already assumed for an arbitrary heat transfer application. Considering Chapter 4 and 5, it is important to choose a heat transfer estimation method for Nusselt number. As it is mentioned in Section 3.2.2, the Nusselt number of nanofluid can also increase with the usage of nanofluids. Moreover, the results in the Chapter 4 shows that the nanofluid heat transfer coefficient cannot be predicted accurately by conventional approaches. However, in this case, it is assumed that there is no abnormal enhancement in nanofluid flow for the primitive analyses done in the current study because of simplicity. Therefore, for the fully developed region of fluid flow and heat transfer, Nusselt numbers for both nanofluid and pure fluid are assumed always 4.364 for CHF case and 3.657 for CWT case [86]. The equation for Nusselt number ratio can be considered as in Equation (110) with no abnormal heat transfer assumption:

$$Nu_r = 1 \tag{110}$$

Thus, this parameter, heat transfer coefficient ratio at constant pumping power, is equal to relative conductivity, $h_r = k_r$, for the first approximation with this method. Therefore, the values can be obtained for Al_2O_3 , CuO and Cu particles with base fluids water and ethylene glycol using Equation (19) by Corcione [28]. The Figures (37) and (38) show distribution of the parameter h_r with the assumption given in Equation (108) as a function volumetric fraction and particle diameter.

The detailed discussion of the thermal conductivity was also given in Chapter 2. Moreover, there is no significant difference for different types of nanoparticles, thus; only Cu particle results are presented.

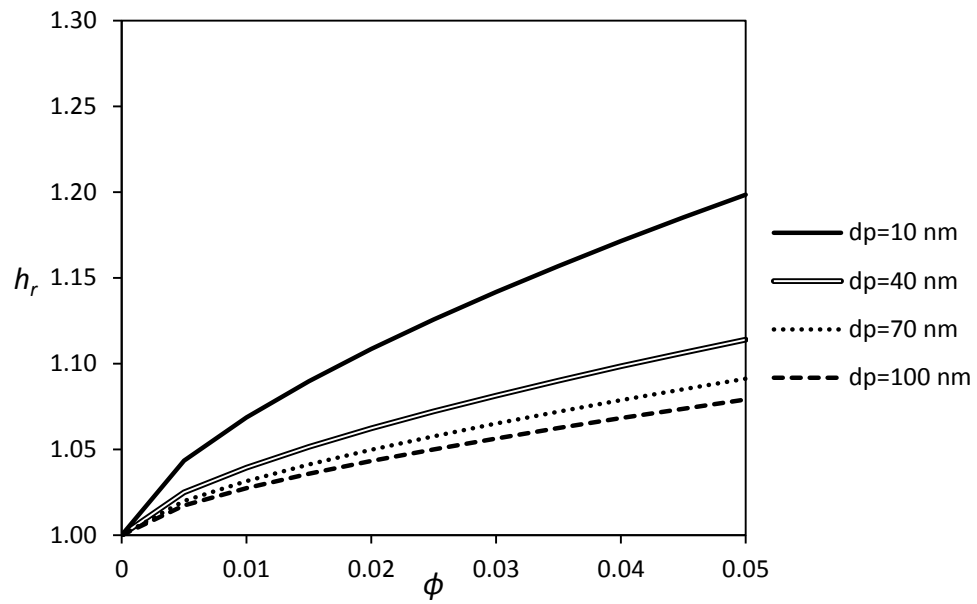


Figure 37 Variation of the parameter h_r with changing volumetric fraction at different particle sizes for Cu/water nanofluid at 20°C (Eq. 19, 103).

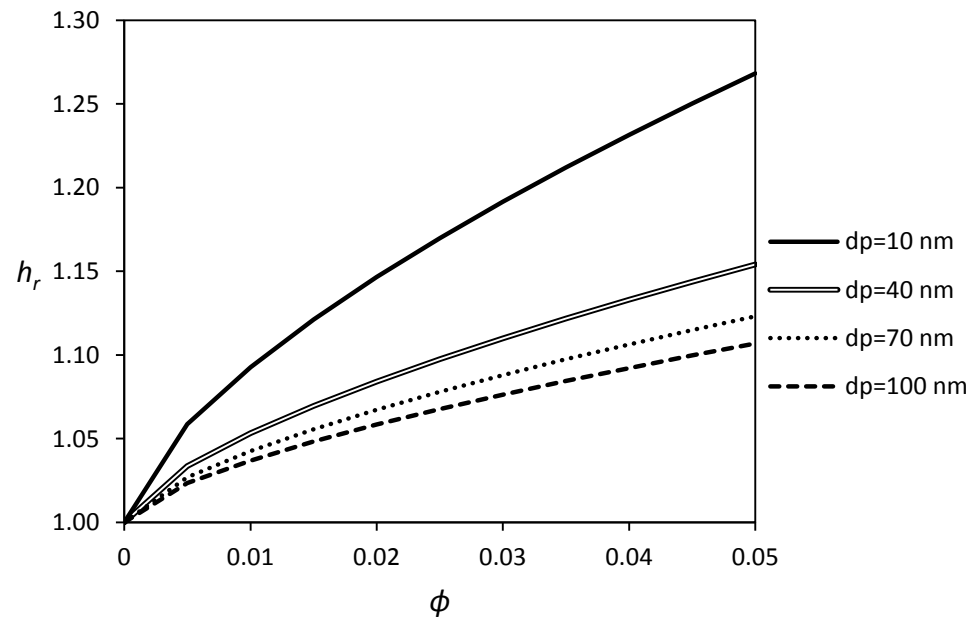


Figure 38 Variation of the parameter h_r with changing volumetric fraction at different particle sizes for Cu/EG nanofluid at 20°C (Eq. 19, 103).

5.7. Maximum Heat Transfer Performance and Optimum Nanofluid Type

As stated in the previous sections, Graetz number depends on the characteristics of the heat transfer problem and very radical changes on it are not possible. On the other hand, the parameters h_r and β are related with nanofluid properties and are subject to change.

Because volumetric fraction of nanoparticles and size of particles in a nanofluid are dominant in determination of these parameters, these are extensively investigated. It can be concluded that h_r and β are oppositely affected by these properties (for example, compare the trends in Figures (35) and (37)) and this situation causes a consideration of optimum nanofluid type for a specific Graetz number.

Therefore, the aim should be the determination of optimum values for different flow configurations with variable Reynolds number, Prandtl number, and length over diameter ratio. Actually, once the solution is obtained for a specific Graetz number, other parameters can be readily calculated for the fully developed region.

Several analyses with various types of Cu/water and Cu/EG nanofluids have been performed. Volumetric fraction variation between 0-5% and particle diameter variation between 10-100 nm are applied to Equation (109). These intervals are determined considering practical nanofluid applications. For example, a nanofluid with nanoparticle diameter 10 nm has not been seen in the literature.

Figures (39) and (40) show heat transfer performance under CHF condition with changing volumetric fractions at different particle diameters for water. The difference between the two figures is the temperature of the working fluid. As seen, there is almost no enhancement at temperature 20°C and a decrement in performance for the nanofluid with respect to the base fluid is observed beyond volumetric fraction 1.5%. However, there is a significant enhancement on the nanofluid performance at 50°C and the enhancement is maximum 6% at 1.5% volumetric fraction in this case. The significant difference between the two fluid temperatures is caused by conductivity and viscosity variation with temperature.

The same analyses are done for Cu/EG nanofluid and a similar trend is obtained as shown in Figures (41) and (42). However, the heat transfer performance enhancement values are larger than Cu/water nanofluid samples. The maximum enhancement is achieved as 11% at nearly 1.8% nanoparticle volumetric fraction.

In addition, it is important to note that the smallest particle diameter ($d_p = 10$ nm) gives the best nanofluid performance for all cases in the current study. A smaller particle diameter is not used because it was not observed smaller nanoparticle diameter in nanofluid research.

These analyses can be repeated for various cases of nanofluids and operational conditions and optimum volumetric fraction and particle diameter for each case can be determined at constant Graetz number. As stated above, the higher base fluid Graetz number means higher performance enhancement and the reverse means poorer performance. Figures (39), (40), (41), and (42) demonstrate the performance of the case $Gz_f = 20$ which is the starting point of the fully developed region. For higher base fluid Graetz number, developing region analysis must be implemented. For lower base fluid Graetz number, the enhancement gradually decreases.

In conclusion, the heat transfer coefficient enhancement at constant Peclet or Reynolds number as is done in most of the literature cannot explain energetic efficiency of nanofluids. One of the alternatives of evaluation of nanofluid heat transfer performance is constant pumping power analysis. In this analysis, pumping power is taken as constant, then; heat transfer rate for CWT condition, or outlet wall temperature for CHF condition is compared between nanofluid and base fluid heat transfer.

The determining parameters on heat transfer performance are found as Graetz number for base fluid, and the parameters h_r and β which depends on relative volumetric heat capacity, viscosity, thermal conductivity, and Nusselt number ratio, that are shown in Equations (101), (102) and (103). All three variables should be high in order to obtain a better heat transfer performance.

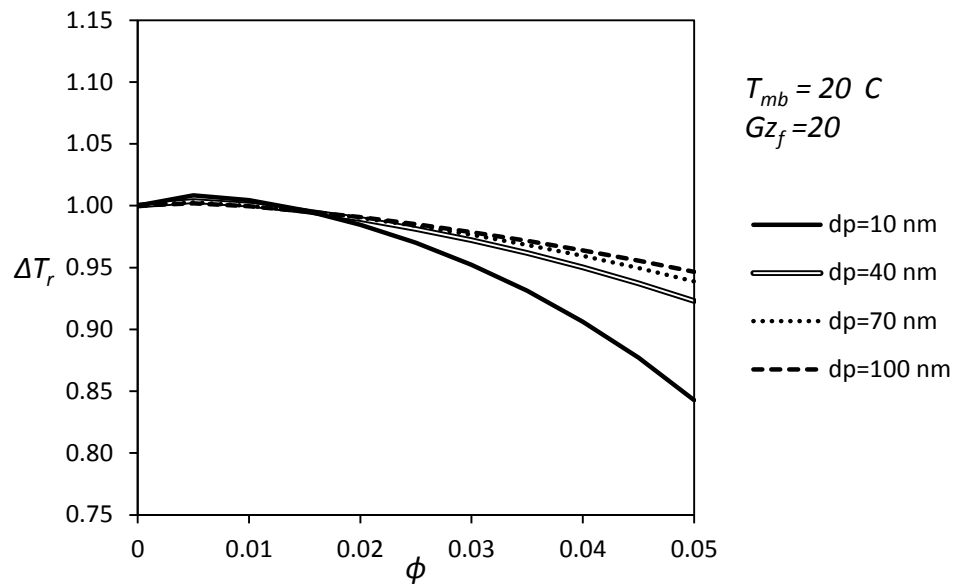


Figure 39 Heat transfer performance ratio for Cu/water nanofluids at different particle diameters for CHF case with fully developed region at Graetz number 20 as a function of volumetric fraction

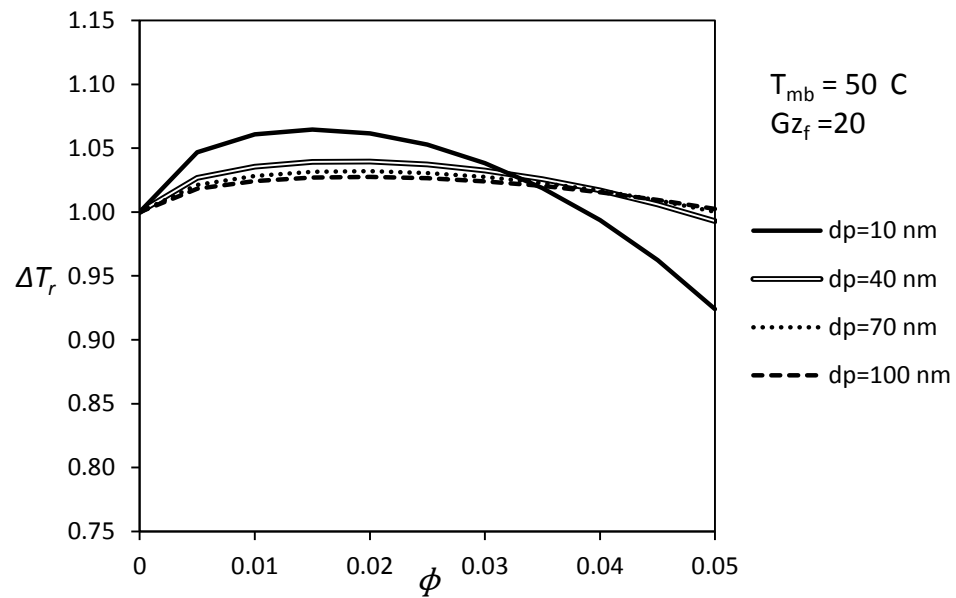


Figure 40 Heat transfer performance ratio for Cu/water nanofluids at different particle diameters for CHF case with fully developed region at Graetz number 20 as a function of volumetric fraction

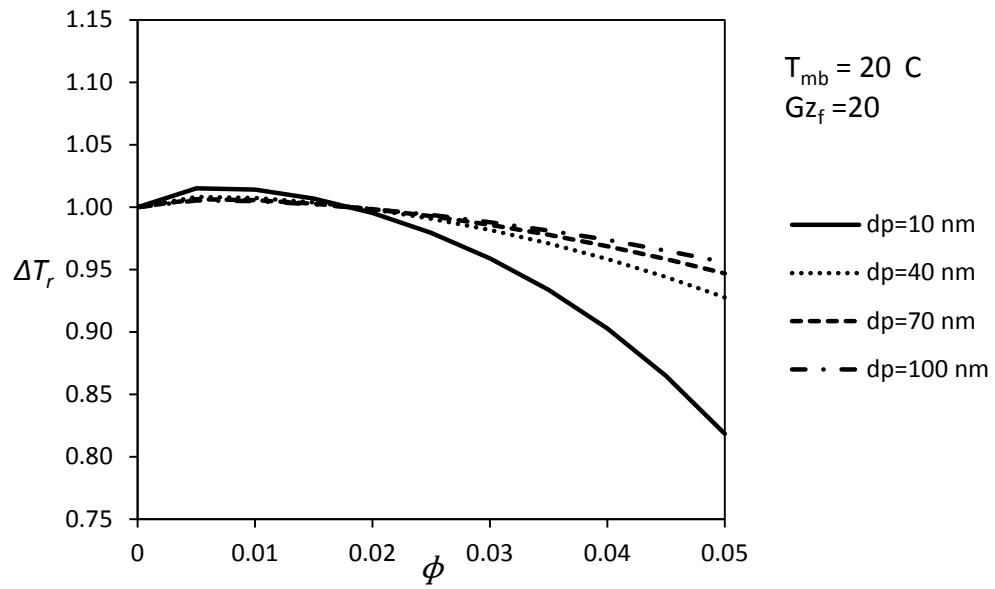


Figure 41 Heat transfer performance ratio for Cu/EG nanofluids at different particle diameters with for CHF case with fully developed region at Graetz number 20 as a function of volumetric fraction

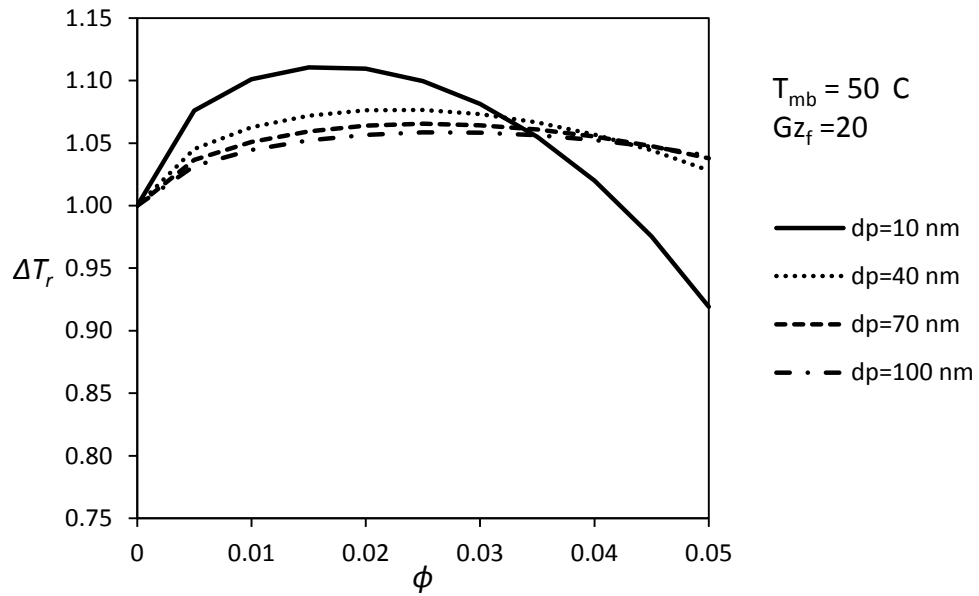


Figure 42 Heat transfer performance ratio for Cu/EG nanofluids at different particle diameters with for CHF case with fully developed region at Graetz number 20 as a function of volumetric fraction

The results show that there may be enhancement or decrement of heat transfer performance by using a nanofluid instead of the base fluid. There is an optimum volumetric fraction value for a specified nanofluid particle size and type, bulk mean temperature, base fluid Graetz number and base fluid type.

The bulk mean temperature of the working fluid significantly affects the enhancement and gives higher enhancement with higher values. Base fluid type also affects the value while there is no significant effect on heat transfer performance enhancement among the three types of nanoparticles, Al_2O_3 , CuO , and Cu . Ethylene glycol as the base fluid provides higher heat transfer performance enhancement compared to water based nanofluids due to change in the properties with the addition of nanoparticles.

Another issue is the Prandtl number effect. If the analyses are performed as a function of base fluid Reynolds number in laminar flow region, EG based nanofluid is going to be more advantageous due to its higher Prandtl number when the Figure (34) and Equation (101) are considered. Here, the constant parameter is always constant pumping power but the nanofluid heat transfer performance is followed only as a function the base fluid Reynolds number. Prandtl numbers of the different heat transfer fluids are also shown in Figure (11) of Chapter 2.

CHAPTER 6

SUMMARY AND CONCLUSION

6.1. Summary

In Chapter 1, the effect on the heat transfer devices of development of engineering systems and possible enhancement on heat transfer are briefly discussed. The heat transfer enhancement can be achieved by increasing the heat transfer area or replacing the heat transfer fluid with a better one. The second subject is the new research area which covers development of nanofluids. Nanofluids are produced by mixing a selected heat transfer fluid and solid nanoparticles at desired volumetric fractions. Nanofluid compositions and preparation techniques are mentioned.

In Chapter 2, thermophysical property estimation of nanofluids in literature and evaluation of thermophysical properties for different nanoparticle and base fluid types are investigated. Thermal conductivity and viscosity for nanofluids especially attract attention, because they do not have a generally predictable behavior. The empirical correlations and theoretical models are investigated for the thermal conductivity and the viscosity, then; suitable models are determined for heat transfer analyses of nanofluids. Finally, all related thermophysical properties are obtained and compared for different nanofluids by using different nanoparticles and base fluids.

In Chapter 3, a literature survey of the convective heat transfer of nanofluids in terms of experimental, theoretical, and numerical studies is done. By considering the survey,

it is decided to use single phase approach for the nanofluid heat transfer modeling in a straight long pipe for constant wall temperature and constant wall heat flux boundary conditions. Single phase assumes that the nanoparticles are homogeneous with the base fluid, hence; these are in thermodynamic equilibrium with the base fluid and there is no relative motion between the particles and the base fluid. The energy equation for the nanofluid convective heat transfer is extracted from the fundamental equations with temperature dependent thermal conductivity and temperature independent density, specific heat, and viscosity assumption. After obtaining the energy equation, it is discretized with finite difference methods and a numerical study is performed with a created original computer code.

In Chapter 4, the results of the numerical study are presented by considering the important parameters in nanofluid convective heat transfer. First, the comparison of the numerical study results with experimental nanofluid results in the literature is performed. Second, the heat transfer coefficients and heat transfer enhancements ($h_r = h_{nf}/h_f$) are evaluated with five different thermal conductivity models for both constant wall temperature and constant wall heat flux boundary conditions. Third, change in the Nusselt number with nanofluids, effect of temperature dependent thermal conductivity on nanofluid prediction, Peclet number, nanoparticle size, axial conduction, and viscous dissipation effects on nanofluid heat transfer are extensively investigated.

In Chapter 5, nanofluid heat transfer performance under consideration of the flow friction is surveyed. It is understood that the most representative approach in evaluation of nanofluid heat transfer performance is to take pumping power as constant and observe heat transfer rate ratio or wall temperature ratio of the nanofluid and base fluid for constant wall temperature or constant wall heat flux boundary condition, respectively. The fundamental equations related with this issue are presented and heat transfer performance Q_r for constant wall temperature boundary condition or ΔT_r for constant wall heat flux boundary condition are extracted from these equations. Then, the effective parameters on heat transfer performance are determined and defined. Finally, some primitive cases are analyzed; maximum heat

transfer performance ratios and optimum nanoparticle volumetric fractions are calculated.

6.2. Conclusion

The nanofluid thermophysical property estimation is vitally important for a realistic convective heat transfer analyses and performance evaluation of the nanofluid heat transfer. Density and specific heat can be accurately predicted by the mixture and thermodynamic equilibrium models, respectively. On the other hand, thermal conductivity and viscosity of the nanofluids cannot be easily predicted and numerous theoretical and empirical models were proposed. Some selected thermal conductivity models are investigated and it is seen that particle diameter, nanoparticle volumetric fraction, a nanofluid temperature are the most important theoretical parameters. In addition, it is observed that Corcione thermal conductivity and viscosity models are the most accurate models for prediction of these nanofluid properties.

An assessment on some selected materials that are candidates to nanoparticle production is made. It is concluded that copper is the best material for nanoparticles. The base fluid effect on nanofluid properties is also investigated for ethylene glycol and water. Ethylene glycol based nanofluids have greater thermal conductivity and viscosity. Because the thermal conductivity and the viscosity have opposite effects on nanofluid heat transfer performance, it is not possible to comment on which one is better.

A literature survey on convective heat transfer of nanofluids showed that the heat transfer behavior of nanofluid may be different than conventional heat transfer fluids. However, there are also nanofluid experimental studies that show the same behavior with conventional fluids. As a result, both single phase and two phase approaches were used in the literature. In the current study, nanofluid convective heat transfer is investigated with temperature dependent thermal conductivity and single phase assumption.

The results showed that the nanofluid usage significantly increases the heat transfer coefficient for laminar flow at constant Peclet number. The promising technology

provides cheaper nanofluid production solutions. Usage of nanofluids in heat transfer applications may become widespread with development of the nanofluid heat transfer research. Another important advantage of the nanofluids is that; they do not require a modified geometry; they can be directly replaced with its substitute heat transfer fluid. Previously designed heat transfer devices are suitable for nanofluid heat transfer operation if an advantage can be obtained. Namely, the cost of design and production of higher heat transfer capable devices may not be required with the aid of nanofluids.

The results from the current numerical study in Chapter 4 give these practical results:

- The large portion of nanofluid heat transfer coefficient enhancement is coming from the thermal conductivity enhancement of nanofluids. The change in the Nusselt number is 1% for the fully developed region while it is below 1% in thermally developing region.
- When constant wall temperature and constant wall heat flux boundary conditions are considered, there is a slightly different trend in heat transfer coefficient enhancement. CWT condition has a relatively constant heat transfer coefficient enhancement while CHF condition has an increasing trend. Because the critical parameter in CHF condition is the outlet wall temperature of the fluid, it can be said that this result is advantageous for the CHF condition.
- Temperature dependent thermal conductivity approach gives more accurate results than constant conductivity assumption along the channel. Even though Nusselt number does not change very much, the difference in heat transfer coefficient values can be up to 20% with the two different approaches.
- Bulk mean temperature of the fluid along the channel changes with changing Peclet number, hence; the heat transfer coefficient, which is strongly dependent on temperature, decreases. In addition, when the effect of the increase in Reynolds number is investigated between the pure fluid and the nanofluid, it is seen that heat transfer coefficient in thermally developing region increases because the nanofluid Prandtl number is higher than the pure fluid Prandtl number.
- The heat transfer coefficient enhancement increases with increasing nanoparticle volumetric fraction. This is true for all thermal conductivity models.

- Nanoparticle size is not important for Hamilton Crosser model while the other four thermal conductivity models, Chon, Corcione, Koo Kleinstreuer, and Sitprasert models, are affected by it. Because the Hamilton Crosser model is proposed for micro and macro sized particles, it does not reflect the reality for the nanofluids. Heat transfer coefficient and thermal conductivity increases with decreasing nanoparticle size.
- Hamilton Crosser provides very low heat transfer coefficient and Sitprasert is very sensitive to nanoparticle size. The other three thermal conductivity models, Chon, Corcione, Koo Kleinstreuer give similar results.
- Because the Corcione model is created by considering extensive experimental data, it is decided that it gives the most accurate results. In addition, the current numerical study results are verified with the Corcione model using experimental convective heat transfer data in the literature. Therefore, it is advised to use this model in order to obtain generalized results.
- There is no difference between nanofluid and pure fluid in regard to the effect of axial conduction on the heat transfer coefficient.
- Viscous dissipation cannot be ignored for certain cases, especially for nanofluid flow and heat transfer in microchannels. It can be checked by evaluating the Brinkman number. Brinkman number is always greater for the nanofluid than the pure fluid at constant Peclet number analysis, because of the increased viscosity of nanofluids.

Evaluation of heat transfer performance is also analyzed by considering constant pumping power case and observing the heat transfer performance criterion, which depends on the boundary condition, for the nanofluids and the base fluids.

It is concluded that heat transfer performance depends on three important parameters for the fully developed region for either CWT or CHF boundary conditions. Actually, the theoretical analysis gives similar results for the two boundary conditions but may have slightly different performance ratios. The three important parameters depend on nanofluid thermophysical properties and nanofluid convective heat transfer behavior. As a first approximation, it is considered that the pure fluid Nusselt number is equal to

the nanofluid Nusselt number for the fully developed region. The results are obtained with this assumption and following discussion is given:

- The parameter Nu_f/Gz_f has a significant effect on nanofluid heat transfer performance. The performance ratio (Q_r or ΔT_r) is between h_r and β depending on the value of Nu_f/Gz_f . If this parameter is very high, the performance enhancement approaches β , which is smaller than 1, thus; a decrement on performance is obtained. In this situation, the nanofluid usage brings a disadvantage instead of providing an enhancement and must not be used. If it is close to zero, the performance ratio is close to h_r , which is always larger than 1 for the fully developed laminar flow. The advantage of the nanofluids can be utilized in this situation.
- The parameter β ($= \rho_r C_r / \mu_r^{1/2}$), has its maximum value, 1, for pure fluids. It decreases with increasing particle diameter and nanoparticle volumetric fraction. However, it should be kept high for better heat transfer performance.
- The parameter h_r ($= Nu_r k_r$), has its minimum value, 1, for pure fluids. It increases with increasing particle diameter and nanoparticle volumetric fraction. It should also be high for better heat transfer performance.
- There is a contradictory result between desired trends of β and h_r . This situation causes to think optimum nanofluid properties that provide the best heat transfer performance for a certain Nu_f/Gz_f value.
- The optimum values are obtained for water and ethylene glycol base fluids with copper nanoparticles using CHF boundary condition at Graetz number 50 and fully developed region ($Nu_f = 4.36$ & $Nu_r = 1$). The sample case shows that the smallest particle diameter (10 nm) always has the highest performance ratio with different nanoparticle volumetric fraction for different cases.

To sum up, it can be said that the property and heat transfer estimation studied in Chapters 2, 3, and 4 are important to observe an accurate heat transfer performance considering pumping power as it is done in Chapter 5. Therefore, Chapter 5

determines the benefit of nanofluid usage and it is the most important issue in the current study.

6.3. Future Work

First, it is seen that the experimental studies in the literature on thermophysical properties contradict each other. More experimental studies are required for a better prediction of heat transfer. Additionally, it is imperative to record all factors that affect the nanofluid thermal conductivity and viscosity in experiments. Moreover, the thermophysical property data for different types of base fluids such as engine oil and R-134a are very limited so that new experiments on this issue are required.

Second, the experimental studies on convective heat transfer of nanofluids are also insufficient to comment on heat transfer behavior of nanofluids. Actually, the researchers should conduct both thermophysical property and convective heat transfer experiments on nanofluids with the same nanofluid. Otherwise, the Nusselt number results calculated from convective heat transfer experiments includes the uncertainty of the thermal conductivity model used in conductivity estimation.

Numerical studies should be performed by considering Buongiorno's arguments [18]. The results can be used to estimate heat transfer coefficient of nanofluids. Then, correlations with wide application ranges can be derived from analyses and they can be compared with experimental studies.

The heat transfer performance evaluation of nanofluids is the most important gap in the literature. An evaluation criterion is created for the nanofluids in Chapter 5. This criterion can be performed for turbulent and developing region of laminar flow. The current study shows a pathway for evaluation, but the analyses are limited to fully developed region with conventional heat transfer analysis approach. Nusselt number ratio can be estimated with newly developed nanofluid heat transfer correlations for more accurate results.

Heat transfer oil based nanofluids should be investigated extensively. They have higher Prandtl number, lower thermal conductivity, thus; they have more nanofluid

heat transfer performance enhancement potential. However, they cannot be theoretically studied because there is no sufficient experimental data or information on their thermophysical properties and convectional heat transfer behaviors.

The theoretical performance analyses can be repeated for different regions of turbulent and nanofluid flow. The length and diameter of the pipe, Reynolds number and Prandtl number effects can be systematically investigated. Various correlations can be derived to determine the optimum nanofluid properties at certain flow and heat transfer cases. Such a study may be similar to Corcione's study [97] but the affecting parameters should be followed for a parametric study.

The analyses for the heat transfer performance ratio can be extended to different types of base fluids and the most suitable heat transfer fluids for the nanofluid heat transfer enhancement can be determined. Therefore, the research can be focused on these fluids.

REFERENCES

- [1] Ahuja A. S., (1975), Augmentation of Heat Transport in Laminar Flow of Polystyrene Suspensions. I. Experiments and Results, *Journal of Applied Physics*, Vol. 46 (8), pp. 3408-3416.
- [2] Ahuja A. S., (1982), Thermal Design of a Heat Exchanger Employing Laminar Flow of Particle Suspensions, *International Journal of Heat and Mass Transfer*, Vol. 25 (5), pp. 725-728.
- [3] Choi S.U.S., (1995), Enhancing thermal conductivity of fluid with nanoparticles, *Developments and Applications of Non-Newtonian Flows*, IN: Siginer D.A., Wang H. P. (Eds.), ASME, New York, FED V. 231/MD-Vol.66, pp. 99-105.
- [4] Das S. K., Putra N., Thiesen P., Roetzel W., (2003), Temperature Dependence of Thermal Conductivity Enhancement for Nanofluids, *Journal of Heat Transfer*, Vol. 125, pp. 567-574.
- [5] Chandrasekar M., Suresh S., Bose A. C., (2010), Experimental investigations and theoretical determination of thermal conductivity and viscosity of Al_2O_3 /water nanofluid, *Experimental Thermal and Fluid Science*, Vol. 34, pp. 210-216.
- [6] Chon, C. H., Kihm, K. D., Lee, S. P., and Choi, S. U. S., (2005), Empirical Correlation Finding the Role of Temperature and Particle Size for Nanofluid (Al_2O_3) Thermal Conductivity Enhancement, *Applied Physics Letters*, Vol. 87(15), pp. 153107.
- [7] Duangthongsuk W., Wongwises S., (2009), Measurements of temperature-dependent thermal conductivity and viscosity of TiO_2 (21 nm)/water nanofluids, *Experimental Thermal and Fluid Science*, Vol. 33, pp. 706-714.
- [8] Hong T. K., Yang H. S., Choi C. J., (2005), Study of the enhanced thermal conductivity of Fe nanofluids, *Journal of Applied Physics*, Vol. 97, 064311.

- [9] Park E. J., Park S. D., Bang I. C., Park Y. B., Park H. W., (2012), Critical heat flux characteristics of nanofluids based on exfoliated graphite nanoplatelets (xGnPs), *Materials Letters*, 81, pp. 193-197.
- [10] Nasiri A., Niasar M. S., Rashidi A. M., Khodafarin R., (2012), Effect of CNT structures on thermal conductivity and stability of nanofluid, *International Journal of Heat and Mass Transfer*, 55, pp. 1529-1535.
- [11] Souza N. S., Rodrigues A. D., Cardoso C. A., Pardo H., Faccio R., Mombru A. W., Galzerani J. C., Lima O. F. de, Sergeenkov S., Moreira F. M. A., (2012), Physical properties of nanofluid suspension of ferromagnetic graphite with high Zeta potential, *Physics Letters A*, Vol. 376, pp. 544-546.
- [12] Nasiri A., Niasar M. S., Rashidi A., Amrollahi A., Khodafarin R., (2011), Effect of dispersion method on thermal conductivity and stability of nanofluid, *Experimental Thermal and Fluid Science*, Vol. 35, pp. 717-723.
- [13] Chen L., Xie H., (2009), Silicon oil based multiwalled carbon nanotubes nanofluid with optimized thermal conductivity enhancement, *Colloids and Surfaces A: Physicochemical and Engineering Aspects*, Vol. 352, pp. 136-140.
- [14] Yu W., Xie H., Li Y., Chen L., Wang Q., (2011), Experimental investigation on the thermal transport properties of ethylene glycol based nanofluids containing low volume concentration diamond nanoparticles, *Colloids and Surfaces A: Physicochemical and Engineering Aspects*, Vol. 380, pp. 1-5.
- [15] Li Y., Zhou J., Tung S., Schneider E., Shengqi X., (2009), A review on development of nanofluid preparation and characterization, *Powder Technology*, Vol. 196, pp. 89-101.
- [16] Pak B. C., Cho Y. I., (1998), Hydrodynamic and heat transfer study of dispersed fluids with submicron metallic oxide particles, *Experimental Heat Transfer: A Journal of Thermal Energy Generation, Transport, Storage, and Conversion*, Vol. 11(2), pp. 151-170.
- [17] Sommers A. D., Yerkes K. L., (2010), Experimental investigation into the convective heat transfer and system level effects of Al₂O₃-propanol nanofluids, *Journal of Nanoparticle Research*, Vol. 12, pp. 1003-1014.

- [18] Buongiorno J., (2006), Convective transport in nanofluids, *Journal of Heat Transfer*, Vol. 128, pp. 240-250.
- [19] Zhou S. Q., Ni R., (2008), Measurement of the specific heat capacity of water based Al_2O_3 nanofluid, *Applied Physics Letters*, Vol. 92, 093123-1.
- [20] Prasher, R., Phelan, P. E., and Bhattacharya, P., (2006), Effect of Aggregation Kinetics on the Thermal Conductivity of Nanoscale Colloidal Solutions (Nanofluid), *Nano Letters*, Vol. 6(7), pp. 1529-1534.
- [21] Maxwell J.C., (1873), *A treatise on electricity and magnetism*, Clarendon Press, Oxford.
- [22] Choi S. U. S., Eastman J. A., (1995), Enhancing Thermal Conductivity of Fluids with Nanoparticles, *ASME International Mechanical Engineering Congress & Exposition*, November 12-17, San Francisco, CA.
- [23] Hamilton, R. L., and Crosser, O. K., (1962), Thermal Conductivity of Heterogeneous Two-Component Systems, *Industrial & Engineering Chemistry Fundamentals*, Vol. 1(3), pp. 187-191.
- [24] Lee, S., Choi, S. U. S., Li, S., and Eastman, J. A., (1999), Measuring Thermal Conductivity of Fluids Containing Oxide Nanoparticles, *Journal of Heat Transfer*, Vol. 121(2), pp. 280-289.
- [25] Koo J., Kleinstreuer C., (2004), A new thermal conductivity model for nanofluids, *Journal of Particle Research*, Vol. 6, pp. 577-588.
- [26] Sitprasert C., Dechaumphai P., Juntasaro V. , (2009), A thermal conductivity model for nanofluids including effect of temperature dependent interfacial layer, *Journal of Nanoparticle Research*, Vol. 11, pp. 1465-1476.
- [27] Leong K. C., Yang C., Murshed S. M. S., (2006), A model for the thermal conductivity of nanofluids – the effect of interfacial layer, *Journal of Nanoparticle Research*, Vol. 8(2), pp. 245-254.
- [28] Corcione M., (2011), Empirical correlating equations for predicting the effective thermal conductivity and dynamic viscosity of nanofluids, *Energy Conversion and Management*, 52, pp. 789–793.

- [29] Masuda H., Ebata A., Teramae K., Hishinuma N., (1993), Alteration of thermal conductivity and viscosity of liquid by dispersing ultra-fine particles (Dispersion of Al_2O_3 , SiO_2 , and TiO_2 ultra-fine particles), *Netsu Bussei*, 4, pp. 227-233.
- [30] Eastman J.A., Choi S. U. S., Li S., Yu W., Thompson L. J., (2001), Anomalously increased effective thermal conductivity of ethylene glycol-based nanofluids containing copper nanoparticles, *Applied Physics Letters*, Vol. 78, pp. 718-720.
- [31] Chon C. H., Kihm K. D., (2005), Thermal conductivity enhancement of nanofluids by Brownian motion, *Journal of Heat Transfer*, 127(8), p. 810.
- [32] Murshed S. M. S., Leong K. C., Yang C., (2008), Investigations of Thermal Conductivity and Viscosity of Nanofluids, *International Journal of Thermal Sciences*, Vol. 47, pp. 560-568.
- [33] Mintsa H.A. , Roy G., Nguyen C. T., Doucet D., (2009), New temperature dependent thermal conductivity data for water-based nanofluids, *International Journal of Thermal Sciences* , Vol. 48, pp. 363–371.
- [34] Xuan Y., Li Q., Zhang X., Fujii M., (2006), Stochastic thermal transport of nanoparticle suspensions, *Jornal of Applied Physics*, Vol. 100, 043507.
- [35] Özerinç S., Kakaç S., Yazıcıoğlu A. G., (2010), Enhanced thermal conductivity of nanofluids: a state of the art review, *Microfluid Nanofluid*, Vol. 8, pp. 145-170.
- [36] Chandrasekar M., Suresh S., Senthilkumar T., (2012), Mechanisms Proposed through experimental investigations on thermophysical properties and forced convective heat transfer characteristics of various nanofluids, *Renewable and Sustainable Energy Reviews*, Vol. 16, pp. 3917-3938.
- [37] Jang S. P., Choi S. U. S., (2007), Effects of various parameters on nanofluid thermal conductivity, *Journal of Heat Transfer* , Vol. 129, pp. 618–623.
- [38] Prasher R., Bhattacharya P., Phelan P. E., (2005), Thermal conductivity of nanoscale colloidal solutions (nanofluids), *Physical Review Letters*, Vol. 94, 025901.
- [39] Kumar D. H., Patel H. E., Kumar V. R. R., Sundararajan T., Pradeep T., Das S. K., (2004), Model for heat conduction in nanofluids, *Physical Review Letters*, Vol. 93, 144301.

- [40] Xuan Y., Li Q., Hu W., (2003), Aggregation structure and thermal conductivity of nanofluids, *AIChE Journal*, Vol. 49, pp. 1038–1043.
- [41] Xie H., Fujii M., Zhang X., (2005), Effect of interfacial nanolayer on the effective thermal conductivity of nanoparticle–fluid mixture, *International Journal of Heat and Mass Transfer*, Vol. 48, pp. 2926–2932.
- [42] Xue Q., Xu W. M., (2005), A model of thermal conductivity of nanofluids with interfacial shells, *Materials Chemistry and Physics*, Vol. 90, pp. 298–301.
- [43] Yu W., Choi S. U. S., (2003), The role of interfacial layers in the enhanced thermal conductivity of nanofluids: a renovated Maxwell model, *Journal of Nanoparticle Research*, Vol. 5, pp. 167–171.
- [44] Wang B. X., Zhou L. P., Peng X. F., (2003), A fractal model for predicting the effective thermal conductivity of liquid with suspension of nanoparticles, *International Journal of Heat and Mass Transfer*, Vol. 46, pp. 2665–2672.
- [45] Feng Y., Yu B., Xu P., Zou M., (2007), The effective thermal conductivity of nanofluids based on the nanolayer and the aggregation of nanoparticles, *Journal of Physics D: Applied Physics*, Vol. 40, pp. 3164–3171.
- [46] Einstein A., (1906), A New Determination of the Molecular Dimensions, *Annalen Der Physik*, Vol. 324(2), pp. 289-306.
- [47] Maiga E. B., Nguyen C. T., Galanis N., Roy G., (2004), Heat transfer behaviors of nanofluids in a uniformly heated tube, *Superlattices and Microstructures*, Vol.35, pp.543 -557.
- [48] Nguyen C. T., Desgranges F., Galanis N., Roy G., Mare T., Boucher S., Mintsa H. A., (2008), Viscosity Data for Al₂O₃/water Nanofluid-Hysteresis: Is Heat Transfer Enhancement Using Nanofluids Reliable, *International Journal of Thermal Sciences*, Vol. 47, pp. 103-111.
- [49] Prasher R., Song D., Wang J., Phelan P., (2006), Measurements of Nanofluid Viscosity and its Implications for Thermal Applications, *Applied Physics Letters*, Vol. 89, 133108.
- [50] Vasheghani M., Marzbanrad E., Zamani C., Aminy M., Raissi B., Ebadzadeh T., Bafrooei H. B., (2011), Effect of Al₂O₃ phases on the enhancement of thermal

- conductivity and viscosity of nanofluids in engine oil, *Heat and Mass Transfer*, Vol. 47, pp. 1401-1405.
- [51] Wang X., Xu X., Choi S.U.S., (1999), Thermal conductivity of nanoparticles-fluid mixture, *Journal of Thermophysics Heat Transfer*, Vol. 13 (4) , pp. 474-480.
- [52] Das S. K., Putra N., Roetzel W., (2003), Pool boiling characteristics of nanofluids. *International Journal of Heat and Mass Transfer*, Vol. 46, pp. 851–862.
- [53] Putra N., Roetzel W., Das S. K., (2003), Natural convection of nano-fluids, *Heat and Mass Transfer*, Vol. 39, pp. 775–784.
- [54] He Y., Jin Y., Chen H., Ding Y., Cang D., Lu H., (2007), Heat transfer and flow behaviour of aqueous suspensions of TiO₂ nanoparticles (nanofluids) flowing upward through a vertical pipe, *International Journal of Heat and Mass Transfer*, Vol. 7(50), pp. 2272–2281.
- [55] Chen H., Ding Y., Tan C., (2007), Rheological behaviour of nanofluids, *New Journal of Physics*, Vol.9, 367.
- [56] Chen H., Ding Y., He Y., Tan C., (2007), Rheological behaviour of ethylene glycol based titania nanofluids, *Chemical Physics Letters*, Vol. 444, pp. 333-337.
- [57] Chevalier J., Tillement O., Ayela F., (2007), Rheological properties of nanofluids flowing through microchannels, *Applied Physics Letters*, Vol. 91, 233103.
- [58] Lee J. H., Hwang K. S., Jang S. P., Lee B. H., Kim J. H., Choi S. U. S., (2008), Effective viscosities and thermal conductivities of aqueous nanofluids containing low volume concentrations of Al₂O₃ nanoparticles, *International Journal of Heat and Mass Transfer*, Vol. 51, 2651–2656.
- [59] Garg J., Poudel B., Chiesa M., Gordon J. B., Ma J. J., Wang J. B., (2008), Enhanced thermal conductivity and viscosity of copper nanoparticles in ethylene glycol nanofluid, *Journal of Applied Physics*, Vol. 103, 074301.
- [60] Kumar P. C. M., Kumar J., Suresh S., (2012), Review on Nanofluid Theoretical Viscosity Models, *International Journal of Engineering Innovation & Research*, Vol. 1(2), pp. 2277-5668.E
- [61] Krieger L. M., Dougherty T. J., (1959), A mechanism for non-Newtonian Flow in Suspensions of Rigid Spheres, *Transactions of the Society of Rheology*, Vol. 3, pp. 137-152.

- [62] Niesen L. E., (1970), Generalized Equation for the Elastic Moduli of Composite Materials, *Journal of Applied Physics*, Vol. 41, pp. 4626-4627.
- [63] Bachelor G. K., (1977), The effect of Brownian Motion on the Bulk Stress in a Suspensions of Spherical Particles, *Journal of Fluid Mechanics*, Vol. 83, pp. 97-117.
- [64] Incropera, F. P., DeWitt D. P., Bergman T. L., Lavine A. S., (2006), *Fundamentals of Heat Transfer*, Sixth ed., John Wiley & Sons, New York.
- [65] Rohsenow W. M., Hartnett J. P., Cho Y. I., (1998), *Handbook of Heat Transfer*, Third Ed., The McGraw-Hill, New York.
- [66] Li Q., Xuan Y., (2002), Convective heat transfer and fluid flow characteristics of Cu-water nanofluid, *Science in China (Series E)*, Vol. 45(4), pp. 408-416.
- [67] Xuan Y., Li Q., (2003), Investigation on convective heat transfer and flow features of nanofluids, *Journal of Heat Transfer*, Vol. 125, pp. 151-155.
- [68] Winterton R. H. S., Where did the Dittus and Boelter equation come from?, *International Journal of Heat and Mass Transfer*, Vol. 41, pp. 809-810.
- [69] Wen D., Ding Y., (2004), Experimental investigation into convective heat transfer of nanofluids at the entrance region under laminar flow conditions, *International Journal of Heat and Mass Transfer*, Vol. 47, pp. 5181-5188.
- [70] Heris, S. Z., Etemad, S., and Esfahany, M. N., (2006), Experimental Investigation of Oxide Nanofluids Laminar Flow Convective Heat Transfer, *International Communications in Heat and Mass Transfer*, Vol. 33(4), pp. 529-535.
- [71] Rea U., McKrell T., Hu L., Buongiorno J., (2009), Laminar convective heat transfer and viscous pressure loss of alumina–water and zirconia–water nanofluids, *International Journal of Heat and Mass Transfer*, Vol. 52, pp. 2042-2048.
- [72] Anoop K.B., Sundararajan T., Das S.K., (2009), Effect of particle size on the convective heat transfer in nanofluid in the developing flow, *International Journal of Heat and Mass Transfer*, Vol. 52, pp. 2189-2195.
- [73] Dunangthongsuk W., Wongwises S., (2010), An experimental study on the heat transfer performance and pressure drop of TiO₂-water nanofluids flowing under a

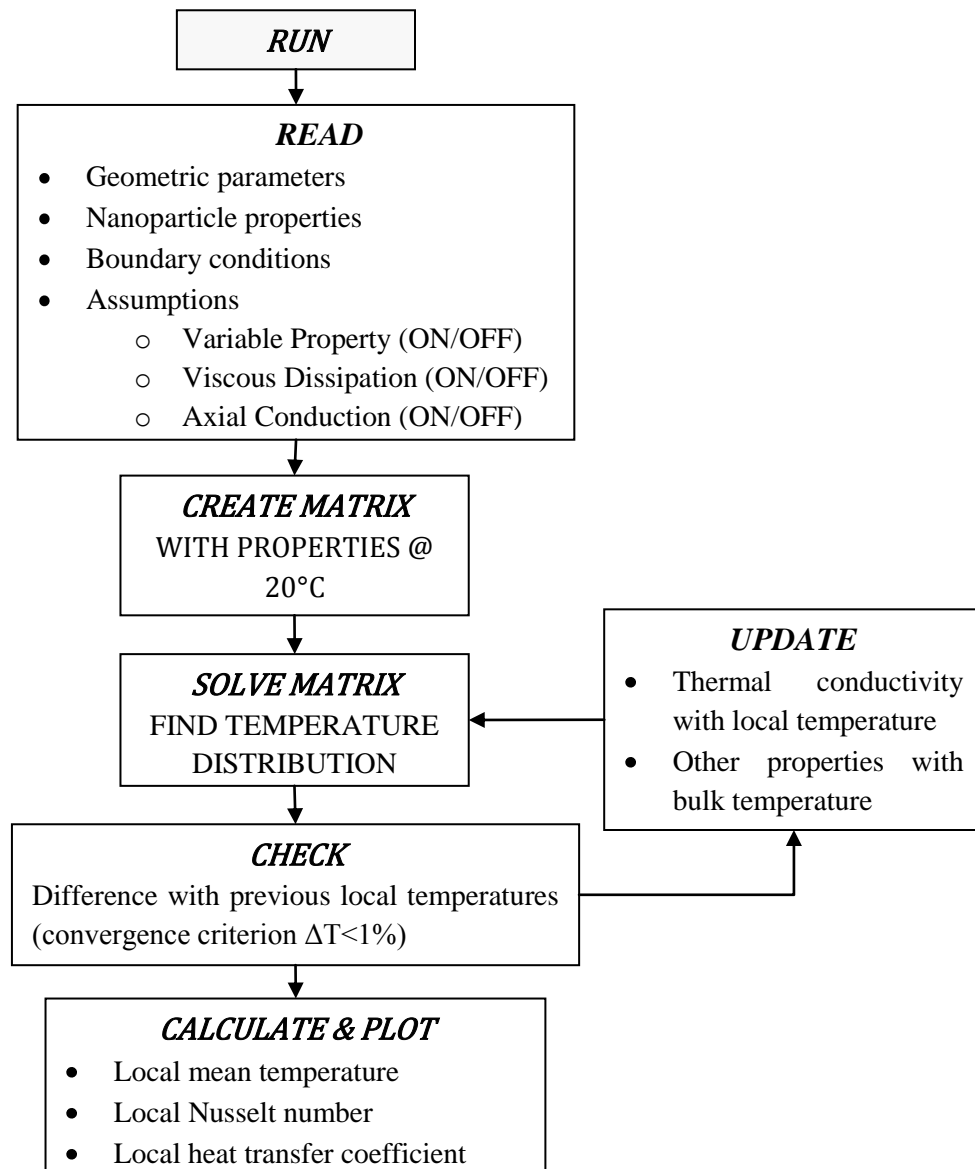
- turbulent flow regime, *International Journal of Heat and Mass Transfer*, Vol. 53, pp. 334-344.
- [74] Kim, D., Kwon, Y., Cho, Y., Li, C., Cheong, S., Hwang, Y., Lee, J., Hong, D., Moon, S., (2009), Convective Heat Transfer Characteristics Of Nanofluids Under Laminar And Turbulent Flow Conditions, *Current Applied Physics*, Vol. 9(2), pp. e119–e123.
- [75] Lai W. Y., Vinod S., Phelan P. E., Prasher R., (2009), Convective heat transfer for water-based Alumina nanofluids in a single 1.02-mm tube, *Journal of Heat Transfer*, Vol. 131, 112401-1.
- [76] Mills P., Snabre P., (1995), Rheology and structure of concentrated suspensions of hard spheres, shear induced particle migration, *Journal of Physics II*, Vol. 5, pp. 1597-1608.
- [77] Chandrasekar M., Suresh S., Bose A. C., (2010), Experimental studies on heat transfer and friction factor characteristics of Al₂O₃/water nanofluid in a circular pipe under laminar flow with wire coil inserts, *Experimental Thermal and Fluid Science*, Vol. 34, pp.122-130.
- [78] Xuan Y., Roetzel W., (2000), Conceptions for heat transfer correlation of nanofluids, *International Journal of Heat and Mass Transfer*, Vol. 43, pp. 3701-3707.
- [79] Pope S. B., (2000), *Turbulent Flows*, Cambridge University Press, Cambridge.
- [80] Gnielinski V., (1976), New Equations for Heat and Mass Transfer in Turbulent Pipe and Channel Flow, *Industrial and Engineering Chemistry*, Vol. 16, pp. 359–368.
- [81] Sarkar J., (2011), A critical review on convective heat transfer correlations of nanofluids, *Renewable and Sustainable Energy Reviews*, Vol. 15, pp. 3271-3277.
- [82] Kakaç S., Pramuanjaroenkij A., (2009), Review of convective heat transfer enhancement with nanofluids, *International Journal of Heat and Mass Transfer*, Vol. 52, pp. 3187-3196.
- [83] Maiga S. B., Palm S. J., Nguyen C. T., Roy G., Galanis N., (2005), Heat transfer enhancement by using nanofluids in forced convection flows, *International Journal of Heat and Fluid Flow*, Vol. 26, pp. 530-546.

- [84] Raisee M., Moghaddami M., (2008), Numerical Investigation of Laminar Forced Convection of Nanofluids through Circular Pipes, *Journal of Enhanced Heat Transfer*, Vol. 15(4), pp. 335-350.
- [85] Bianco V., Chiacchio F., Manca O., Nardini S., (2009), Numerical investigation of nanofluids forced convection in circular tubes, *Applied Thermal Engineering*, Vol. 29, pp. 3632-3642.
- [86] Kakaç, S., Yener, Y., (1995), *Convective Heat Transfer*, Second Ed., CRC-Press, Boca Raton.
- [87] Bejan A., Kraus A. D., (2003), *Heat Transfer Handbook*, John Wiley & Sons, Hoboken, New Jersey.
- [88] Özerinç S., (2010), Heat Transfer Enhancement with Nanofluids (Master's thesis), Middle East Technical University, Ankara, Turkey.
- [89] Özışık, M. N., (1994), *Finite Difference Methods in Heat Transfer*, CRC-Press, Boca Raton.
- [90] Lienhard IV J.H., Lienhard V J.H., (2002), *A Heat Transfer Textbook*, Second Ed., Phlogiston Press, Cambridge, Massachusetts.
- [91] Chiesa M., Garg J., Kang Y. T., Chen G., (2008), Thermal conductivity and viscosity of water-in-oil nanoemulsions, *Colloids and Surfaces A: Physicochemical and Engineering Aspects*, Vol. 326, pp. 67-72.
- [92] Etherington H., (1958), *Nuclear Engineering Handbook*, Vol. 36, McGraw-Hill, New York.
- [93] Singh P. K., Anoop K.B., Sundararajan T., Das S. K., (2010), Entropy generation due to flow and heat transfer in nanofluids, *International Journal of Heat and Mass Transfer*, Vol. 53, pp. 4757-4767.
- [94] Bejan A., (1982), *Entropy Generation through Heat and Fluid Flow*, John Wiley & Sons, New York.
- [95] Liu L., Kim E. S., Park Y. G., Jacobi A. M., (2012), The potential impact of nanofluid enhancements on the performance of heat exchangers, *Heat Transfer Engineering*, Vol. 33(1), pp. 31-41.

- [96] Falahat A., (2011), Second law analysis of nanofluid flow in coiled tube under constant heat flux, *International Journal of Multidisciplinary Sciences and Engineering*, Vol. 2, 5.
- [97] Routbort J. L., Singh D., Timofeeva E. V., Yu W., France D. M., (2011), Pumping power of nanofluids in a flowing system, *Journal of Nanoparticle Research*, Vol. 13, pp. 931-937.
- [98] Corcione M., Cianfrini M., Quintino A., (2012), Heat transfer of nanofluids in turbulent pipe flow, *International Journal of Thermal Sciences*, Vol. 56, pp. 58-69.
- [99] Li J., Kleinstreuer C., (2010), Entropy generation analysis for nanofluid flow in microchannels, *Journal of Heat Transfer*, Vol. 132, 122401-1.
- [100] Mohhaddami M., Mohammadzade A., Esfenahi S. A. V., (2011), Second law analysis of nanofluids, *Energy Conversion and Management*, Vol. 52, pp. 1397-1405.
- [101] Shokoumand H., Moghaddami M., Siavashi M., Second law analysis of nanofluid flow through circular pipe, *Proceedings of the ASME 2010 10th Biennial Conference on Engineering Systems Design and Analysis ESDA 2010*, Jul 12-14, 2010, Istanbul, Turkey.

APPENDIX A

NUMERICAL STUDY CODE ALGORITHM



APPENDIX B

CONVECTIVE HEAT TRANSFER ANALYSIS DIMENSIONAL VALUES AND RESULTS

Table 4 Dimensional Geometrical and Boundary Condition Values for the Figures (18-30)

Fluid mean inlet temperature	$T_{m,i}$	20 °C
Channel diameter	D	0.01 m
Channel length	L	1 m
CWT case wall condition	T_w	50 °C
CHF case wall condition	q''	5660 W/m ²

Table 5 Constant and Variable Property Results of Al₂O₃ (50nm) /water Nanofluid in the Fully Developed Region for Different Peclet Numbers

D= 0.02m		CHF, $q_w = 500 \text{ W/m}^2$				CWT, $T_w = 70^\circ\text{C}$			
Property		Constant		Variable		Constant		Variable	
Pe		$\phi=0$	$\phi=0.05$	$\phi=0$	$\phi=0.05$	$\phi=0$	$\phi=0.05$	$\phi=0$	$\phi=0.05$
1000	Nu_L	4.36	4.36	4.36	4.38	3.66	3.66	3.66	3.66
	h_L (W/m ² K)	141	172	146	218	116	144	121	181
4000	Nu_L	4.36	4.36	4.37	4.39	3.66	3.66	3.67	3.72
	h_L (W/m ² K)	134	150	137	158	116	139	121	170
7000	Nu_L	4.36	4.36	4.37	4.39	3.69	3.69	3.71	3.83
	h_L (W/m ² K)	132	147	134	152	115	135	119	162

Table 6 Effect of Axial Conduction for Al₂O₃ (50nm) /water Nanofluid in the Fully Developed Region

D= 0.02m		CHF, $q_w = 2000 \text{ W/m}^2$				CWT, $T_w = 70^\circ\text{C}$			
Axial Conduction		OFF		ON		OFF		ON	
Pe		$\phi=0$	$\phi=0.05$	$\phi=0$	$\phi=0.05$	$\phi=0$	$\phi=0.05$	$\phi=0$	$\phi=0.05$
10	Nu _L	4.400	4.474	4.441	4.511	3.657	3.651	3.684	3.690
	h_L (W/m ² K)	140.3	171.2	141.3	171.6	121.2	181.1	122.0	182.5
100	Nu _L	4.400	4.474	4.400	4.474	3.657	3.651	3.658	3.652
	h_L (W/m ² K)	140.3	171.2	140.3	171.2	121.2	181.1	121.2	181.1
1000	Nu _L	4.400	4.474	4.400	4.474	3.657	3.651	3.657	3.651
	h_L (W/m ² K)	140.3	171.2	140.3	171.2	121.2	181.1	121.2	181.1

Table 7 Effect of Viscous Dissipation for Al₂O₃ (50nm) /water Nanofluid in the Fully Developed Region

Pe = 4000		CHF, $q_w = 2000 \text{ W/m}^2$				CWT, $T_w = 70^\circ\text{C}$			
Viscous Dissipation		OFF		ON		OFF		ON	
D (m)		$\phi=0$	$\phi=0.05$	$\phi=0$	$\phi=0.05$	$\phi=0$	$\phi=0.05$	$\phi=0$	$\phi=0.05$
0.02	$Br \times 10^{-7}$	1.40	3.00	1.40	3.00	0.20	0.37	0.20	0.37
	Nu _L	4.371	4.385	4.371	4.385	3.687	3.777	3.687	3.777
	h_L (W/m ² K)	136.6	158.2	136.6	158.2	120.0	166.1	120.0	166.1
0.002	$Br \times 10^{-4}$	1.40	3.00	1.40	3.00	0.02	0.04	0.02	0.04
	Nu _L	4.354	4.353	4.348	4.342	3.687	3.777	3.687	3.777
	h_L (W/m ² K)	1360	1570	1359	1568	1200	1660	1200	1661
0.0002	$Br \times 10^{-2}$	1.40	3.00	1.40	3.00	0.02	0.04	0.02	0.04
	Nu _L	4.354	4.353	3.880	3.463	3.687	3.777	3.674	3.749
	h_L (W/m ² K)	13600	15710	12220	13080	12000	16610	11960	16490

APPENDIX C

PARAMETRIC STUDY OF CHAPTER 5

